



# **GeoTechnical Investigations for the Dalton Highway Innovation Project As A Case Study of the Ice-Rich Syngenetic Permafrost**

**Prepared By:**

Yuri Shur  
Mikhail Kanevskiy  
Matthew Dillon  
Eva Stephani  
Jonathan O'Donnell

**February 2010**

**Prepared By:**

Alaska University Transportation Center  
Duckering Building Room 245  
P.O. Box 755900  
Fairbanks, AK 99775-5900

Alaska Department of Transportation  
Research, Development, and Technology  
Transfer  
2301 Peger Road  
Fairbanks, AK 99709-5399

**INE/ AUTC 11.11**

**DOT # FHWA-AK-RD-10-06**

**REPORT DOCUMENTATION PAGE**

Form approved OMB No.

Public reporting for this collection of information is estimated to average 1 hour per response, including the time for reviewing instructions, searching existing data sources, gathering and maintaining the data needed, and completing and reviewing the collection of information. Send comments regarding this burden estimate or any other aspect of this collection of information, including suggestion for reducing this burden to Washington Headquarters Services, Directorate for Information Operations and Reports, 1215 Jefferson Davis Highway, Suite 1204, Arlington, VA 22202-4302, and to the Office of Management and Budget, Paperwork Reduction Project (0704-1833), Washington, DC 20503

1. AGENCY USE ONLY (LEAVE BLANK)

FHWA-AK-RD-10-06

2. REPORT DATE

September 2010

3. REPORT TYPE AND DATES COVERED

Final Report (04/2008-03/2010)

4. TITLE AND SUBTITLE

Geotechnical Investigations for the Dalton Highway Innovation Project as a Case Study of the Ice-Rich Syngenetic Permafrost

5. FUNDING NUMBERS

AUTC #207122  
DTRT06-G-0011  
T2-08-19

6. AUTHOR(S)

Yuri Shur, Mikhail Kanevskiy, Matthew Dillon, Eva Stephani, Jonathan O'Donnell

7. PERFORMING ORGANIZATION NAME(S) AND ADDRESS(ES)

Alaska University Transportation Center  
P.O. Box 755900  
Fairbanks, AK 99775-5900

8. PERFORMING ORGANIZATION REPORT NUMBER

INE/AUTC # 11.11

9. SPONSORING/MONITORING AGENCY NAME(S) AND ADDRESS(ES)

Alaska Department of Transportation  
Research, Development, and Technology Transfer  
2301 Peger Road  
Fairbanks, AK 99709-5399

10. SPONSORING/MONITORING AGENCY REPORT NUMBER

FHWA-AK-RD-10-06

11. SUPPLEMENTARY NOTES

12a. DISTRIBUTION / AVAILABILITY STATEMENT

No restrictions

12b. DISTRIBUTION CODE

13. ABSTRACT (Maximum 200 words)

ADOT&PF plans to construct a new section of the James W. Dalton Highway in northern Alaska. The new three-mile-long section of road will avoid a steep climb, making the road safer to drive. Preliminary work shows that this new section of highway will cross an area of extremely complex permafrost conditions. The area is characterized by ice-rich, syngenetic Pleistocene permafrost, which can be up to 100 feet thick and contain huge ice wedges. ("Syngenetic" describes frozen ground that slowly grows upwards in size as sediments are deposited on the surface.) Any human activity in this sensitive area can trigger thaw settlement of soils and permafrost degradation. The durability of roads crossing such complex conditions depends on a design based on the best geotechnical information available, continuous monitoring, and timely maintenance. The better the design, the less maintenance work required. AUTC permafrost experts Yuri Shur and Mikhail Kanevskiy helped prepare for this construction project by performing a geotechnical investigation of the area, training ADOT&PF engineers in the nature of permafrost behavior, and providing guidance in developing a methodology for describing, sampling, and testing the ice-rich syngenetic Pleistocene permafrost. In addition to supporting the best design possible for the Dalton Highway, project results will be useful for construction projects throughout the circumpolar North and will contribute to educating a new generation of engineers at the University of Alaska.

14. KEYWORDS: Permafrost, Polar regions, Geotechnical engineering

15. NUMBER OF PAGES

156

16. PRICE CODE

N/A

17. SECURITY CLASSIFICATION OF REPORT

Unclassified

18. SECURITY CLASSIFICATION OF THIS PAGE

Unclassified

19. SECURITY CLASSIFICATION OF ABSTRACT

Unclassified

20. LIMITATION OF ABSTRACT

N/A

### **Notice**

This document is disseminated under the sponsorship of the U.S. Department of Transportation in the interest of information exchange. The U.S. Government assumes no liability for the use of the information contained in this document.

The U.S. Government does not endorse products or manufacturers. Trademarks or manufacturers' names appear in this report only because they are considered essential to the objective of the document.

### **Quality Assurance Statement**

The Federal Highway Administration (FHWA) provides high-quality information to serve Government, industry, and the public in a manner that promotes public understanding. Standards and policies are used to ensure and maximize the quality, objectivity, utility, and integrity of its information. FHWA periodically reviews quality issues and adjusts its programs and processes to ensure continuous quality improvement.

### **Author's Disclaimer**

Opinions and conclusions expressed or implied in the report are those of the author. They are not necessarily those of the Alaska DOT&PF or funding agencies.

# SI\* (MODERN METRIC) CONVERSION FACTORS

## APPROXIMATE CONVERSIONS TO SI UNITS

Symbol	When You Know	Multiply By	To Find	Symbol
<b>LENGTH</b>				
in	inches	25.4	millimeters	mm
ft	feet	0.305	meters	m
yd	yards	0.914	meters	m
mi	miles	1.61	kilometers	km
<b>AREA</b>				
in <sup>2</sup>	square inches	645.2	square millimeters	mm <sup>2</sup>
ft <sup>2</sup>	square feet	0.093	square meters	m <sup>2</sup>
yd <sup>2</sup>	square yard	0.836	square meters	m <sup>2</sup>
ac	acres	0.405	hectares	ha
mi <sup>2</sup>	square miles	2.59	square kilometers	km <sup>2</sup>
<b>VOLUME</b>				
fl oz	fluid ounces	29.57	milliliters	mL
gal	gallons	3.785	liters	L
ft <sup>3</sup>	cubic feet	0.028	cubic meters	m <sup>3</sup>
yd <sup>3</sup>	cubic yards	0.765	cubic meters	m <sup>3</sup>
NOTE: volumes greater than 1000 L shall be shown in m <sup>3</sup>				
<b>MASS</b>				
oz	ounces	28.35	grams	g
lb	pounds	0.454	kilograms	kg
T	short tons (2000 lb)	0.907	megagrams (or "metric ton")	Mg (or "t")
<b>TEMPERATURE (exact degrees)</b>				
°F	Fahrenheit	5 (F-32)/9 or (F-32)/1.8	Celsius	°C
<b>ILLUMINATION</b>				
fc	foot-candles	10.76	lux	lx
fl	foot-Lamberts	3.426	candela/m <sup>2</sup>	cd/m <sup>2</sup>
<b>FORCE and PRESSURE or STRESS</b>				
lbf	poundforce	4.45	newtons	N
lbf/in <sup>2</sup>	poundforce per square inch	6.89	kilopascals	kPa
<b>APPROXIMATE CONVERSIONS FROM SI UNITS</b>				
Symbol	When You Know	Multiply By	To Find	Symbol
<b>LENGTH</b>				
mm	millimeters	0.039	inches	in
m	meters	3.28	feet	ft
m	meters	1.09	yards	yd
km	kilometers	0.621	miles	mi
<b>AREA</b>				
mm <sup>2</sup>	square millimeters	0.0016	square inches	in <sup>2</sup>
m <sup>2</sup>	square meters	10.764	square feet	ft <sup>2</sup>
m <sup>2</sup>	square meters	1.195	square yards	yd <sup>2</sup>
ha	hectares	2.47	acres	ac
km <sup>2</sup>	square kilometers	0.386	square miles	mi <sup>2</sup>
<b>VOLUME</b>				
mL	milliliters	0.034	fluid ounces	fl oz
L	liters	0.264	gallons	gal
m <sup>3</sup>	cubic meters	35.314	cubic feet	ft <sup>3</sup>
m <sup>3</sup>	cubic meters	1.307	cubic yards	yd <sup>3</sup>
<b>MASS</b>				
g	grams	0.035	ounces	oz
kg	kilograms	2.202	pounds	lb
Mg (or "t")	megagrams (or "metric ton")	1.103	short tons (2000 lb)	T
<b>TEMPERATURE (exact degrees)</b>				
°C	Celsius	1.8C+32	Fahrenheit	°F
<b>ILLUMINATION</b>				
lx	lux	0.0929	foot-candles	fc
cd/m <sup>2</sup>	candela/m <sup>2</sup>	0.2919	foot-Lamberts	fl
<b>FORCE and PRESSURE or STRESS</b>				
N	newtons	0.225	poundforce	lbf
kPa	kilopascals	0.145	poundforce per square inch	lbf/in <sup>2</sup>

\*SI is the symbol for the International System of Units. Appropriate rounding should be made to comply with Section 4 of ASTM E380.  
(Revised March 2003)



## TABLE OF CONTENT

<b>SUMMARY</b> .....	<b>7</b>
<b>1. INTRODUCTION</b> .....	<b>9</b>
<b>2. METHODS</b> .....	<b>12</b>
<b>3. NATURE OF SYNGENETIC PERMAFROST</b> .....	<b>14</b>
<b>4. PREVIOUS PERMAFROST INVESTIGATIONS IN THE AREA</b> .....	<b>28</b>
<b>5. AUTC AND AKDOT INVESTIGATIONS IN 2008</b> .....	<b>33</b>
5.1. LOCATION, TOPOGRAPHY, GEOLOGY, AND PERMAFROST FEATURES .....	33
5.2. BOREHOLE LOGGING.....	36
<i>Borehole # AUTC08-2</i> .....	36
<i>Borehole # AUTC08-3</i> .....	48
<i>Borehole # AUTC08-4</i> .....	57
<i>Borehole # AUTC08-5</i> .....	68
<i>Borehole # AUTC08-6</i> .....	77
<i>Borehole # AUTC08-7</i> .....	90
<i>Borehole # AUTC08-8</i> .....	102
<i>Borehole # AUTC08-9</i> .....	112
5.3. SOIL CHARACTERISTICS .....	124
<i>Grain-size analyses</i> .....	124
<i>Moisture content of soil between ice wedges</i> .....	127
5.4. IDENTIFICATION OF ALIGNMENT SECTIONS WITH DIFFERENT PERMAFROST PROPERTIES .....	128
<i>Section #1</i> .....	133
<i>Section #2</i> .....	136
<i>Section #3</i> .....	137
<i>Section #4</i> .....	138
5.5. THAW STRAIN OF FROZEN SOILS.....	140
<b>CONCLUSIONS</b> .....	<b>147</b>
<b>REFERENCES</b> .....	<b>149</b>

## FIGURES

- Figure 1.1.** Location of AUTC and DOT boreholes, Dalton Highway Innovation Project, May-June 2008 (total number of boreholes – 62). Locations of eight AUTC hollow stem boreholes are marked with red squares.
- Figure 2.1.** Drill rig at the Dalton Highway Innovation Project field site, May 2008.
- Figure 2.2.** Simplified classification of cryostructures of mineral soils (ice is black).
- Figure 3.1.** Mechanisms of formation of epigenetic (A) and syngenetic (B) permafrost.
- Figure 3.2.** Appearance of wedge-ice, sample obtained by coring (Dalton Highway innovation project area, Interior Alaska).
- Figure 3.3.** Main cryostructures of syngenetic permafrost.
- Figure 3.4.** Micro-porphyritic cryostructure of syngenetic permafrost (Northern Alaska).
- Figure 3.5.** Micro-lenticular and latent micro-lenticular cryostructures of syngenetic permafrost, depth 46 ft (14 m), label is 1.25x1.25 cm (CRREL Permafrost tunnel, Fox, Interior Alaska).
- Figure 3.6.** Micro-braided cryostructure of syngenetic permafrost (Dalton Highway innovation project area, Interior Alaska).
- Figure 3.7.** Micro-ataxitic and micro-braided cryostructures of syngenetic permafrost (Dalton Highway innovation project area, Interior Alaska).
- Figure 3.8.** Belt-like cryostructure (combined with micro-braided cryostructure) of syngenetic permafrost (Dalton Highway innovation project area, Interior Alaska).
- Figure 3.9.** Exposure of the late Pleistocene syngenetic permafrost (Northern Alaska).
- Figure 3.10.** Possible interpretations of massive ice bodies encountered by drilling at different depths. A – tabular massive ice; B – syngenetic ice wedges.
- Figure 3.11.** Typical sequence of syngenetic permafrost in the core, ice is black (idealized image, not to scale).
- Figure 3.12.** Typical sequence of the upper part of the ice-rich syngenetic permafrost. 1 – Active layer; 2 – Transient layer; 3 – Intermediate layer with thin contemporary ice wedge; prevailing cryostructures – ataxitic and reticulate; 4 – Late Pleistocene syngenetic permafrost with big buried ice wedge; prevailing cryostructure – micro-lenticular.
- Figure 4.1.** Ice wedge exposed during construction of the pipeline haul road near Hess Creek (Andersland & Anderson 1978).
- Figure 4.2.** Location of boreholes drilled by Alyeska Pipeline Service Company in 1970 projected on the aerial photograph, Alyeska Pipeline Service Company, August 10, 1969 (Kreig & Reger 1982).
- Figure 4.3.** Location of boreholes drilled by Alyeska Pipeline Service Company in 1970 (Kreig & Reger 1982) projected on AKDOT&PF map.
- Figure 4.4.** Occurrence of massive ice in the boreholes located along the line A-A' (Kreig & Reger 1982). Location of the boreholes is shown in Figures 4.2, 4.3.
- Figure 4.5.** Occurrence of massive ice in the boreholes from *a* to *h* (based on the data from Kreig & Reger 1982). Location of the boreholes is shown in Figures 4.2, 4.3.
- Figure 4.6.** Temperature distribution (from Tart, 2003).
- Figure 5.1.** Aerial photograph of the project area.
- Figure 5.2.** Burned black spruce forest in the project area.
- Figure 5.3.** Cryogenic structure (ice is black) and properties of frozen soil, borehole AUTC-2, depth 0-11.5 ft (0-3.5 m).
- Figure 5.4.** Cryogenic structure (ice is black) and properties of frozen soil, borehole AUTC-2, depth 11.5-23 ft (3.5-7 m).
- Figure 5.5.** Cryogenic structure (ice is black) and properties of frozen soil, borehole AUTC-2, depth 23-34.5 ft (7-10.5 m).
- Figure 5.6.** Cryogenic structure (ice is black) and properties of frozen soil, borehole AUTC-2, depth 34.5-39 ft (10.5-11.84 m).

**Figure 5.7.** Gravimetric moisture content of frozen soil, borehole AUTC-2. Up to 9 m – thawed and refrozen sediments. From 9 m – syngenetic permafrost.

**Figure 5.8.** Silt with porous cryostructure (no visible ice), borehole AUTC-2, depth 2.80-2.94 m, gravimetric moisture content 46%.

**Figure 5.9.** Silt with porous cryostructure (no visible ice), borehole AUTC-2, depth 7.20-7.44 m, gravimetric moisture content 45%.

**Figure 5.10.** Silt with porous cryostructure (no visible ice), borehole AUTC-2, depth 8.60-8.73 m, gravimetric moisture content 45%.

**Figure 5.11.** Silt with micro-porphyrritic cryostructure, borehole AUTC-2, depth 9.2-9.3 m, gravimetric moisture content 64%.

**Figure 5.12.** Silt with micro-lenticular – micro-braided cryostructure, borehole AUTC-2, depth 10.95-11.05 m, gravimetric moisture content 81%.

**Figure 5.13.** Silt with small ice vein, typical of syngenetic permafrost, borehole AUTC-2, depth 11.43-11.55 m.

**Figure 5.14.** Cryogenic structure (ice is black) and properties of frozen soil, borehole AUTC-3, depth 0-18 ft (0-5.5 m).

**Figure 5.15.** Cryogenic structure (ice is black) and properties of frozen soil, Dalton Highway Innovation Project, borehole AUTC-3, depth 18-29.5 ft (5.5-9 m).

**Figure 5.16.** Gravimetric moisture content of frozen soil, borehole AUTC-3. Syngenetic permafrost, from 1.8 to 4.8 m wedge-ice. From 6.1 m – epigenetic permafrost.

**Figure 5.17.** Silt with micro-braided – micro-lenticular cryostructure, borehole AUTC-3, depth 1.03-1.15 m.

**Figure 5.18.** Silt with reticulate incomplete cryostructure, borehole AUTC-3, depth 1.65-1.76 m, gravimetric moisture content 68%.

**Figure 5.19.** Silt with micro-ataxitic – micro-braided cryostructure, borehole AUTC-3, depth 5.62-5.72 m, gravimetric moisture content 233%.

**Figure 5.20.** Silt with micro-braided – micro-layered cryostructure, borehole AUTC-3, depth 6.0-6.13 m.

**Figure 5.21.** Silt with layered – braided cryostructure, borehole AUTC-3, depth 6.65-6.75 m, gravimetric moisture content 45%.

**Figure 5.22.** Cryogenic structure (ice is black) and properties of frozen soil, borehole AUTC-4, depth 0-11.5 ft (0-3.5 m).

**Figure 5.23.** Cryogenic structure (ice is black) and properties of frozen soil, borehole AUTC-4, depth 11.5-23 ft (3.5-7 m).

**Figure 5.24.** Cryogenic structure (ice is black) and properties of frozen soil, borehole AUTC-4, depth 23-34.5 ft (7-10.5 m).

**Figure 5.25.** Cryogenic structure (ice is black) and properties of frozen soil, borehole AUTC-4, depth 34.5-40 ft (10.5-12.2 m).

**Figure 5.26.** Gravimetric moisture content of frozen soil, borehole AUTC-4. From 0.7 to 1.5 m – intermediate layer; from 1.5 to 3 m – thawed and refrozen sediments; from 3 to 10.2 m – syngenetic permafrost; from 10.2 m – epigenetic permafrost (gravel).

**Figure 5.27.** Silt with micro-braided – micro-ataxitic cryostructure, borehole AUTC-4, depth 0.84-0.95 m.

**Figure 5.28.** Silt with micro-porphyrritic cryostructure, borehole AUTC-4, depth 3.16-3.28 m, gravimetric moisture content 47%.

**Figure 5.29.** Silt with micro-lenticular – micro-braided cryostructure, borehole AUTC-4, depth 8.15-8.25 m, gravimetric moisture content 92%. Note inclination of ice lenses indicating proximity of ice wedge.

**Figure 5.30.** Silt with coarse sand and gravel, with crustal / micro-braided cryostructure, borehole AUTC-4, depth 9.63-9.70 m, gravimetric moisture content 67%.

**Figure 5.31.** Gravel with crustal cryostructure, borehole AUTC-4, depth 12.08-12.20 m, gravimetric moisture content 14%.

**Figure 5.32.** Cryogenic structure (ice is black) and properties of frozen soil, borehole AUTC-5, depth 0-11.5 ft (0-3.5 m).

**Figure 5.33.** Cryogenic structure (ice is black) and properties of frozen soil, borehole AUTC-5, depth 11.5-23 ft (3.5-7 m).

**Figure 5.34.** Cryogenic structure (ice is black) and properties of frozen soil, borehole AUTC-5, depth 23-24.5 ft (7-7.48 m).

**Figure 5.35.** Gravimetric moisture content of frozen soil, borehole AUTC-5, syngenetic permafrost

**Figure 5.36.** Silt with micro-braided cryostructure, borehole AUTC-5, depth 0.8-0.9 m, gravimetric moisture content 92%.

**Figure 5.37.** Silt with latent micro-lenticular cryostructure (inclined), borehole AUTC-5, depth 2.03-2.14 m, gravimetric moisture content 66%.

**Figure 5.38.** Silt with latent micro-lenticular cryostructure, borehole AUTC-5, depth 2.74-2.85 m, gravimetric moisture content 74%.

**Figure 5.39.** Silt with micro-lenticular – micro-braided cryostructure, borehole AUTC-5, depth 4.55-4.64 m, gravimetric moisture content 90%.

**Figure 5.40.** Silt with micro-ataxitic – micro-braided cryostructure, borehole AUTC-5, depth 7.30-7.38 m, gravimetric moisture content 126%.

**Figure 5.41.** Cryogenic structure (ice is black) and properties of frozen soil, borehole AUTC-6, depth 0-11.5 ft (0-3.5 m).

**Figure 5.42.** Cryogenic structure (ice is black) and properties of frozen soil, borehole AUTC-6, depth 11.5-46 ft (3.5-14 m).

**Figure 5.43.** Cryogenic structure (ice is black) and properties of frozen soil, borehole AUTC-6, depth 46-57.5 ft (14-17.5 m).

**Figure 5.44.** Cryogenic structure (ice is black) and properties of frozen soil, borehole AUTC-6, depth 57.5-69 ft (17.5-21.05 m).

**Figure 5.45.** Gravimetric moisture content of frozen soil, borehole AUTC-6. Thawed and refrozen sediments on top, from 3.2 m – syngenetic permafrost. From 18.6 m – epigenetic permafrost.

**Figure 5.46.** Silt with micro-lenticular cryostructure (0-4cm – porous invisible), borehole AUTC-6, depth 0.76-0.88 m, gravimetric moisture content 56% (0.8-0.86 m).

**Figure 5.47.** Silt with porous cryostructure (no visible ice), borehole AUTC-6, depth 2.25-2.36 m, gravimetric moisture content 39%.

**Figure 5.48.** Organic silt with porous cryostructure (no visible ice), borehole AUTC-6, depth 2.90-3.03 m, gravimetric moisture content 63%.

**Figure 5.49.** Silt with micro-lenticular – micro-braided cryostructure, borehole AUTC-6, depth 14.11-14.18 m, gravimetric moisture content 99%.

**Figure 5.50.** Ice-rich silt, boundary with ice wedge, borehole AUTC-6, depth 7.30-7.38 m.

**Figure 5.51.** Ice-poor silt (epigenetic permafrost) with porous – lenticular cryostructure, borehole AUTC-6, depth 18.67-18.77 m, gravimetric moisture content 39%.

**Figure 5.52.** Gravelly sandy silt (epigenetic permafrost) with crustal cryostructure, borehole AUTC-6, depth 18.67-18.77 m, gravimetric moisture content 24%.

**Figure 5.53.** Cryogenic structure (ice is black) and properties of frozen soil, borehole AUTC-7, depth 0-11.5 ft (0-3.5 m).

**Figure 5.54.** Cryogenic structure (ice is black) and properties of frozen soil, borehole AUTC-7, depth 11.5-23 ft (3.5-7 m).

**Figure 5.55.** Cryogenic structure (ice is black) and properties of frozen soil, borehole AUTC-7, depth 23-34.5 ft (7-10.5 m).

**Figure 5.56.** Cryogenic structure (ice is black) and properties of frozen soil, borehole AUTC-7, depth 34.5-39 ft (10.5-11.9 m).

**Figure 5.57.** Gravimetric moisture content of frozen soil, borehole AUTC-7, syngenetic permafrost. From 1 to 1.8 m – thawed and refrozen sediments.

**Figure 5.58.** Silt with reticulate – braided cryostructure, borehole AUTC-7, depth 2.66-2.76 m, gravimetric moisture content 157%.

**Figure 5.59.** Organic silt with micro-braided cryostructure, borehole AUTC-7, depth 3.00-3.08 m, gravimetric moisture content 183%.

**Figure 5.60.** Silt with micro-lenticular – micro-braided cryostructure, borehole AUTC-7, depth 4.25-4.35 m, gravimetric moisture content 81%.

**Figure 5.61.** Silt with braided – micro-braided cryostructure, borehole AUTC-7, depth 11.5-11.6 m, gravimetric moisture content 73%.

**Figure 5.62.** Ice-rich silt, boundary with ice wedge, borehole AUTC-7, depth 11.77-11.9 m.

**Figure 5.63.** Sediment-rich wedge-ice with vertical foliation, borehole AUTC-7, depth 11.9 m.

**Figure 5.64.** Cryogenic structure (ice is black) and properties of frozen soil, borehole AUTC-8, depth 0-11.5 ft (0-3.5 m).

**Figure 5.65.** Cryogenic structure (ice is black) and properties of frozen soil, borehole AUTC-8, depth 11.5-23 ft (3.5-7 m).

**Figure 5.66.** Cryogenic structure (ice is black) and properties of frozen soil, borehole AUTC-8, depth 23-48 ft (7-14.6 m).

**Figure 5.67.** Gravimetric moisture of frozen soil, borehole AUTC-8 (syngenetic permafrost). From 14.2 m – epigenetic permafrost (presumably thawed and refrozen sediments).

**Figure 5.68.** Silt with micro-braided – micro-ataxitic cryostructure, borehole AUTC-8, depth 0.64-0.72 m, gravimetric moisture content 182%.

**Figure 5.69.** Organic silt with organic-matrix – micro-braided cryostructure, borehole AUTC-8, depth 3.60-3.72 m, gravimetric moisture content 93%.

**Figure 5.70.** Organic silt with organic-matrix – micro-braided cryostructure, sub-vertical, borehole AUTC-8, depth 4.67-4.77 m, gravimetric moisture content 121%.

**Figure 5.71.** Silt with micro-braided – micro-lenticular cryostructure, inclined, borehole AUTC-8, depth 6.9-7.0 m, gravimetric moisture content 118%.

**Figure 5.72.** Ice-poor silt with layered – lenticular cryostructure, borehole AUTC-8, depth 14.28-14.43 m, gravimetric moisture content 36% (14.4-14.5 m, almost without visible ice).

**Figure 5.73.** Cryogenic structure (ice is black) and properties of frozen soil, borehole AUTC-9, depth 0-34.5 ft (0-10.5 m).

**Figure 5.74.** Cryogenic structure (ice is black) and properties of frozen soil, borehole AUTC-9, depth 34.5-46 ft (10.5-14 m).

**Figure 5.75.** Cryogenic structure (ice is black) and properties of frozen soil, borehole AUTC-9, depth 46-59 ft (14-18 m).

**Figure 5.76.** Cryogenic structure (ice is black) and properties of frozen soil, borehole AUTC-9, depth 59-70 ft (18-21.35 m).

**Figure 5.77.** Gravimetric moisture content of frozen soil, borehole AUTC-9 (syngenetic permafrost).

**Figure 5.78.** Silt with micro-braided – micro-ataxitic cryostructure, borehole AUTC-9, depth 0.91-1.02 m, gravimetric moisture content 160%.

**Figure 5.79.** Silt with latent micro-lenticular – micro-porphyrific cryostructure, with small ice veins, borehole AUTC-9, depth 13.75-13.85 m, gravimetric moisture content 62%.

**Figure 5.80.** Silt with latent micro-lenticular – micro-lenticular cryostructure, borehole AUTC-9, depth 17.44-17.55 m, gravimetric moisture content 51%.

**Figure 5.81.** Silt with micro-braided – micro-lenticular cryostructure, borehole AUTC-9, depth 19.16-19.28 m, gravimetric moisture content 81%.

**Figure 5.82.** Silt with micro-braided – micro-lenticular cryostructure, with ice veins, borehole AUTC-9, depth 21.30-21.35 m, gravimetric moisture content 90%.

**Figure 5.83.** Example of DOT drilling log, Dalton Highway Innovation Project, test hole TH08-003 (for location, see **Figure 5.96**, DOT borehole #3).

**Figure 5.84.** Grain size distribution, boreholes AUTC-2 – AUTC-7.

**Figure 5.85.** Organic matter content, DOT boreholes (based on AKDOT&PF data).

**Figure 5.86.** Gravimetric moisture content (without wedge ice) with depth (based on the data from eight AUTC boreholes, 189 samples). Average value: 85.5%.

**Figure 5.87.** Volumetric vs gravimetric moisture contents (based on 99 samples with measured volume from eight AUTC boreholes).

**Figure 5.88.** Ice-rich and relatively ice-poor sections (map).

**Figure 5.89.** Division of alignment in ice-rich and relatively ice-poor sections (profile).

**Figure 5.90.** Wedge-ice occurrence with depth, sections #1 (left) and #3 (right).

Numbers in parentheses show number of boreholes (both AUTC and DOT), which reached this depth interval. For locations of sections #1 and #3, see Figures 5.88, 5.89.

**Figure 5.91.** Gravimetric moisture content with depth, Section #1, based on DOT and AUTC data (four and 22 boreholes, correspondingly).

**Figure 5.92.** Distribution of ground ice volume with depth (Section #1). Numbers in parentheses show number of boreholes (both AUTC and DOT), which reached this depth interval. Volumetric ice content distribution is based on AUTC data.

**Figure 5.93.** Gravimetric moisture content with depth, Section #2, based on DOT and AUTC data (eight and four boreholes, correspondingly).

**Figure 5.94.** Gravimetric moisture content with depth, Section #3, based on DOT data (nine boreholes).

**Figure 5.95.** Gravimetric moisture content with depth, Section #4, based on DOT data (15 boreholes).

**Figure 5.96.** Cryostratigraphic profile. AUTC boreholes marked by green squares and the rest are DOT boreholes. Boundaries of sections #1 (ice-rich) and #2 (relatively ice-poor) are shown in Figures 5.88, 5.89.

**Figure 5.97.** Expected wedge-ice distribution in different sections of the proposed alignment (not to scale).

**Figure 5.98.** Correlation between thaw strain of mineral and organic-rich soil (without external load) and their moisture content (based on data from AUTC boreholes, 44 samples).

**Figure 5.99.** Correlation between thaw strain of mineral soil (without external load) and their moisture content (based on the data for 35 samples from AUTC boreholes).

**Figure 5.100.** Correlation between thaw strain of organic-mineral soil (without external load) and their moisture content (based on the data for 9 samples from AUTC boreholes).

**Figure 5.101.** Thaw strain analysis of soils, borehole AUTC-4, depth 9.7 m, elapsed time 7 hrs.

**Figure 5.102.** Consolidation of organic-mineral soils.

**Figure 5.103.** Consolidation of mineral soils.

**Figure 5.104.** Thaw strain of mineral soil vs moisture content. 1 – without external load (based on experimental data, see Figure 5.99); 2 – under the stress 50 kPa; 3 – under the stress 140 kPa.

## TABLES

**Table 1.1.** Proposed tasks and objectives of the Dalton Highway innovation project.

**Table 5.1.** General characteristics of sections of ice-rich and relatively ice-poor sections. Based on drilling logs, AUTC and DOT boreholes.

**Table 5.2.** Wedge-ice occurrence at different depth intervals, sections 1-4.



## Summary

This project addresses the Alaska University Transportation Center (AUTC) theme in the areas of *Designing for Permafrost: exploring and developing designs that will perform better over these sensitive areas* through studying the geotechnical conditions of ice-rich syngenetic Pleistocene permafrost and developing best approaches to geotechnical investigations of such permafrost.

Soil in the Dalton Highway innovation project area is the ice-rich syngenetic Pleistocene permafrost. Such permafrost widely occurs in the Interior Alaska, on Seward Peninsula, on the Arctic Foothills of the Brooks Range and can be encountered in other areas, which had remained unglaciated during the late Pleistocene. Till recently, this type of permafrost has been understudied in Alaska and investigations for engineering projects usually do not provide sufficient information for its characterization.

The report presents results of collaborative geotechnical investigations of ice-rich Pleistocene permafrost conducted directly for one of the ADOT Northern Region projects in the Interior Alaska. The cooperative efforts between the University of Alaska Fairbanks (UAF) and the Alaska Department of Transportation and Public Facilities (AKDOT&PF) included core logging, soil sampling, and laboratory testing. Field geotechnical investigations along the proposed alignment of the highway between MP 8 and MP 12 were performed in May 2008. The frozen cores were analysed at UAF-CEE laboratory. During the field and laboratory work, three AKDOT geologists were trained in detailed permafrost description.

Field data proved our preliminary evaluation of permafrost genesis and its properties in the project area. Most of soils in the project area are extremely ice-rich and have excessive thaw settlement upon thawing. Four sections with different permafrost properties are identified along the proposed alignment:

**Section #1 (542+00...590+00)** has a thick sequence of ice-rich syngenetically frozen silt (from 52 ft to more than 85 ft) with very high wedge-ice occurrence (35%) and gravimetric moisture content of perennially frozen silt (102% average). The average thaw strain due to segregated ice reaches 32%, so the total thaw strain (due to wedge-ice and segregated ice) reaches 56%.

**Section #2 (509+00...542+00)** is presented by 31-39-ft-thick sequence of silt (partially ice-rich syngenetically frozen, partially ice-poor thawed and refrozen); very small wedge-ice occurrence (2%), but relatively high gravimetric moisture content of perennially frozen silt (79% average). The average thaw strain due to segregated ice reaches 23%, total thaw strain reaches 25%.

**Section #3 (492+00...509+00)** is characterized by 30-46-ft-thick sequence of ice-rich syngenetically frozen silt, extremely high wedge-ice occurrence (47%) and gravimetric moisture content of perennially frozen silt (81% average). The average thaw strain due to segregated ice reaches 23%, total thaw strain reaches 59%.

**Section #4 (433+00...492+00)** is very thin (2-13-ft-thick) sequence of silt overlaying gravel and weathered bedrocks; wedge-ice occurrence is very small (3%), but the gravimetric moisture content of perennially frozen silt is still relatively high (63% average). The average thaw strain due to segregated ice reaches 13%, total thaw strain reaches 16%.

Sections #1 and #3 are extremely ice-rich and permafrost thawing in these parts of alignment will bring unbearable settlement. Wedge-ice occurrence at sections #2 and #4 is not so significant, but

the soils themselves contain great amount of segregated ice, and the thaw settlement cannot be neglected.

In the study area, ice wedges are usually separated from the base of the active layer by 3-13-ft-thick protective layer of thawed and refrozen soils. Existence of the intermediate layer and the ice-poor stratum of thawed and refrozen soils on top of original syngenetic permafrost and could protect it in fill areas. In cut areas, this layer will be destroyed, therefore permafrost will be more vulnerable to climatic and local impacts. This ice-poor layer can significantly reduce the period of stabilization of exposed surfaces of cut slopes (in cases when large massive ice bodies are located right below the permafrost table, the process of complete stabilization of exposed bluffs can take dozens of years) .

Extremely high ice content of the ice-rich syngenetic permafrost with ice wedges defines its high thaw susceptibility and settlement harmful to any structures. The main potential hazards are following: (1) significant thaw settlement of soils beneath the road; (2) rapid retreat of permafrost slopes in cut areas; (3) contamination of surface water due to thawing of ice-rich silts at the slopes; (4) formation of ponds in the road-side ditches, which will increase the rate of permafrost thawing and thaw settlement of sediments beneath the water.

Information on the ice-rich syngenetic permafrost obtained for the Dalton Highway innovative project sets baseline for future applied investigations in Alaska in widely occurred areas with such permafrost. This information is representative for this type of permafrost and can be considered an example for future projects where such permafrost occurs. Information from the project will be used in UAF courses on permafrost and frozen ground engineering.



# 1. Introduction

The Alaska Department of Transportation and Public Facilities (AKDOT&PF) is proposing to construct a new alignment of the Dalton Highway between Mile Post (MP) 8 and MP 12. Our preliminary analysis of geotechnical conditions showed that a new alignment crosses the area with extremely complex permafrost conditions. An analysis of existing data obtained during previous geotechnical investigations in the area by AKDOT&PF and by Alyeska Pipeline Company identified existence of ice-rich permafrost including massive ice. The area is also located in the discontinuous permafrost zone where permafrost is slowly degrading.

Our work on the Dalton Highway innovation project the AUTC theme in the areas of *Designing for Permafrost: exploring and developing designs that will perform better over these sensitive areas* through studying the geotechnical conditions of ice-rich syngenetic Pleistocene permafrost and developing best approaches to geotechnical investigations of such permafrost. Proposed tasks and objectives of this project are shown in **Table 1.1**.

**Table 1.1.** Proposed tasks and objectives of the Dalton Highway innovation project.

Tasks	Objectives
T1: Provide comprehensive evaluation of permafrost conditions.	<p>O1.1: Preliminary identify permafrost conditions using available information.</p> <p>O1.2: Conduct detail field studies of permafrost along a new alignment.</p> <p>O1.3: Evaluate geotechnical properties of frozen and thawing soils.</p> <p>O1.4: Provide comprehensive characteristic of permafrost conditions.</p>
T2: Assist AKDOT in choosing design alternatives including experimental approaches increasing road integrity in areas of ice-rich degrading permafrost. In cooperation with design engineers, evaluate monitoring program and identify boreholes for installation monitoring equipment.	<p>O2.1: Provide assistance to AKDOT design engineers in evaluation of design alternatives.</p> <p>O2.2: In cooperation with design engineers, evaluate monitoring program and identify boreholes for installation monitoring equipment</p>
T3: Disseminate knowledge on syngenetic Pleistocene permafrost, its properties and behaviour in the base of roads and slope.	<p>O3.1: Develop best practice guide to study of ice-rich syngenetic permafrost for road design and construction.</p> <p>O3.2: Present a workshop on genesis, morphology, and engineering properties of syngenetic ice-rich permafrost for AKDOT geologists and engineers.</p>

The Dalton Highway innovation project requires extensive geotechnical investigations because it is located in the area with syngenetic Pleistocene permafrost. This extremely ice-rich and highly thaw-susceptible permafrost is potentially highly hazardous and requires special engineering measures to protect integrity of any structures built on it. In engineering practice, there is usually not enough information characterizing such permafrost and till recently, this type of permafrost was understudied in Alaska.

Long-term road integrity in such conditions depends on a design based on the best geotechnical information, continuous monitoring, and timely maintenance. The better design the less maintenance work will be required. To justify solutions implemented in design, geotechnical information should be sufficient and should clearly and adequately define the nature of massive ice and properties of permafrost soils covering and surrounding massive ice. Permafrost conditions along potential cuts should be characterized specifically well to predict thaw settlement of soils, behavior of slopes, and an environmental impact of slope erosion.

In May 2008, we performed field geotechnical investigations for the Dalton Highway innovation project as a case study of the ice-rich syngenetic permafrost. This study was developed as a cooperative effort between UAF and the AKDOT&PF. It included core logging, soil sampling, and laboratory testing of frozen samples. Drilling operations were conducted by AKDOT&PF.

Field work was performed at the proposed alignment of the Dalton Highway between Milepost 8.5 and Milepost 11.5 (**Figure 1.1**). Hollow stem drilling was conducted by AKDOT&PF. UAF participants (Yuri Shur, Mikhail Kanevskiy, Matthew Dillon, Jonathan O'Donnell) supervised drilling, collected samples, and logged boreholes. They described continuous cores from eight boreholes. Total length of obtained core was 358.7 ft (109.4 m). Laboratory study and testing of frozen samples was performed by Mikhail Kanevskiy, Matthew Dillon, and Eva Stephani. In further descriptions these boreholes are called AUTC boreholes. During the field and laboratory work, three AKDOT geologists were trained in detailed permafrost description. In May-June 2008, AKDOT added 54 solid stem drilled boreholes described by AKDOT geologists (in further descriptions they are called DOT boreholes). Information on soil from ADOT boreholes was available to AUTC and partly analyzed in this report.

This report is prepared by Y. Shur, M. Kanevskiy, M. Dillon, E. Stephani, and J. O'Donnell.

We appreciate good job of the drilling crew Tom Johnson and Jason Cline, cooperation in the field with ADOT geologists Julie Rowland and Ronald Brooks, and discussion at the different stages of the project with Billy Connor, Jessie Reinikainen, Steve Masterman, James Sweeney, and Leo Woster.

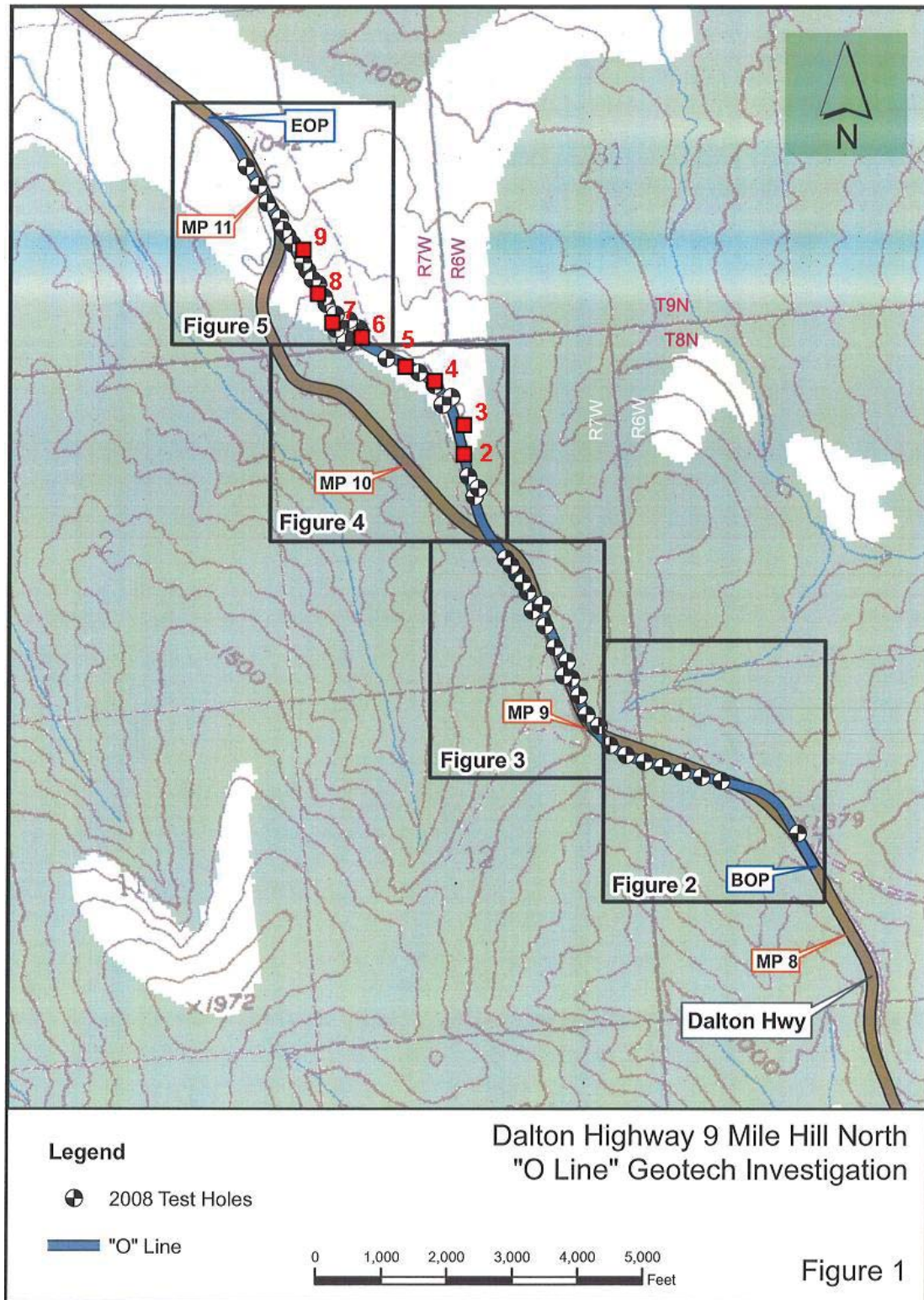


**Figure 1.1.** Location of AUTC and DOT boreholes, Dalton Highway Innovation Project, May-June 2008 (total number of boreholes – 62). Locations of eight AUTC hollow stem boreholes are marked with red squares.



## 2. Methods

**Drilling, logging, and sampling.** Hollow stem drilling was conducted by AKDOT&PF with the drill rig (Figure 2.1) equipped with modified CME sampler (2" inside diameter). Eight boreholes from 24.5 ft (7.5 m) up to 70.5 ft (21.5 m) deep were cored by AKDOT crew (drillers Tom Johnson and Jason Cline) and logged by the AUTC scientists. Total length of obtained core in these boreholes reached 358.7 ft (109.4 m).



**Figure 2.1.** Drill rig at the Dalton Highway Innovation Project field site, May 2008.

**Permafrost description.** For geotechnical investigations in the areas with the ice-rich permafrost, specific methods of permafrost investigations can be successfully applied. In our study, we used the cryofacial method (Katasonov 1962, 1978). It is based upon two concepts, (1) the shape, size and spatial pattern of ice inclusions (i.e. cryostructures) depend on the conditions under which the sediment was deposited and then frozen, and (2) every cryofacies has its own specific cryostructures. The method is based on a close relationship between cryogenic structure of soils and specific terrain units, and reveals the way of permafrost formation. Study of cryostructures helps (1) to understand the nature of permafrost, (2) to distinguish layers with specific cryogenic structure and properties, and (3) to estimate the ice distribution within the section. The cryofacial method has been especially useful for study of syngenetic permafrost.

For description of soil cryogenic structure, we used a classification of cryostructures (cryostructure – a pattern formed by ice inclusions in the frozen soil), which is based on several Russian and North

American classifications (Gasarov 1963, Pihlainen & Johnston 1963, Linell and Kaplar 1966, Katasonov 1969, Kudryavtsev 1978, Zhestkova 1982, Popov et al. 1985, Murton and French 1994, Shur and Jorgenson 1998, Melnikov and Spesivtsev 2000, French 2007). Simplified classification of cryostructures of mineral soils is shown in **Figure 2.2**.

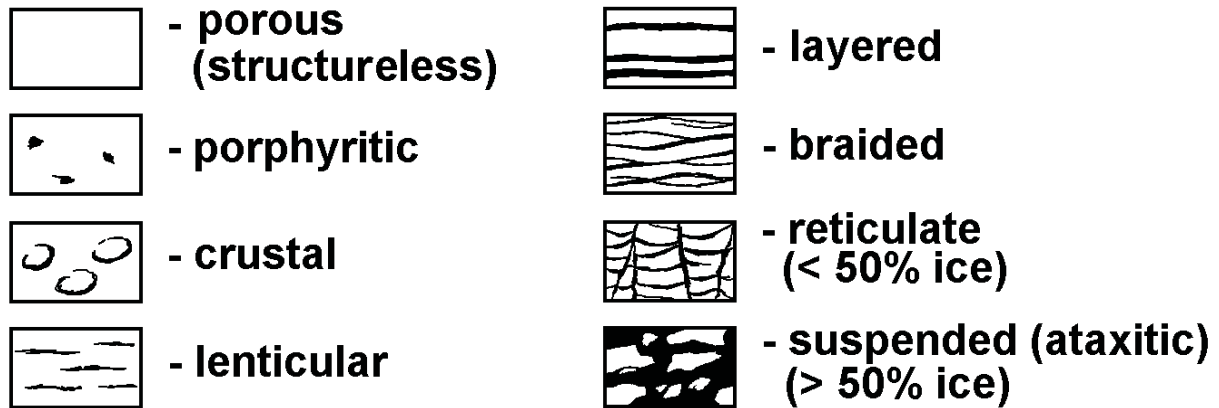


**Figure 2.2.** Simplified classification of cryostructures of mineral soils (ice is black).

Wedge-ice occurrence and its distribution with depth were evaluated on the base of the data obtained from 8 AUTC boreholes and 54 DOT boreholes.

**Soil testing.** The grain size analyses of the sediments were performed with sieves and hydrometers (ASTM D 422). Analyses were carried out on 25 samples obtained from six AUTC boreholes (AUTC08-2 – AUTC08-7). *Gradistat* software was used for the analysis of grain-size distributions (Blout and Pye, 2001).

Ice content of frozen soil between ice wedges was evaluated by oven-drying (90°C, 72 h) of samples. The samples were obtained from all AUTC boreholes (AUTC08-2 – AUTC08-9). Gravimetric moisture contents (on a dry-weight basis) were calculated for 189 soil samples. For volumetric moisture contents, 99 samples with cylindrical shape (for the most precise volume calculations) were selected. Volumetric moisture content was calculated as the ratio of the volume of ice (mass of the ice in a sample / 0.9 g/cm<sup>3</sup>) to the volume of the whole sample (van Everdingen 1998).

The thaw strain (the amount that frozen ground compresses upon thawing) is equal to the thaw settlement divided by the original thickness of the frozen ground before thawing (van Everdingen 1998). Thaw strain of ice-rich soil from the studied site was evaluated for two conditions. 44 samples obtained from seven AUTC boreholes (AUTC08-3 – AUTC08-9) were thawed without external load. Consolidation test of thawed soils was performed on five samples.

### 3. Nature of syngenetic permafrost

Geotechnical investigations for the Dalton Highway innovation project require special attention because syngenetic Pleistocene permafrost present in the area has not been well studied and well understood in Alaska. This extremely ice-rich and highly thaw-susceptible permafrost is potentially highly hazardous and requires special engineering measures to protect integrity of any structures built on it. In engineering practice, there is usually not enough information characterizing ice-rich syngenetic permafrost and till recently, this type of permafrost was understudied in Alaska.

There are two main types of permafrost: epigenetic and syngenetic (**Figure 3.1**). These types are characterized by differing mechanisms of formation, structure, and properties. The type of permafrost usually can be distinguished by its cryogenic structure, which is formed within perennially frozen soils by inclusions of pore, segregated, and massive ice.

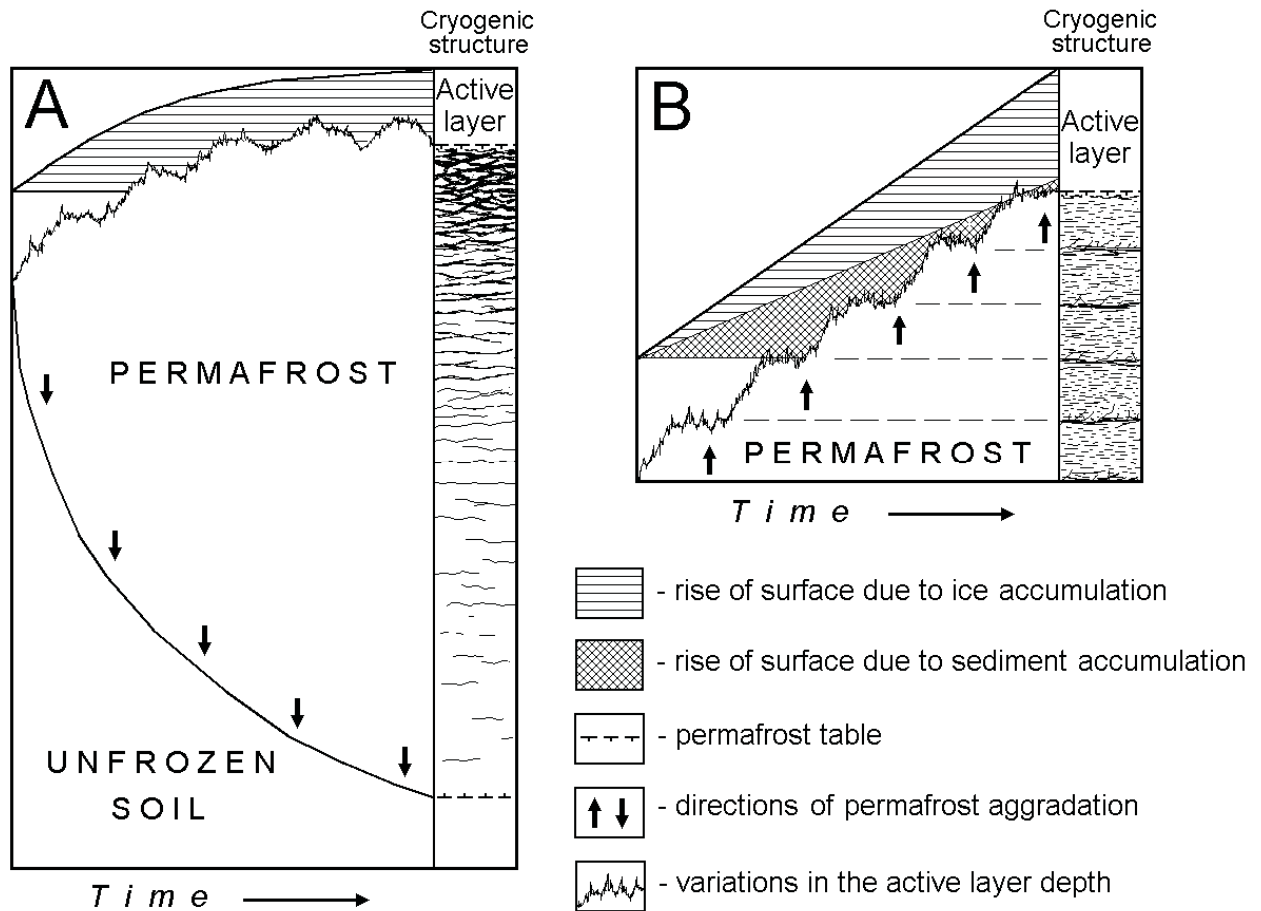


**Figure 3.1.** Mechanisms of formation of epigenetic (A) and syngenetic (B) permafrost.

**Epigenetic permafrost** – permafrost that forms through lowering of the permafrost base in previously deposited sediment or other earth material (van Everdingen 1998). Aggradation of epigenetic permafrost proceeds downward. Epigenetic freezing of unconsolidated saturated soils

results in accumulation of ice mostly in the upper part of section (**Figure 3.1A**). Ice distribution relates to the rate of freezing, which slows down with depth. Generally, when there are no additional sources of water, ice content of epigenetically frozen soil decreases with depth and its density increases.

**Syngenetic permafrost** forms through rise of the permafrost table during the deposition of additional sediment or other earth material on the ground surface (van Everdingen 1998).

Syngenetic permafrost formation is a complex process related to sedimentation in cold conditions, when the base of the active layer rises following accumulation of new sediment on the soil surface. Mechanism of syngenetic permafrost formation can be illustrated by **Figure 3.1B** based on the scheme suggested by Popov (1967). According to this scheme, syngenetic permafrost formation is connected with consequential addition of bottom portions of the frozen active layer to permafrost, which is going along with new sediment accumulation on the soil surface.

Syngenetic permafrost forms in response to sedimentation (alluvial, slope, aeolian, lacustrine, etc.) that causes the base of the active layer to aggrade upwards. Transformation of a part of the active layer into a perennially-frozen state occurs virtually simultaneously with sedimentation. Typically, syngenetically-frozen sediments are silty, or loess-like (up to 70-80% silt fraction), and ice-rich (the soil gravimetric moisture content may exceed 100-200%). They also contain significant amount of organic matter, buried peat horizons, and they have rhythmically-organized generally layered cryogenic structures. Occurrence of almost undecomposed rootlets indicates relatively small gap in time between sedimentation and freezing of sediments.

The syngenetic permafrost is usually extremely ice-rich and contains ice wedges throughout its entire thickness. Several systems of ice wedges, which can be found at different depths, are also common. Formation of ice wedges is triggered by repeated contraction cracking of the soil (Leffingwell 1915, Lachenbruch 1962, Popov 1967, Romanovskii 1993). During abrupt temperature drops during the winter the frozen soil contracts and forms a crack up to 2-cm-wide. In the following spring, surface water flows into the crack and freezes. Because ice is weaker than the surrounding frozen soil, a crack forms in the same place the next winter and the process repeats itself. Thickening of ice wedges causes deformation of previously accumulated sediments and development of inclined and even vertically oriented cryostructures.

In contrast to epigenetic permafrost, in which ice wedges rarely exceed 10-15 ft (4-5 m) in depth, ice wedges in syngenetic permafrost may extend through the entire strata, reaching 30-140 ft (10-50 m) in depth and 6-17 ft (2-6 m) in width. Their varying width and depth reflect the varying rates of sedimentation and climate conditions. In syngenetic permafrost, wedge-ice can occupy 20-50% (and even more in some cases) of the total section.

Wedge-ice has foliated structure and numerous air bubbles (**Figure 3.2**). Vertical foliation of ice is formed by particles of silt and organic matter, which penetrate inside the ice body with the water coming through the frost (contraction) cracks in the spring time. Wedge-ice is usually grey to yellow in color, depending on the color of soil particles.





**Figure 3.2.** Appearance of wedge-ice, sample obtained by coring (Dalton Highway innovation project area, Interior Alaska).

The main cryostructure of syngenetic permafrost is micro-lenticular (Shur et al. 2004, Kanevskiy 1991, 2003, Kanevskiy et al. 2008). The term “lenticular” is used in several existing classifications of cryostructures (e.g. Zhestkova 1982, Popov et al. 1985, Murton & French 1994, Melnikov & Spesivtsev 2000, French 2007). The term “micro-lenticular” generally means the occurrence of very small sub-horizontal (sometimes wavy), relatively short ice lenses. The thickness of uniformly distributed ice lenses (and spacings between them as well) usually does not exceed 0.5 mm. Inexperienced observers often do not pay enough attention to recognition of numerous but tiny ice inclusions and describe soil with such a cryostructure as without visible ice.

Our studies in Russia and Alaska show several varieties of micro-lenticular cryostructure, which very often have similar appearance (because of small size of ice lenses) but after thorough examination significant differences can be found. Very often instead of short separate lenses we can see rather long wavy intercrossing ice layers with lens-like thickenings (i.e. such cryostructure has braided appearance). Sometimes we can notice tiny elongated mineral blocks suspended in the ice.



Thus, we can distinguish the following sequence of close-related cryostructures (ranked approximately in the order of the ice content increase): latent micro-lenticular — micro-porphyrritic (porous visible) — micro-lenticular — micro-layered lenticular — micro-layered — micro-braided lenticular — micro-braided — micro-ataxitic (suspended). In many sections, these cryostructures can easily transform into each other.

**Figure 3.3** shows generalized images of these varieties of micro-lenticular cryostructure. It should be mentioned, that very small size of ice inclusions, especially for latent micro-lenticular and micro-porphyrritic cryostructures, makes it difficult to distinguish the occurrence of ice lenses. In the cores, ice lenses often reveal themselves only when the core is partly melted. That explains why such cryostructures are often distinguished as porous invisible (or structureless, according to Murton & French 1994).

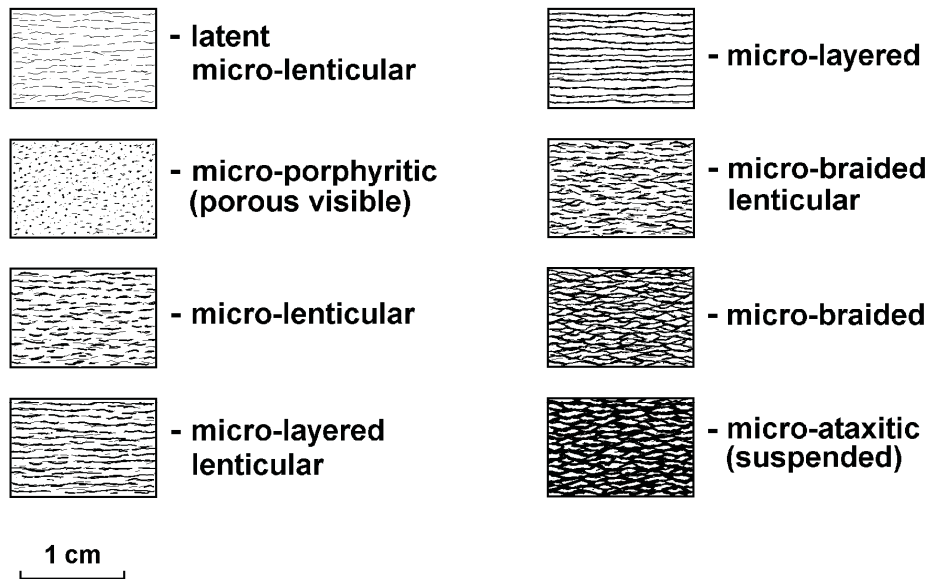


**Figure 3.3.** Main cryostructures of syngenetic permafrost.

Micro-lenticular cryostructure (including all its varieties) is the most typical for syngenetic permafrost and usually it forms not less than 60% of the entire thickness of such sections (Kanevskiy 1991, 2003). Ice content of the sediments with micro-lenticular cryostructure can be very high, despite the small size of the ice lenses. Gravimetric moisture content for such sediments varies from 40-50% (for latent micro-lenticular and micro-porphyrritic cryostructures) up to 200% and even more (for micro-ataxitic cryostructure).

The other feature typical for syngenetic permafrost is the occurrence of distinct layers of ice from several millimeters up to several centimeters thick (ice ‘belts’ in the Russian permafrost literature). Belts usually divide more or less uniform layers with different varieties of micro-lenticular cryostructure (**Figure 3.1B**). Photographs of cryostructures typical for syngenetic permafrost are shown in **Figures 3.4-3.8**.



**Figure 3.4.** Micro-porphyrific cryostructure of syngenetic permafrost (Northern Alaska).





**Figure 3.5.** Micro-lenticular and latent micro-lenticular cryostructures of syngenetic permafrost, depth 46 ft (14 m), label is 1.25x1.25 cm (CRREL Permafrost tunnel, Fox, Interior Alaska).





**Figure 3.6.** Micro-braided cryostructure of syngenetic permafrost (Dalton Highway innovation project area, Interior Alaska).





**Figure 3.7.** Micro-ataxitic and micro-braided cryostructures of syngenetic permafrost (Dalton Highway innovation project area, Interior Alaska).





**Figure 3.8.** Belt-like cryostructure (combined with micro-braided cryostructure) of syngenetic permafrost (Dalton Highway innovation project area, Interior Alaska).



Ice-rich syngenetic permafrost with large ice wedges can be easily recognized in natural (thermoerosional gullies, banks of rivers, lakes, and seas) or artificial (quarries, mines, road cuts) exposures (**Fig. 3.9**). It is not so easy to distinguish this type of permafrost if the only kind of available data are the results of drilling. For example, massive ice bodies encountered by drilling at different depths can be interpreted either as layers of tabular massive ice (**Fig. 3.10A**) or as syngenetic ice wedges (**Fig. 3.10B**). That is why the knowledge of permafrost nature and ground ice origin is so important.



**Figure 3.9.** Exposure of the late Pleistocene syngenetic permafrost (Northern Alaska).

Wedge-ice in the core can be recognized by its color (usually yellow, grey or brown), vertical foliation, and abundant air bubbles, usually evenly distributed (**Fig. 3.2**). Sometimes it is not easy because the ice core is often destroyed by drilling. In some cases ice wedges are formed by very clean water and no vertical foliation can be observed. At the same time most of late Pleistocene wedges contain a lot of mineral particles or organic matter distributed vertically. Study of samples of frozen soil obtained by coring also can help to distinguish syngenetic permafrost. The main diagnostic features are the following:

- Prevalence of micro-lenticular cryostructure and its varieties (**Fig. 3.3**);
- Portions with uniform cryostructures are rhythmically-organized and often divided by ice ‘belts’ (**Fig. 3.11**);
- Inclination of ice lenses, which commonly increases near the boundaries of ice wedges (**Fig. 3.11**);
- Occurrence of almost undecomposed rootlets;
- Occurrence of buried peat horizons.

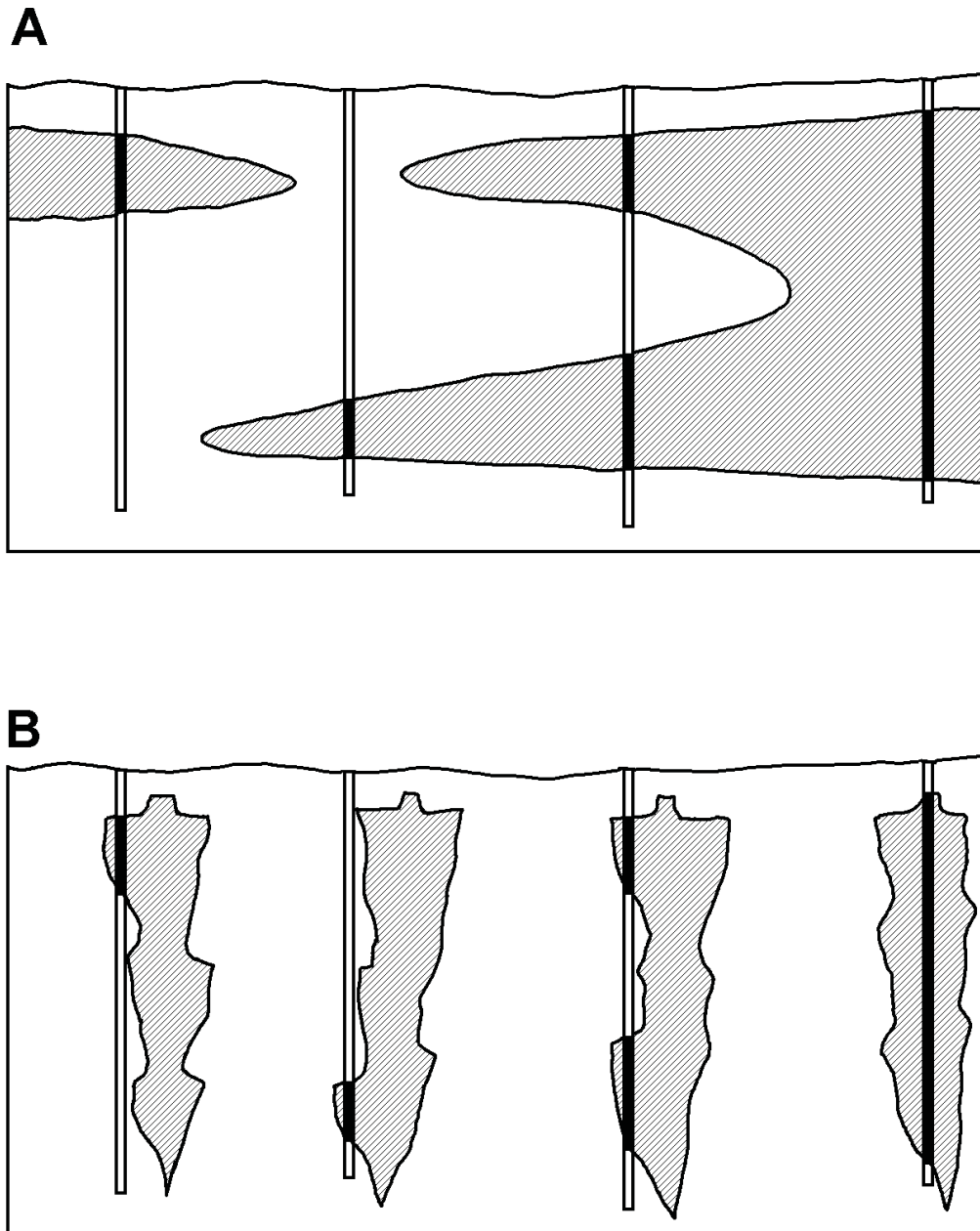


**Figure 3.10.** Possible interpretations of massive ice bodies encountered by drilling at different depths. A – tabular massive ice; B – syngenetic ice wedges.



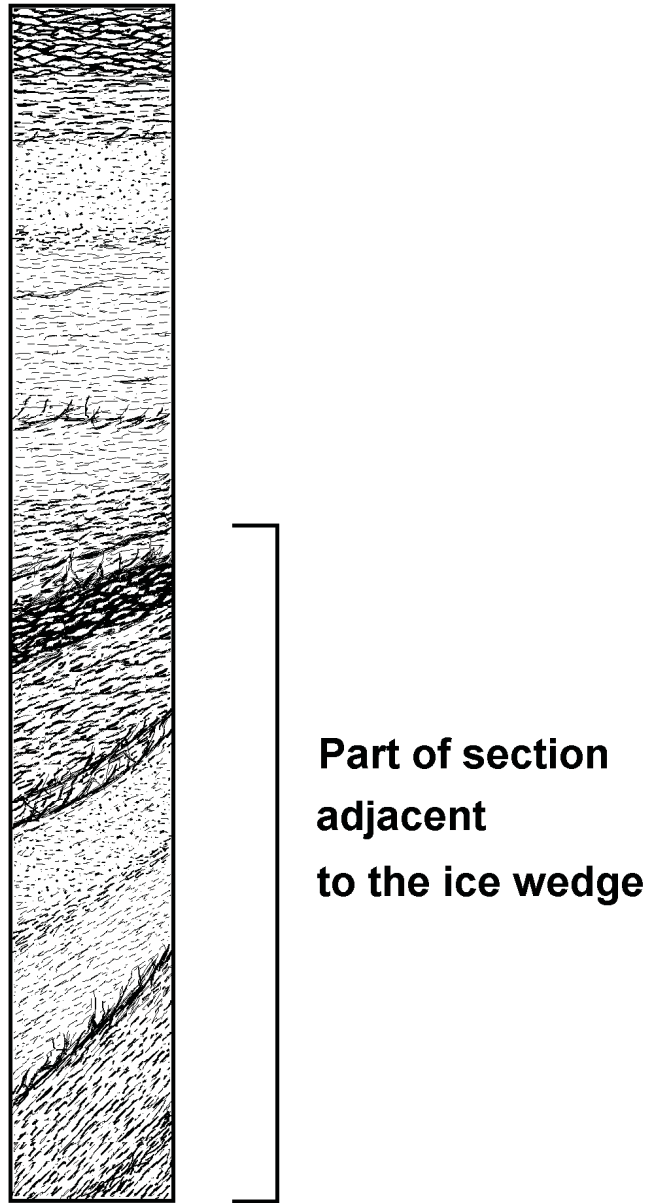


**Figure 3.11.** Typical sequence of syngenetic permafrost in the core, ice is black (idealized image, not to scale).

Properties of the upper part of permafrost are especially important because permafrost behaviour (and first of all the development of thermokarst, thermal erosion and other hazardous processes) strongly depends on properties of the near-surface permafrost. The concept of transition zone (Shur et al. 2005) helps to describe the interactions between the active layer and the permafrost. The upper part of the transition zone is known as the transient layer that is typically a part of the uppermost permafrost but which, under certain conditions, occasionally joins the active layer (Yanovskiy 1933). During most warm years, the transient layer protects the underlying ice-rich soils from thaw. The relative thickness of the transient layer varies widely depending on climate and soil, and in some cases can exceed 30% of the active-layer thickness (Shur et al. 2005).

The lower part of the transition zone is formed by the ice-rich intermediate layer (Shur 1988a, 1988b), whose structure and properties have provided stability of the late Pleistocene permafrost during last 10,000 years in climate much warmer than during its formation. Intermediate layer forms as a result of gradual decrease of the active layer thickness after termination of sedimentation (Shur 1988). Decrease of the active layer thickness can be connected with succession of vegetation, changes of surface conditions, and various local factors. As a result, significant part of the active layer transforms into perennially frozen state due to freezing from below. Along with this process the surface rises gradually as a result of ice formation in the freezing layer. This process resembles syngenetic permafrost formation but without continuing sedimentation on the surface.

Intermediate layer is extremely ice-rich; it is characterized by thick up to 0.5 ft (10-15 cm) ice 'belts' and specific cryostructures (ataxitic and reticulate mostly) with relatively thick (up to 1-2 cm) ice lenses. In the conditions of relatively warm permafrost (including the climatic conditions of the Interior Alaska) however, micro-braided and micro-ataxitic cryostructures are more typical for the intermediate layer. Intermediate layer is widespread in different permafrost regions; its thickness of usually varies from 2 to 5 ft (0.5 to 1.5 m).

Intermediate layer divides the transient layer from the original permafrost and prevents massive ice from thawing. This protective role of the intermediate layer is especially important for conservation of the ice-rich syngenetic permafrost with large ice wedges (Shur 1988a). Besides contemporary intermediate layer, buried intermediate layers very often occur at various depths in the sections of syngenetic permafrost as lenses and layers of extremely ice-rich soil with the thickness of up to 6-10 ft (2-3 m) (Kanevskiy 1991, 2003). These layers usually correspond to the periods of termination or slowdown of sedimentation, which are often related to changes of surface conditions. In many cases such layers can be found beneath organic-rich horizons (buried soils); frequently they overlay buried ice wedges.

The general sketch of the soil sequence common for the ice-rich syngenetic permafrost illustrating the structure of upper permafrost (including transient and intermediate layers) and typical distribution of wedge-ice and segregated ice is shown in **Figure 3.12**.

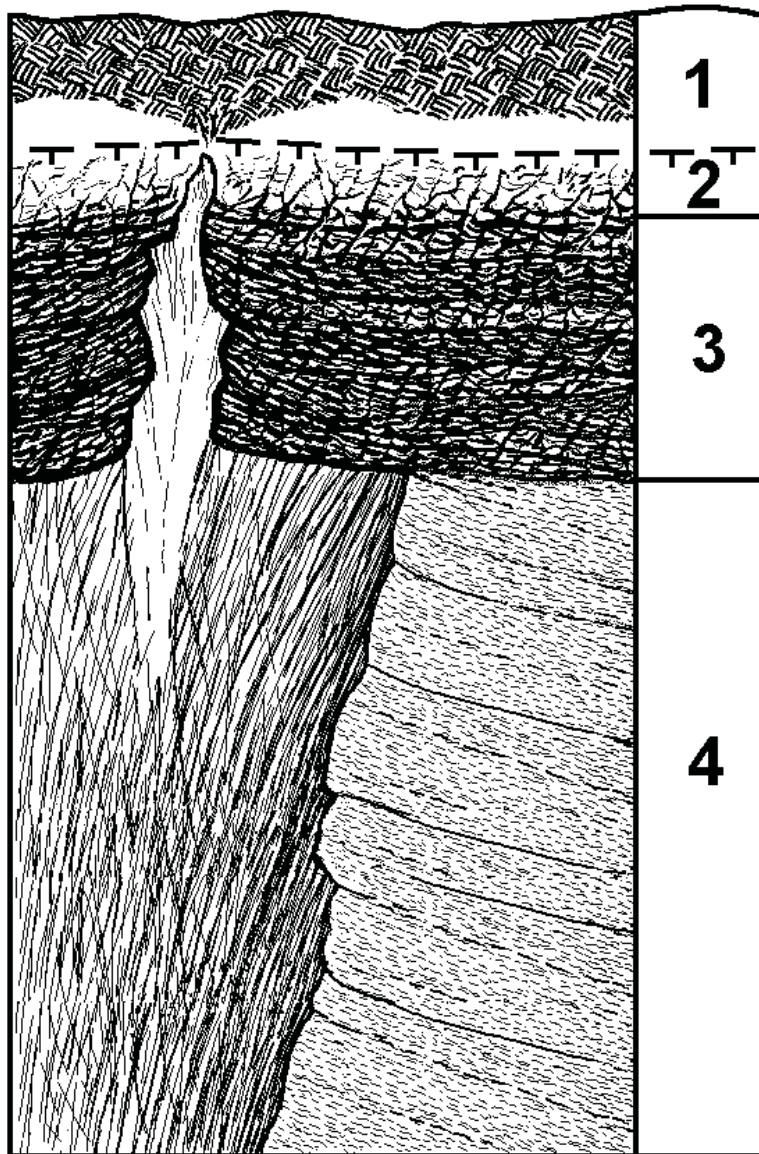


**Figure 3.12.** Typical sequence of the upper part of the ice-rich syngenetic permafrost. 1 – Active layer; 2 – Transient layer; 3 – Intermediate layer with thin contemporary ice wedge; prevailing cryostructures – ataxitic and reticulate; 4 – Late Pleistocene syngenetic permafrost with big buried ice wedge; prevailing cryostructure – micro-lenticular.

In Alaska, ice-rich syngenetic permafrost with deep and thick ice wedges occurs in the Interior, at the Seward Peninsula, and in some areas of the Arctic Foothills. In the Interior Alaska, ice-rich sediments, which we can interpret as late Pleistocene syngenetic permafrost, have been observed in numerous sites (Wilkerson 1932, Tuck 1940, Williams 1962, Péwé 1975, Black 1978, Hamilton 1979, Kreig & Reger 1982, Brown & Kreig 1983, Porter 1986, Porter 1988, Matheus et al. 2003, Meyer 2008). Cryogenic structure of these sediments have been studied extensively in the well-known CRREL permafrost tunnel in Fox, located near Fairbanks (Sellmann 1967, Hamilton et al. 1988, Shur et al. 2004, Bray et al. 2006, Fortier et al. 2008, Kanevskiy et al. 2008).

## 4. Previous permafrost investigations in the area

In the study area, soil is expected to be ice-rich eolian and colluvial silt, whose accumulation took place in the periglacial environment during the Late Pleistocene. At this period, very cold climate was favorable for formation of syngenetic permafrost. During investigations for the Trans-Alaska Pipeline, the ice wedges occurring in the boreholes were often interpreted as continuous buried ice. Large ice wedges were exposed during construction of the pipeline haul road (**Figure 4.1**). In the study area, according to available information, continuous ice wedges can reach 65 ft (20 m) and more in depth. Lotspeich (1971) described the road cuts construction in the ice-rich silts on the Livengood-Yukon section of the haul road and suggested procedures for minimizing the environmental impact of the ground ice thawing. Smith & Berg (1973) described ice-rich soils with massive ice in the eight relatively deep cuts located from 31 to 39 km (19 to 24 miles) of the haul road (Dalton Highway); the authors presented the results of observations on stabilization of slopes of these cuts.



**Figure 4.1.** Ice wedge exposed during construction of the pipeline haul road near Hess Creek (Andersland & Anderson 1978).



Locations of boreholes drilled by Alyeska Pipeline Service Company in 1970 (Kreig & Reger 1982) are shown in **Figures 4.2, 4.3**. Boreholes *e, f, g, h*, and line **A-A'** are located mostly along the proposed alignment (**Figure 4.3**). Sections of the most part of these boreholes show the presence of massive ice (**Figures 4.4, 4.5**). The deepest boreholes revealed more than 18 m of the ice-rich silt (see **Figure 4.4**). Massive ice shown in these figures we interpret as a wedge ice. Our experience shows that during the drilling in the areas with the ice-rich syngenetic permafrost, wedge ice can be found at any depth. It can be related to (1) occurrence of wedges buried at different depths; (2) step-like contact of ice wedges with adjacent sediments; (3) variability of the wedges' thickness with depth; (4) inclination of wedges. Thus we can presume the wedges penetration through the entire silt strata.

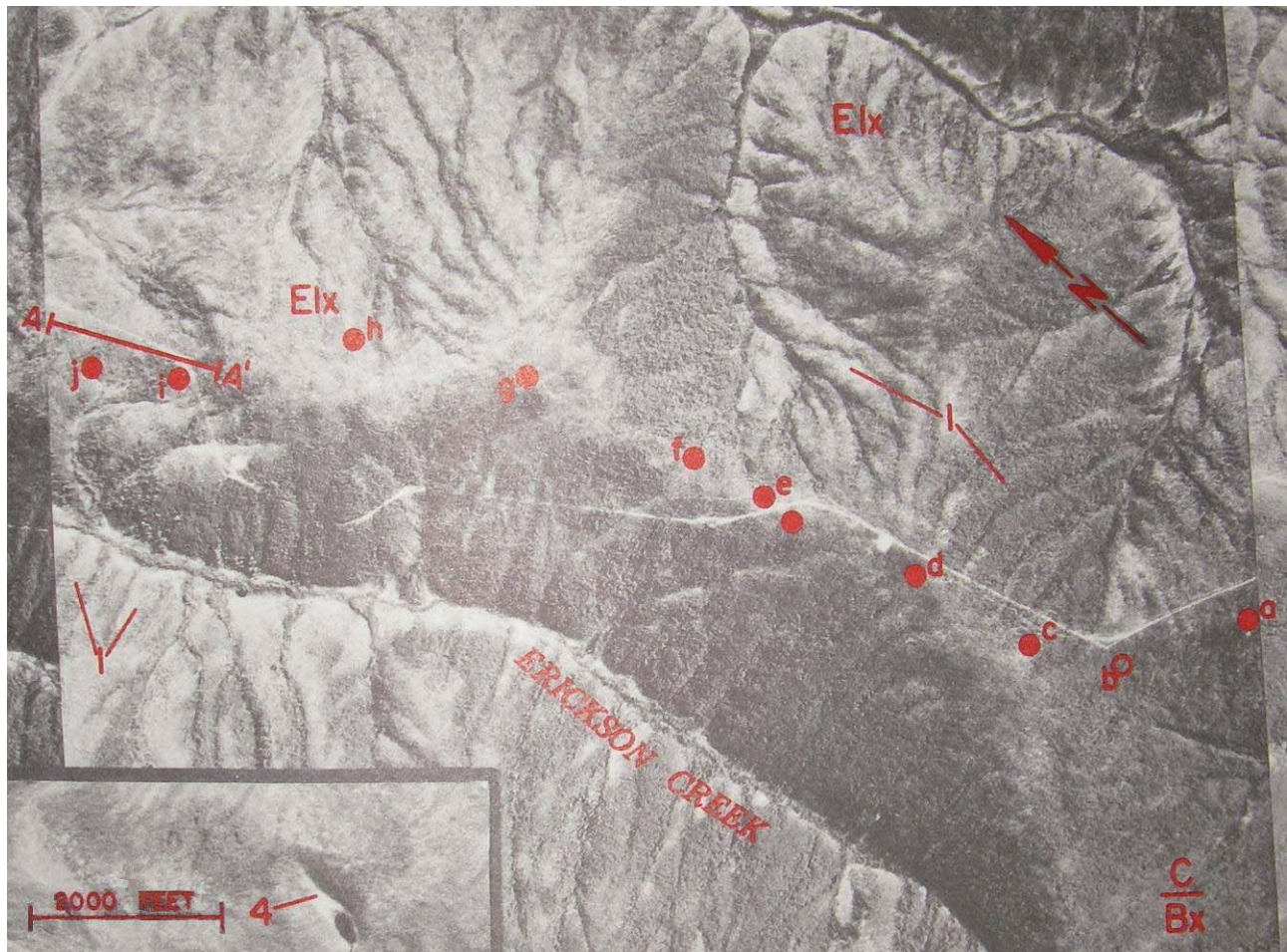


**Figure 4.2.** Location of boreholes drilled by Alyeska Pipeline Service Company in 1970 projected on the aerial photograph, Alyeska Pipeline Service Company, August 10, 1969 (Kreig & Reger 1982).

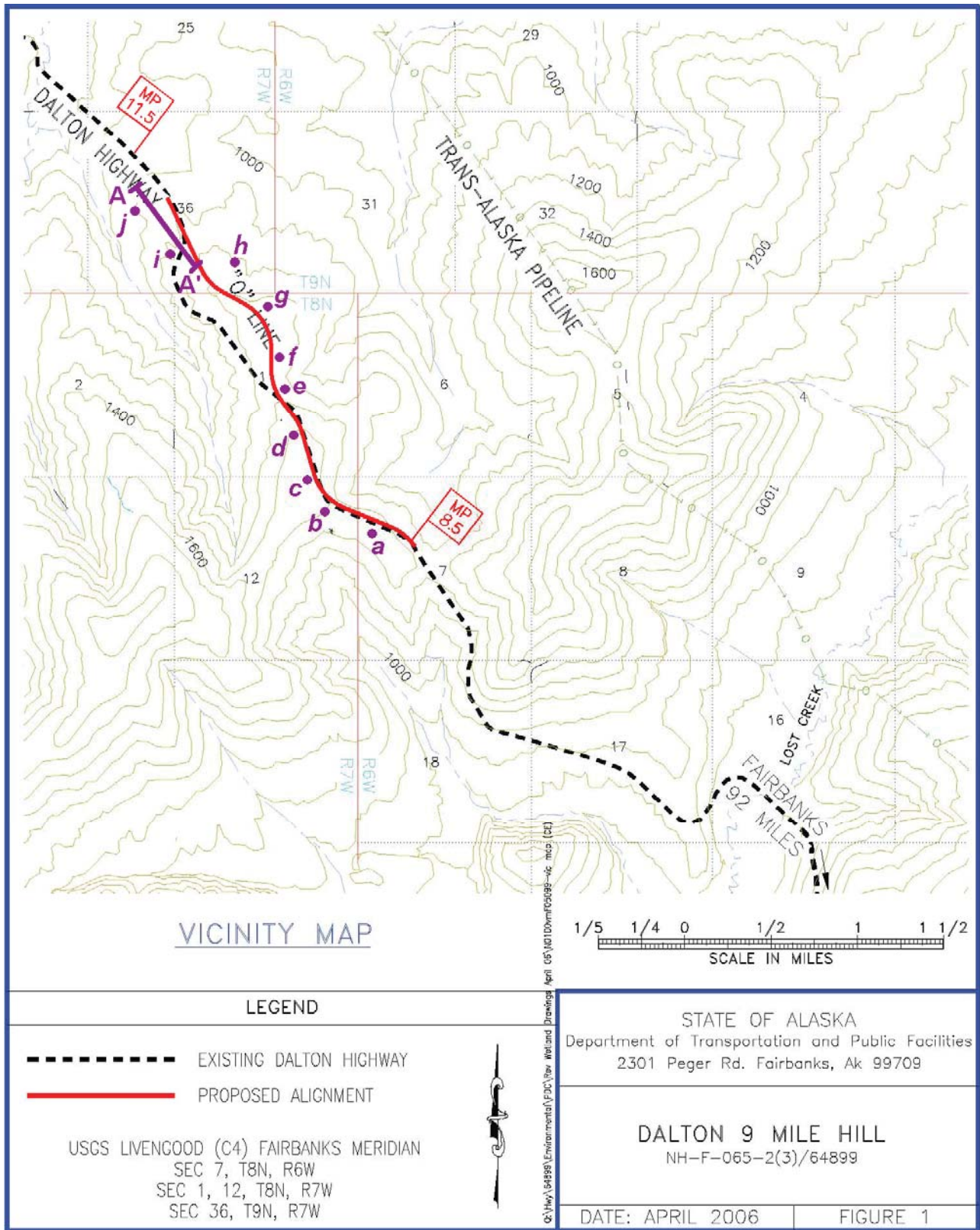


**Figure 4.3.** Location of boreholes drilled by Alyeska Pipeline Service Company in 1970 (Kreig & Reger 1982) projected on AKDOT&PF map.



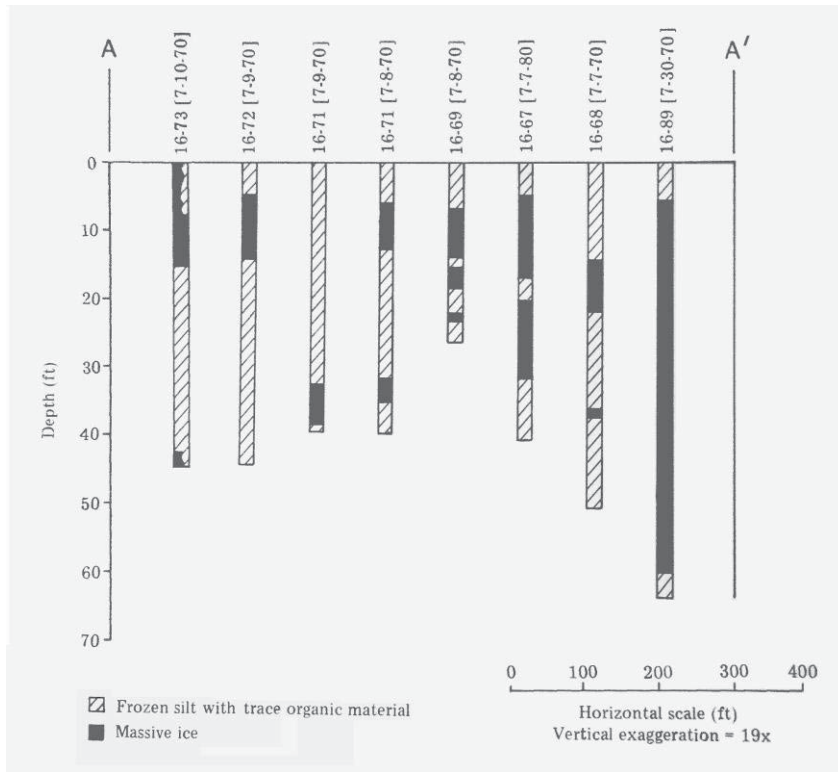


**Figure 4.4.** Occurrence of massive ice in the boreholes located along the line A-A' (Kreig & Reger 1982). Location of the boreholes is shown in **Figures 4.2, 4.3**.

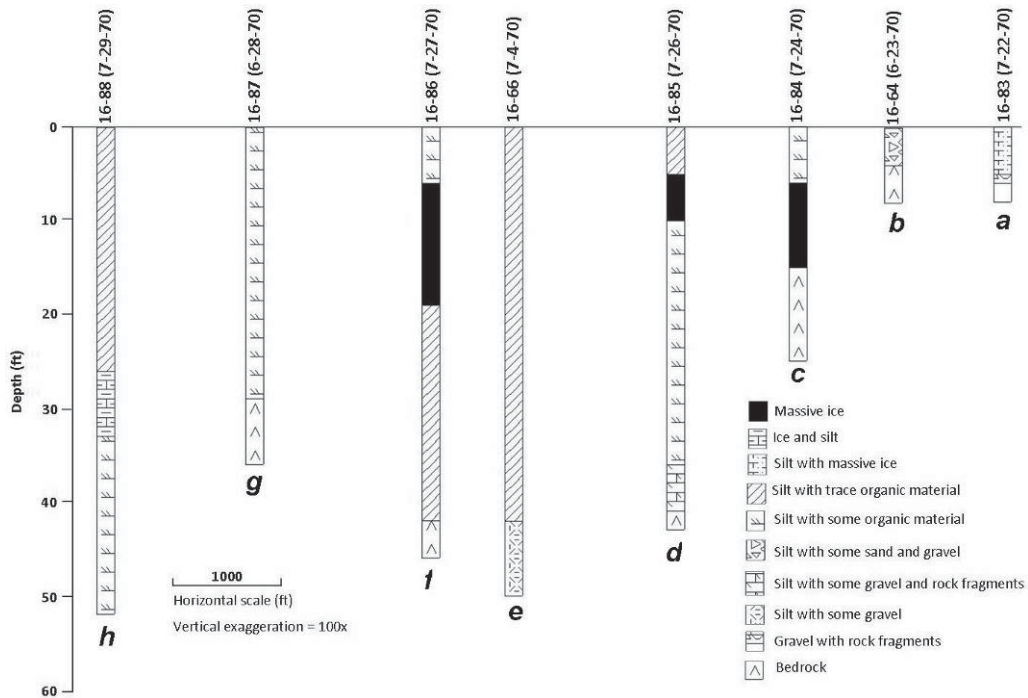


**Figure 4.5.** Occurrence of massive ice in the boreholes from **a** to **h** (based on the data from Kreig & Reger 1982). Location of the boreholes is shown in **Figures 4.2, 4.3**.

The ice-rich syngenetic permafrost of the Alaska Interior is a relic and it can survive in the contemporary climate only if it is protected by thick layer of moss and peat. Even though, permafrost is degrading in the area and its temperature is at the melting point (**Figure 4.6**). Contemporary degradation occurs mainly from the permafrost bottom. Stripping of vegetation will lead to permafrost degradation from the top too.

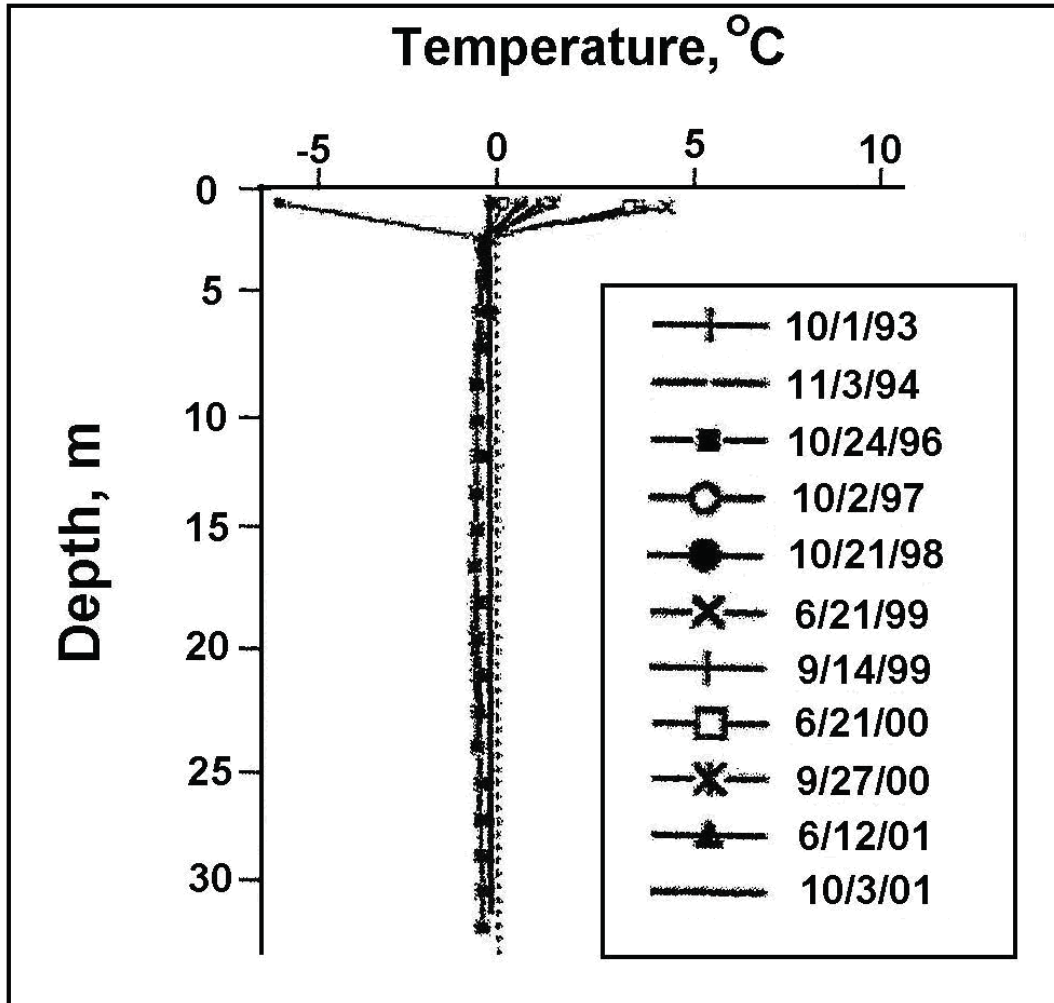


**Figure 4.6.** Temperature distribution (from Tart, 2003).

In 1990 and 1991, AKDOT&PF investigated geotechnical conditions in the area to find a safer alignment between MP 8 and MP 12. In 1990, 45 test holes were drilled, and additional 29 test holes were drilled in 1991. It was found that permafrost is continuous throughout projected area, a thickness of massive ice varies from a few feet to dozens of feet; high natural moisture and high content of organic matter were reported. In 2004, seismic survey was performed (Geotechnical report 2006).



## 5. AUTC and AKDOT investigations in 2008

### 5.1. Location, topography, geology, and permafrost features

The project area is located approximately 10 miles east of Livengood and about 80 miles north of Fairbanks. The Trans-Alaska Pipeline parallels the Dalton Highway and is located about 1.5 miles to the east of the project location.

The study area belongs to the Yukon-Tanana Upland formed by generally rolling low mountains (Wahrhaftig 1965). The proposed alignment is within the low mountain ridge dividing the Erickson Creek and the Lost Creek watersheds. The three mile (4.5 km) long alignment is sloping gently to the north-west from approximately 1300 to 900 ft (450 to 300 m) above the sea level. The study area is drained by the Yukon River.

Bedrock in the study area is represented mostly by highly deformed weathered sedimentary rocks. Main stratigraphic units in the study area are Livengood Dome Chert (Ordovician) and Wickersham unit (Earliest Cambrian and Late Proterozoic) presented by argillite, phillite, and quartzite (Weber et al. 1997). Bedrock is overlain by silt (loess) and muck cover 1.5–70-ft-thick (0.5-25-m). At the base of silt section, colluvial and fluvial gravelly soils occur.

The study area is located within the discontinuous permafrost zone (Pewe 1975, Jorgenson et al. 2008). Permafrost temperature is close to the melting point (Tart 2003). Active layer thickness varies mostly from 1.5 to 3 ft (0.5 to 1 m). Main permafrost related processes in the area are thermokarst and creep. Change in the relief and surface water patterns can trigger thermal erosion. There is no contemporary growth of ice wedges in the area. Potential wedge-ice development in the Interior Alaska can be expected only in organic soils, usually at the flat surface with limited drainage, mostly in peat bogs (Hamilton et al. 1983). All ice wedges in the project area were formed in the late Pleistocene during the syngenetic permafrost formation.

Thermokarst features in the areas with large late Pleistocene ice wedges usually are characterized by deep troughs above melting ice wedges, small thaw ponds at the crossings of ice wedges and so called thermokarst mounds (baidzharakhs) surrounded by troughs. A local relief (difference between a bottom of a pond and a top of a mound) reaches up to 9 ft (3 m). In the area adjacent to the proposed alignment, well developed thermokarst relief was not observed (except man-triggered features). Despite the recent forest fire, which could trigger permafrost thawing, thermokarst in the project area is limited by shallow irregular thermokarst scars; thaw settlement does not exceed 1.5 to 3 ft (0.5 to 1 m). We could not find any distinct thermokarst troughs above melting ice wedges using both the high-resolution aerial photograph (**Fig. 5.1**) and our surface observations (**Fig. 5.2**). We relate it to (1) good drainage conditions due to rugged topography, and (2) thick protective layer of moss, peat and relatively ice-poor frozen soil above ice wedges. Numerous gullies can be observed in the study area (**Fig. 5.1**), but most of them do not show any evidences of the active contemporary thermal erosion.



**Figure 5.1.** Aerial photograph of the project area.





**Figure 5.2.** Burned black spruce forest in the project area.

## 5.2. Borehole logging

Soil description, its cryogenic structure (patterns of ice inclusions in frozen soil), moisture contents, and photographs of core with typical cryostructures for eight hollow stem boreholes (AUTC08-2 – AUTC08-9) are shown in **Figures 5.3-5.82**. Generalized images of different types of cryostructures are shown in **Figures 2.2, 3.3**. Example of DOT drilling log (for one of 54 DOT test holes) is shown in **Figure 5.83**. Location of boreholes is shown in **Figures 1.1, 5.88, and 5.96**.

**Borehole # AUTC08-2 (Figures 5.3-5.13).** May 13, 2008.

Latitude N 65°33'4"; Longitude W 148°53'47".

General description: burned black spruce forest (Erickson Creek fire 2003); low severity burn, patchy burned and unburned moss; organic mat thickness ranging from 10-20 cm; ~ 70% standing dead; ~ 30% down woody debris, shallow thermokarst depressions.

Vascular Plant Species: *Ledum palustre*, *Vaccinium vitis-idaea*.

Moss Species: *Pleurozium schreberi*, *Hylocomium splendens*, *Ceratodon purpureus*.

- 0.00-0.22 m Dark-brown peat. Cryostructure: organic-matrix porphyritic.
- 0.22-1.27 m Yellow-grey silt with very fine sand, slightly oxidized, with small inclusions of organic matter (rootlets). Cryostructure: micro-lenticular, ice lenses up to 0.02-cm-thick, spacings up to 0.5-cm-thick. From 0.35 m – the same soil, dense, homogeneous, no visible ice. Cryostructure: porous invisible. Position of the permafrost table is not clear (presumably 1 m).
- 1.27-1.56 m The same soil. Cryostructures: combination of porous invisible, porous visible (micro-porphyritic), and vein (ice lenses up to 0.05-cm-thick).
- 1.56-8.95 m Dark grey and yellow-grey dense silt. From appr. 3.0 m – more inclusions of organic matter (black and brown). Cryostructure: mostly porous invisible. Between 4.4 m and 6.2 m – several small increments with micro-lenticular cryostructure (ice-poor). Gravimetric moisture content 23-52%. Presumably thawed and refrozen sediments.
- 8.95-11.84 m The same soil. Cryostructures: combination of latent micro-lenticular (prevails in the section), porous visible (micro-porphyritic), vein, porous invisible, and micro-lenticular (ice lenses up to 0.05-cm-thick); several ice lenses up to 0.2-cm-thick (at 10.2-10.3 m, 11.0-11.1 m); at 11.2-11.5 m – several ice veins up to 0.2-cm-thick. Gravimetric moisture content 40-116%.



Depth		Ground ice	Moisture content, %		Thaw strain %	Description of soil
ft	m		grav.	vol.		
						0.00-0.22 m Dark-brown peat. Cryostructure: organic-matrix porphyritic.
1.0						0.22-0.35 m Yellow-grey silt with very fine sand, slightly oxidized, with small inclusions of organic matter (rootlets). Cryostructure: micro-lenticular, ice lenses up to 0.02-cm-thick, spacings up to 0.5-cm-thick.
	0.5		31	48		
2.0						0.35-1.27 m Yellow-grey silt with very fine sand, slightly oxidized, with small inclusions of organic matter, dense, homogeneous, no visible ice. Cryostructure: porous invisible. Position of the permafrost table is not clear (presumably 1 m).
	2.0		28	45		
3.0		1.0				Grain size, depth 0.9 m: sand 0.6%, silt 81.4%, clay 18%.
	3.0	?				
4.0			39	55		1.27-1.56 m The same soil. Cryostructures: porous invisible, porous visible (micro-porphyritic), and vein (ice lenses up to 0.05-cm). Presumably thawed and refrozen sediments.
	4.0					
5.0			49	65		1.56-3.50 m Dark grey and yellow-grey dense silt, with rare small inclusions of organic matter. Cryostructure: mostly porous invisible. Presumably thawed and refrozen sediments.
	5.0					
6.0						Grain size, depth 2.9 m: sand 2.5%, silt 81.1%, clay 16.4%.
	6.0		23	40		
7.0						2.25-2.95 m No data
	7.0					
8.0		2.5				
	8.0	no data				
9.0						
	9.0		46	65		2.95-3.50 m Dark grey and yellow-grey dense silt. From appr. 3.0 m – more inclusions of organic matter (black and brown). Cryostructure: mostly porous invisible, from 3.25 to 3.45 m – micro-porphyritic. Presumably thawed and refrozen sediments.
10.0						
	10.0	3.0				
11.0			47	65		
	11.0					

**Figure 5.3.** Cryogenic structure (ice is black) and properties of frozen soil, borehole AUTC-2, depth 0-11.5 ft (0-3.5 m).

Depth		Ground ice	Moisture content, %		Thaw strain, %	Description of soil
ft	m		grav.	vol.		
12.0						3.50-4.40 m Dark grey and yellow-grey dense silt, with inclusions of organic matter (black and brown). Cryostructure: mostly porous invisible. Presumably thawed and refrozen sediments.
			46	60		
13.0	4.0					
14.0			41	62		
15.0	4.5		42	60		4.40-6.20 m Dark grey and yellow-grey dense silt, with inclusions of organic matter (black and brown). Cryostructure: mostly porous invisible with several small increments with micro-lenticular cryostructure (ice-poor). Presumably thawed and refrozen sediments.
16.0	5.0		47	64		
17.0			43	59		Grain size, depth 5.3 m: sand 2.3%, silt 78.8%, clay 18.9%.
18.0	5.5		43	59		
19.0						
20.0	6.0		52			
21.0	6.5		42	61		6.20-7.00 m Dark grey and yellow-grey dense silt, with inclusions of organic matter (black and brown). Cryostructure: porous invisible. Presumably thawed and refrozen sediments.
22.0			42	61		

**Figure 5.4.** Cryogenic structure (ice is black) and properties of frozen soil, borehole AUTC-2, depth 11.5-23 ft (3.5-7 m).

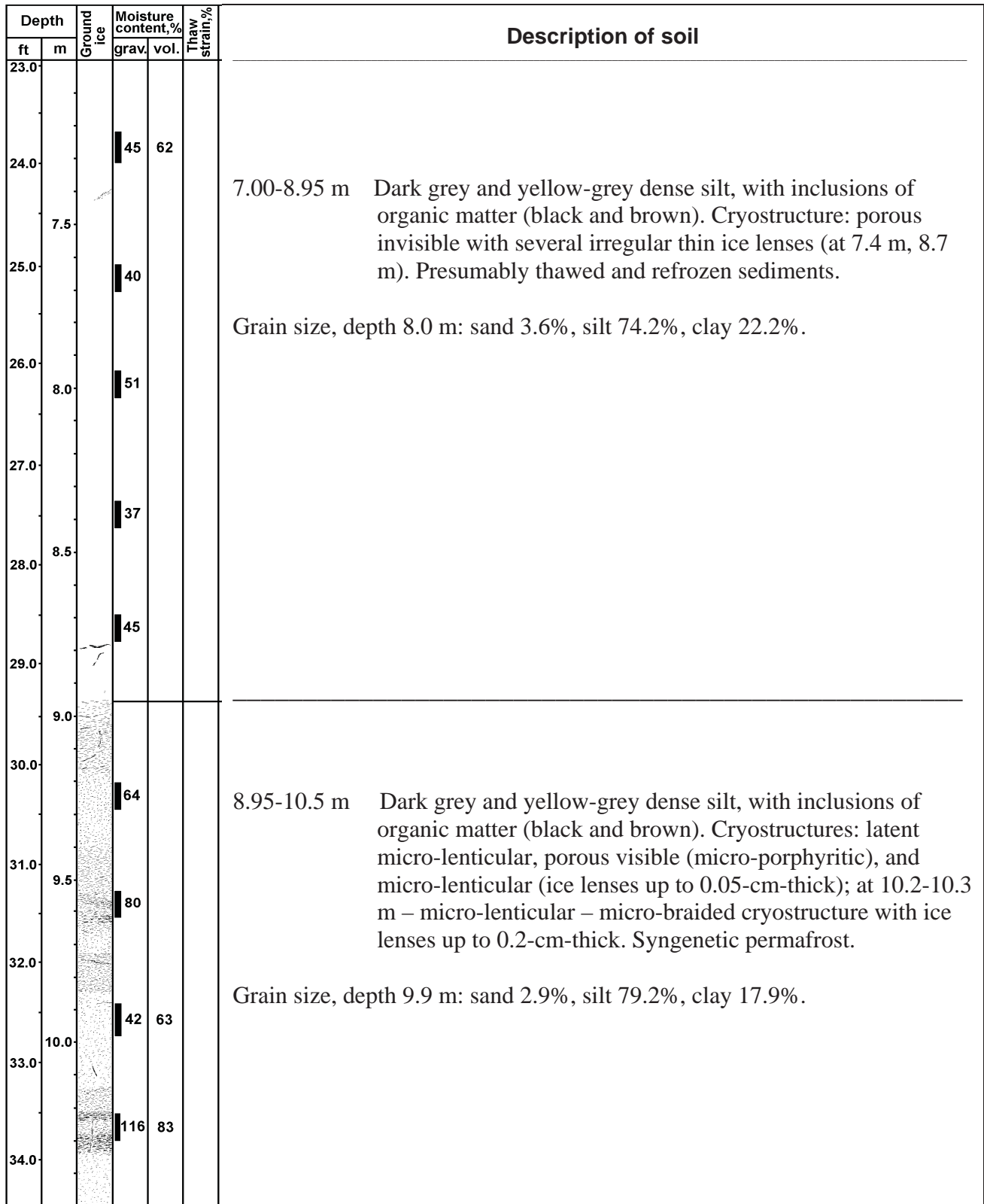


**Figure 5.5.** Cryogenic structure (ice is black) and properties of frozen soil, borehole AUTC-2, depth 23-34.5 ft (7-10.5 m).



Depth		Ground ice	Moisture content, %		Thaw strain, %	Description of soil
ft	m		grav.	vol.		
35.0			44	61		<p>10.5-11.84 m Dark grey and yellow-grey dense silt, with inclusions of organic matter (black and brown). Cryostructures: latent micro-lenticular, porous visible (micro-porphyratic), micro-braided, vein, porous invisible, and micro-lenticular (ice lenses up to 0.05-cm-thick); at 11.0-11.1 m – several ice lenses up to 0.2-cm-thick; at 11.2-11.5 m – several ice veins up to 0.2-cm-thick. Syngenetic permafrost.</p> <p>Grain size, depth 11.65 m: sand 10.2%, silt 74.5%, clay 15.3%.</p>
36.0	11.0		81	77		
37.0			73	74		
38.0	11.5		40	62		

**Figure 5.6.** Cryogenic structure (ice is black) and properties of frozen soil, borehole AUTC-2, depth 34.5-39 ft (10.5-11.84 m).

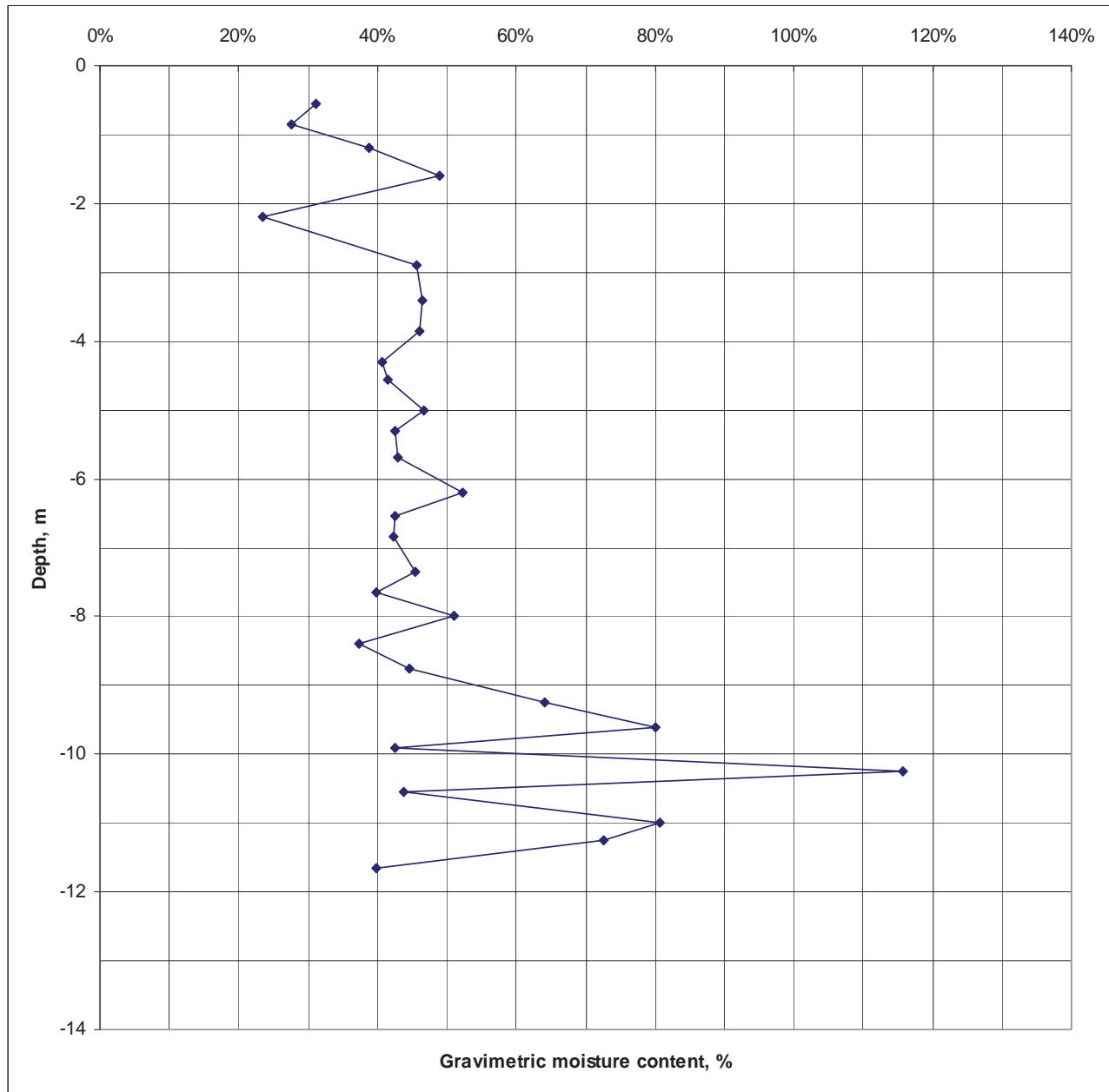


**Figure 5.7.** Gravimetric moisture content of frozen soil, borehole AUTC-2. Up to 9 m – thawed and refrozen sediments. From 9 m – syngenetic permafrost.



**Figure 5.8.** Silt with porous cryostructure (no visible ice), borehole AUTC-2, depth 2.80-2.94 m, gravimetric moisture content 46%.





**Figure 5.9.** Silt with porous cryostructure (no visible ice), borehole AUTC-2, depth 7.20-7.44 m, gravimetric moisture content 45%.





**Figure 5.10.** Silt with porous cryostructure (no visible ice), borehole AUTC-2, depth 8.60-8.73 m, gravimetric moisture content 45%.





**Figure 5.11.** Silt with micro-porphyrific cryostructure, borehole AUTC-2, depth 9.2-9.3 m, gravimetric moisture content 64%.





**Figure 5.12.** Silt with micro-lenticular – micro-braided cryostructure, borehole AUTC-2, depth 10.95-11.05 m, gravimetric moisture content 81%.





**Figure 5.13.** Silt with small ice vein, typical of syngenetic permafrost, borehole AUTC-2, depth 11.43-11.55 m.

**Borehole # AUTC08-3 (Figures 5.14-5.21).** May 13, 2008.

Latitude N 65°33' 10"; Longitude W 148°53' 50".

General description: burned black spruce forest (Erickson Creek 2003); low severity burn, patchy burned and unburned moss; organic mat thickness ranging from 10-20 cm; ~ 70% standing dead; ~ 30% down woody debris. Random thermokarst depressions up to 0.8-m-deep, up to 3 m in diameter, no visible polygons.

Vascular Plant Species: *Ledum palustre*.

Moss Species: dead *Pleurozium schreberi*, dead *Hylocomium splendens*, *Ceratodon purpureus*.

Organic horizon characteristics:

0-1 cm: live *Hylocomium* and *Ceratodon*

1-4 cm: dead *Hylocomium* and charred organic matter

4-10 cm: fibric organic matter; dense root matrix; some recognizable plant parts; no amorphous

10+ cm: frozen

- 0.00-0.19 m Dark-brown peat. Cryostructure: organic-matrix porphyritic, ice inclusions up to 0.4-cm-thick.
- 0.19-0.72 m Yellow-grey silt, up to 0.39 m – strongly oxidized, with numerous inclusions of organic matter (rootlets, thin peat layers). Cryostructures: micro-lenticular to micro-braided, ice lenses up to 0.03-cm-thick; from 0.30 m – latent micro-lenticular; from 0.39 m – porous invisible, from 0.60 m – the soil is very dry (gravimetric moisture content – 27%). Permafrost table – 0.72 m.
- 0.72-0.95 m The same soil, extremely ice-rich. Cryostructures: micro-ataxitic, micro-braided, ice lenses up to 0.3-cm-thick. Gravimetric moisture content: 145-180%. Presumably contemporary intermediate layer.
- 0.95-1.62 m The same soil, from 1.30 m – brown-grey silt with organic material (15%). Cryostructures: micro-lenticular, micro-braided, ice lenses up to 0.15-cm-thick. Gravimetric moisture content: 58-92%. Presumably syngenetic permafrost.
- 1.62-1.80 m Brown-grey silt with organic material (40-50%). Cryostructure: reticulate incomplete, ice lenses up to 0.05-cm-thick. Presumably thawed and refrozen sediments.
- 1.80-4.80 m Wedge-ice. Vertical foliation, air bubbles.
- 4.80-5.25 m Ice-rich breccia. Presumably contact with ice wedge.
- 5.25-5.76 m Grey silt with inclusions of organic material. Cryostructures: ataxitic, from 5.40 m – transitional to micro-ataxitic, ice lenses up to 0.8-cm-thick. From 5.60 – micro-ataxitic, micro-braided. Gravimetric moisture content: 117-233%. Presumably buried intermediate layer.
- 5.76-6.11 m The same soil. Cryostructures: micro-lenticular and micro-braided. Gravimetric moisture content: 95%.
- 6.11-9.00 m Grey silt, slightly oxidized, with organic material; from 7.5 m – mostly brown-grey silt, with numerous organic-rich layers, wavy, slightly inclined; from 8.4 m – grey silt with strong oxidation. Cryostructure: layered to braided, ice lenses up to 0.1-cm-thick (rarely – 0.2 cm), spacings 0.2-1 cm (from 6.9 m – up to 3-4 cm). From 7.3 m prevailing cryostructure is reticulate incomplete, ice lenses up to 0.1-cm-thick (rarely – 0.2 cm). Gravimetric moisture content: 39-46%. Epigenetic permafrost, possibly – thawed and refrozen sediments.



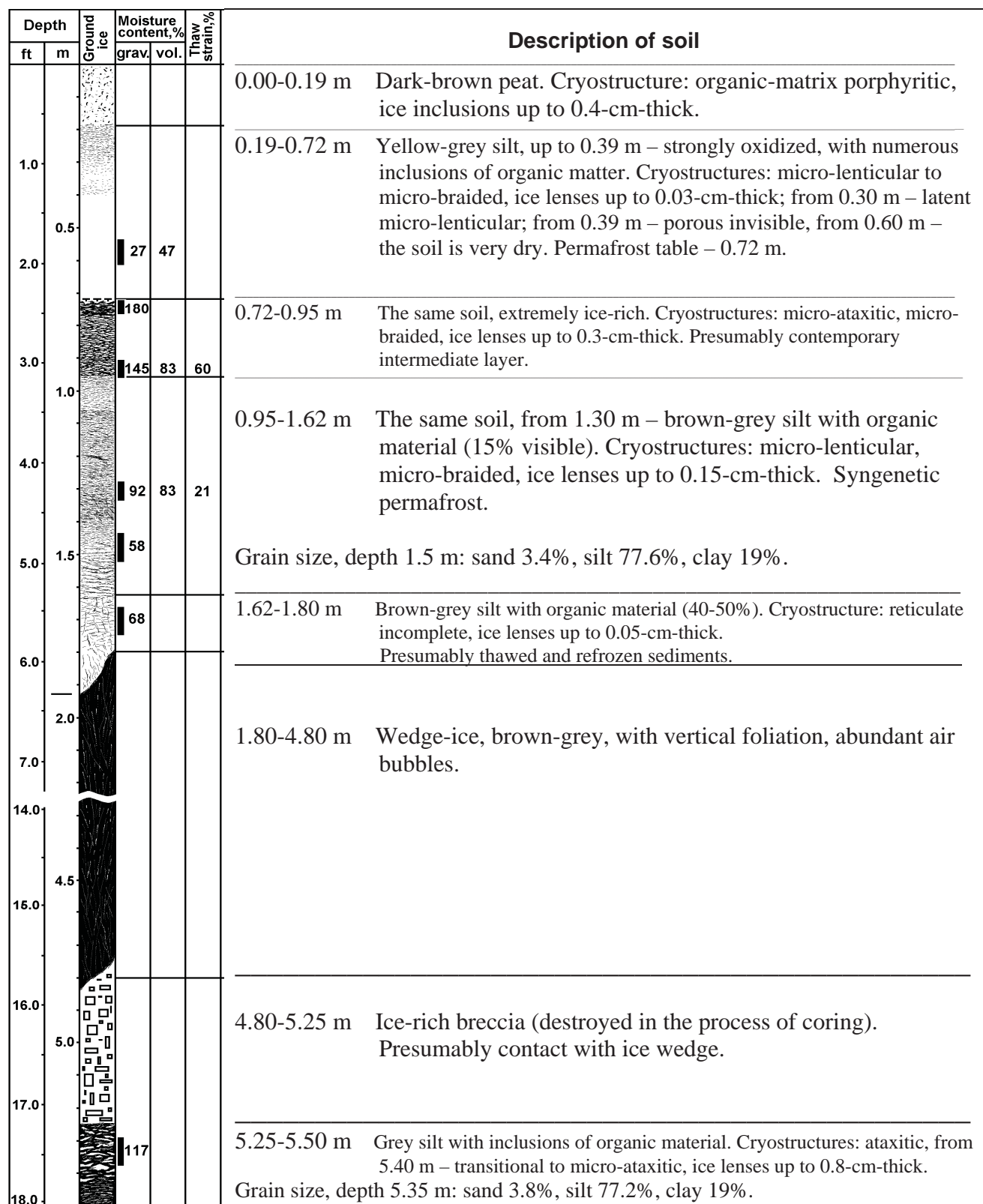


**Figure 5.14.** Cryogenic structure (ice is black) and properties of frozen soil, borehole AUTC-3, depth 0-18 ft (0-5.5 m).

Depth		Ground ice	Moisture content, %		Thaw strain, %	Description of soil
ft	m		grav.	vol.		
			233			5.50-5.76 m Grey silt with inclusions of organic material. Cryostructures: ataxitic (transitional to micro-ataxitic), ice lenses up to 0.8-cm-thick. From 5.60 – micro-ataxitic, micro-braided. Presumably buried intermediate layer.
19.0	6.0		95	80	40	5.76-6.11 m Grey silt with inclusions of organic material. Cryostructures: The same soil. Cryostructures: micro-lenticular and micro-braided. Syngenetic permafrost.
20.0			44			
21.0	6.5					6.11-7.30 m Grey silt, slightly oxidized, with organic material. Cryostructure: layered to braided, ice lenses up to 0.1-cm-thick (rarely – 0.2 cm), spacings 0.2-1 cm (from 6.9 m – up to 3-4 cm). Epigenetic permafrost, possibly – thawed and refrozen sediments.
22.0			45	64		
	7.0		44			
24.0			40			
25.0	7.5					7.30-9.00 m Brown-grey silt, with numerous organic-rich layers, wavy, slightly inclined; from 8.4 m – grey silt with strong oxidation. Cryostructure: mostly reticulate incomplete, ice lenses up to 0.1-cm-thick (rarely – 0.2 cm). Epigenetic permafrost, possibly – thawed and refrozen sediments.
26.0	8.0		46	59		
27.0						Grain size, depth 8.55 m: sand 2.7%, silt 81.3%, clay 16.3%.
28.0	8.5		41	55		
29.0			39			

**Figure 5.15.** Cryogenic structure (ice is black) and properties of frozen soil, Dalton Highway Innovation Project, borehole AUTC-3, depth 18-29.5 ft (5.5-9 m).

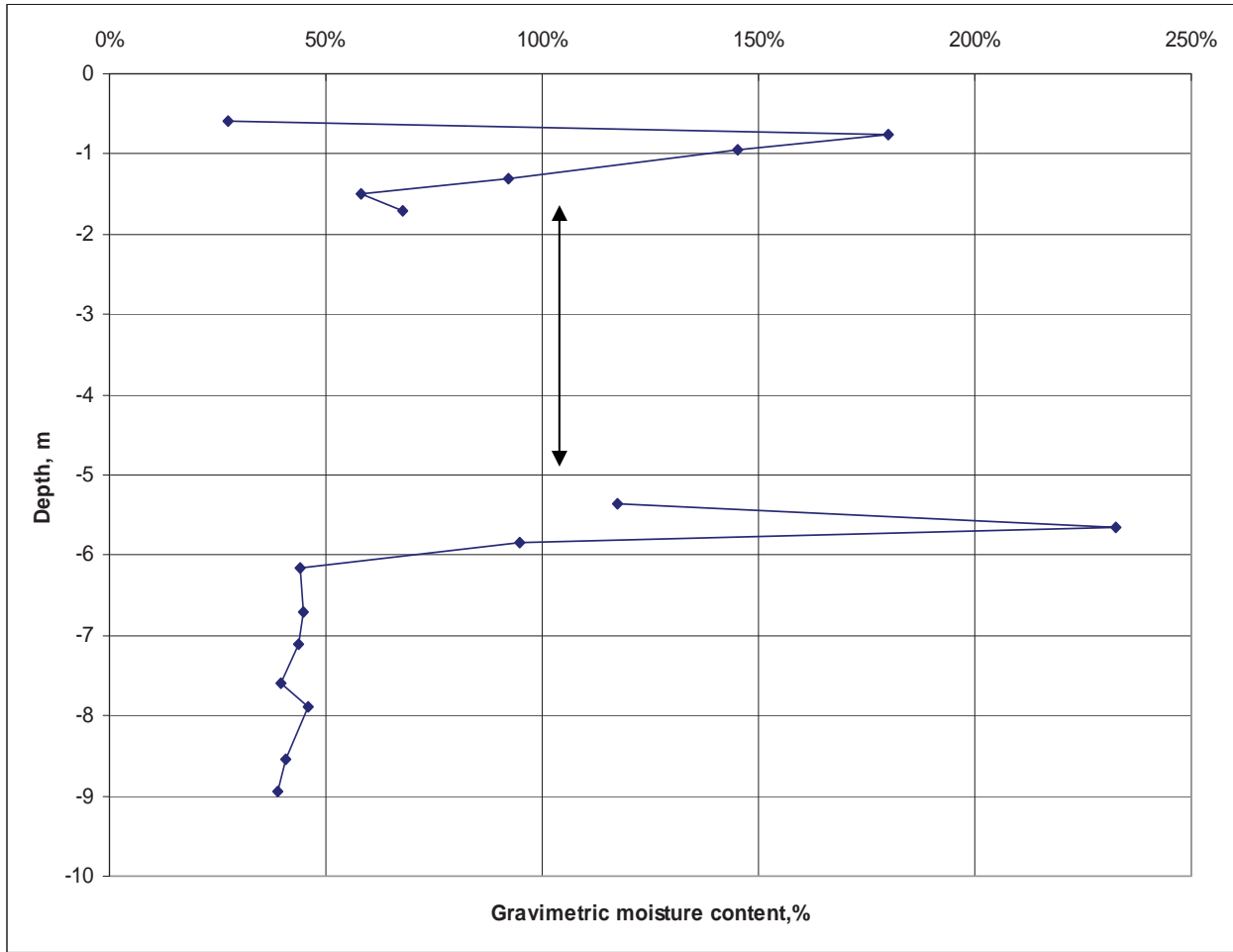


**Figure 5.16.** Gravimetric moisture content of frozen soil, borehole AUTC-3. Syngenetic permafrost, from 1.8 to 4.8 m wedge-ice. From 6.1 m – epigenetic permafrost.





**Figure 5.17.** Silt with micro-braided – micro-lenticular cryostructure, borehole AUTC-3, depth 1.03-1.15 m.





**Figure 5.18.** Silt with reticulate incomplete cryostructure, borehole AUTC-3, depth 1.65-1.76 m, gravimetric moisture content 68%.





**Figure 5.19.** Silt with micro-ataxitic – micro-braided cryostructure, borehole AUTC-3, depth 5.62-5.72 m, gravimetric moisture content 233%.





**Figure 5.20.** Silt with micro-braided – micro-layered cryostructure, borehole AUTC-3, depth 6.0-6.13 m.





**Figure 5.21.** Silt with layered – braided cryostructure, borehole AUTC-3, depth 6.65-6.75 m, gravimetric moisture content 45%.

**Borehole # AUTC08-4 (Figures 5.22-5.31).** May 14, 2008.

Coordinates: Latitude N 65°33'15"; Longitude W 148°53'55".

General description: mix stand of unburned and burned black spruce forest (Erickson Creek 2003); drill site is unburned; random thermokarst depressions, small and shallow.

Vascular Plant Species: *Ledum palustre*, *Epilobium angustifolium*, *Vaccinium vitis-idaea*, *Salix spp.*

Moss Species: *Pleurozium schreberi*, *Hylocomium splendens*, *Ceratodon purpureus*, *Sphagnum fuscum*.

Lichen species: *Cladina mitis*, *cladonia scabriuscula*, *Cladonia rangiferina*, *Peltigera aphosa*.

- 0.00-0.25 m Dark-brown peat. Cryostructure: organic-matrix porphyritic, ice-poor. At 0.23 m – ice layer 0.3 cm; ice-rich from 0.23 m.
- 0.25-0.42 m Yellow-grey and brown-grey silt, up to 0.39 m – strongly oxidized, with numerous inclusions of organic matter (rootlets, thin peat layers). Cryostructures: micro-lenticular to micro-braided, ice lenses up to 0.03-cm-thick; from 0.28 m – latent micro-lenticular (ice content decreases with depth).
- 0.42-0.71 m The same soil, ice-poor. Cryostructure: porous invisible. From 0.62 m – several ice veins up to 0.2-cm-thick. Permafrost table – 0.71 m.
- 0.71-1.50 m Grey and yellow-grey silt, oxidized, with organic material (up to 5%). Cryostructures: micro-ataxitic, micro-braided, ice lenses up to 0.15-cm-thick. Gravimetric moisture content: 71-133%. Modern intermediate layer.
- 1.50-3.00 m The same soil, ice-poor. Cryostructure: porous invisible. Gravimetric moisture content: 42-45%. Thawed and refrozen sediments.
- 3.00-4.45 m The same soil. Cryostructures: micro-lenticular, micro-braided, latent micro-lenticular, micro-porphyritic; ice lenses up to 0.03-cm-thick. Gravimetric moisture content: 47-85%. Syngenetic permafrost.
- 4.45-7.47 m Brown organic silt with layers of grey silt (4.52-4.64; 5.62-5.68; 6.05-6.37). Cryostructures: micro-lenticular, latent micro-lenticular, micro-braided, reticulate incomplete, micro-porphyritic; ice lenses up to 0.05-cm-thick (rarely – up to 0.2-cm-thick). Gravimetric moisture content: 95-168%. Syngenetic permafrost.
- 7.47-9.52 m Grey and yellow-grey silt, with organic material (up to 5%). Cryostructures: latent micro-lenticular, micro-braided, micro-lenticular, micro-porphyritic; ice lenses up to 0.05-cm-thick. Gravimetric moisture content: 48-160%. Syngenetic permafrost.
- 9.52 -10.2? m Grey silt with coarse sand and gravel, weathered, sub-angular to sub-rounded, up to 2 cm (20%). Cryostructures: crustal (ice crusts 0.3-0.4 cm), micro-braided, micro-lenticular, micro-ataxitic; ice lenses up to 0.05-cm-thick. Gravimetric moisture content: 50-67%. Syngenetic permafrost.
- 10.2?-12.0? m The same soil, ice-poor. Gravimetric moisture content: 14. Epigenetic permafrost.
- 12.0?-12.20 m Gravel with some silt, sub-angular to sub-rounded, up to 2 cm. Cryostructure: crustal (ice crusts up to 0.5 cm). Gravimetric moisture content: 14. Epigenetic permafrost.



Depth		Ground ice	Moisture content, %		Thaw strain, %	Description of soil
ft	m		grav.	vol.		
						0.00-0.25 m Dark-brown peat. Cryostructure: organic-matrix porphyritic, ice-poor. At 0.23 m – ice layer 0.3 cm; ice-rich from 0.23 m.
1.0			39			0.25-0.42 m Yellow-grey and brown-grey silt. Cryostructures: micro-lenticular to micro-braided; from 0.28 m – latent micro-lenticular.
	0.5					0.42-0.71 m The same soil, ice-poor. Cryostructure: porous invisible. From 0.62 m – several ice veins up to 0.2-cm-thick. Permafrost table – 0.71 m.
2.0						
			133	82	56	
3.0						0.71-1.50 m Grey and yellow-grey silt, oxidized, with organic material (5% visible). Cryostructures: micro-ataxitic, micro-braided, ice lenses up to 0.15-cm-thick. Modern intermediate layer.
	1.0					
			130	92	47	
4.0						
			125			
			71			
5.0						1.50-2.08 m Grey and yellow-grey silt, oxidized, with organic material (5% visible), ice-poor. Cryostructure: porous invisible. Thawed and refrozen sediments.
	1.5					
			45	64		Grain size, depth 1.95 m: sand 3.6%, silt 82.5%, clay 13.9%.
6.0						
	2.0					
7.0						2.08-2.63 m No data
		no data				
8.0						
	2.5					
			42	60		2.63-2.76 m The same soil (see 1.50-2.08 m)
9.0						
		no data				2.76-3.05 m No data
	3.0					
10.0						
			47	60	6	3.05-3.50 m Grey and yellow-grey silt, oxidized, with organic material. Cryostructures: micro-lenticular, micro-braided, latent micro-lenticular, micro-porphyritic; ice lenses up to 0.03-cm-thick. Syngenetic permafrost.
11.0						

**Figure 5.22.** Cryogenic structure (ice is black) and properties of frozen soil, borehole AUTC-4, depth 0-11.5 ft (0-3.5 m).

Depth		Ground ice	Moisture content, %		Thaw strain, %	Description of soil
ft	m		grav.	vol.		
12.0			67	71	19	3.50-4.45 m Grey and yellow-grey silt, oxidized, with organic material Cryostructures: micro-lenticular, micro-braided, latent micro-lenticular, micro-porphyrritic; ice lenses up to 0.03-cm-thick. Syngenetic permafrost.  Grain size, depth 4.1 m: sand 9.3%, silt 73.5%, clay 17.2%.
13.0	4.0		51			
14.0			85			
15.0	4.5					4.45-4.52 m Brown organic silt. Cryostructure: latent micro-lenticular.
						4.52-4.64 m Grey silt. Cryostructures: micro-lenticular, latent micro-lenticular.
16.0			95			4.64-5.62 m Brown organic silt. Cryostructures: micro-lenticular, latent micro-lenticular, micro-braided, reticulate incomplete, micro-porphyrritic; ice lenses up to 0.05-cm-thick (rarely – up to 0.2-cm-thick). Syngenetic permafrost.
17.0	5.0		133			
18.0	5.5		168			5.62-5.68 m Grey silt. Cryostructures: micro-lenticular, reticulate incomplete.
19.0			118			
20.0	6.0					5.68-6.05 m Brown organic silt. Cryostructures: reticulate incomplete, micro-porphyrritic, micro-lenticular. Syngenetic permafrost.
21.0			130			6.05-6.37 m Grey silt. Cryostructures: micro-lenticular, micro-braided, latent micro-lenticular. Syngenetic permafrost.
22.0	6.5		116			
			113	94		6.37-7.00 m Brown organic silt. Cryostructures: micro-lenticular, latent micro-lenticular, micro-braided, reticulate incomplete, micro-porphyrritic. Syngenetic permafrost.  Grain size, depth 6.65 m: sand 2.9%, silt 79.3%, clay 17.8%.

**Figure 5.23.** Cryogenic structure (ice is black) and properties of frozen soil, borehole AUTC-4, depth 11.5-23 ft (3.5-7 m).

Depth		Ground ice	Moisture content, %		Thaw strain, %	Description of soil
ft	m		grav.	vol.		
23.0			113	94		7.00-7.47 m Brown organic silt. Cryostructures: micro-lenticular, latent micro-lenticular, micro-braided. Syngenetic permafrost.
24.0			164	92	42	
	7.5					7.47-9.52 m Grey and yellow-grey silt, with organic material (5% visible). Cryostructures: latent micro-lenticular, micro-braided, micro-lenticular, micro-porphyrific; ice lenses up to 0.05-cm-thick. Syngenetic permafrost.
25.0			160			
26.0			92	77	23	
27.0			93	76	37	
28.0			52	64	5	
29.0			48	63	0.2	
	9.0					9.52 -9.96 m Grey silt with coarse sand and gravel, weathered, sub-angular to sub-rounded, up to 2 cm (20% visible). Cryostructures: crustal (ice crusts 0.3-0.4 cm), micro-braided, micro-lenticular, micro-ataxitic; ice lenses up to 0.05-cm-thick. Syngenetic permafrost.
30.0			67	71	24	
	9.5		50			Grain size, depth 9.65 m: gravel 15.3%, sand 15.5%, silt 39.7%, clay 14.0%.
31.0		no data				9.96-10.22 m No data
32.0						10.22-10.50 m Grey silt with coarse sand and gravel, ice-poor. Cryostructure: crustal. Epigenetic permafrost.
33.0			14			
34.0						

**Figure 5.24.** Cryogenic structure (ice is black) and properties of frozen soil, borehole AUTC-4, depth 23-34.5 ft (7-10.5 m).



Depth		Ground ice	Moisture content, %		Thaw strain, %	Description of soil
ft	m		grav.	vol.		
35.0		no data				10.50-12.03 m No data
36.0	11.0					
37.0		no data				10.22-10.50 m Gravel with some silt, sub-angular to sub-rounded, up to 2 cm. Cryostructure: crustal (crusts up to 0.5 cm). Epigenetic permafrost.
38.0	11.5					
39.0		no data				10.22-10.50 m Gravel with some silt, sub-angular to sub-rounded, up to 2 cm. Cryostructure: crustal (crusts up to 0.5 cm). Epigenetic permafrost.
40.0	12.0					

**Figure 5.25.** Cryogenic structure (ice is black) and properties of frozen soil, borehole AUTC-4, depth 34.5-40 ft (10.5-12.2 m).

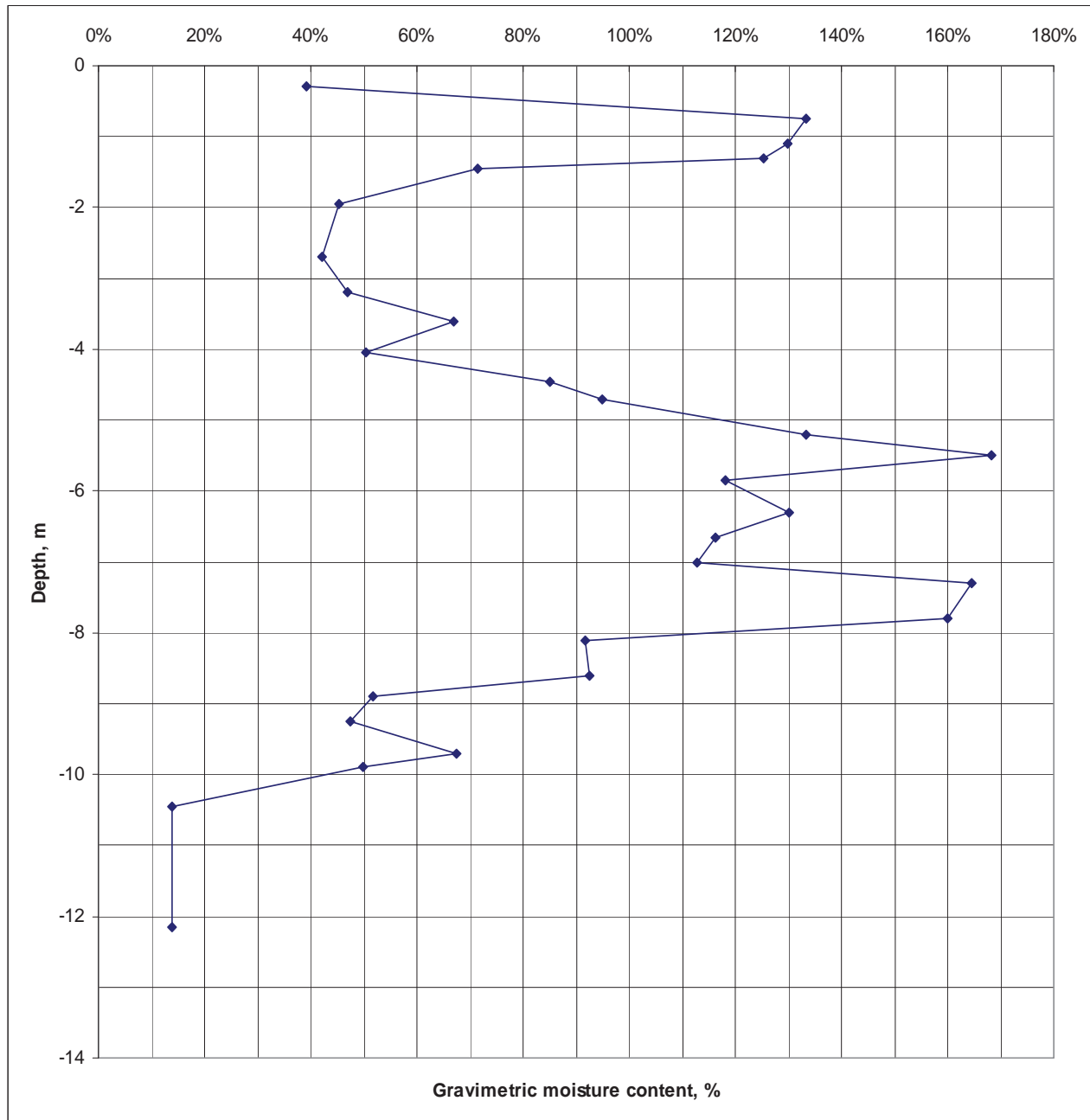


**Figure 5.26.** Gravimetric moisture content of frozen soil, borehole AUTC-4. From 0.7 to 1.5 m – intermediate layer; from 1.5 to 3 m – thawed and refrozen sediments; from 3 to 10.2 m – syngenetic permafrost; from 10.2 m – epigenetic permafrost (gravel).



**Figure 5.27.** Silt with micro-braided – micro-ataxitic cryostructure, borehole AUTC-4, depth 0.84-0.95 m.





**Figure 5.28.** Silt with micro-porphyrific cryostructure, borehole AUTC-4, depth 3.16-3.28 m, gravimetric moisture content 47%.





**Figure 5.29.** Silt with micro-lenticular – micro-braided cryostructure, borehole AUTC-4, depth 8.15-8.25 m, gravimetric moisture content 92%. Note inclination of ice lenses indicating proximity of ice wedge.





**Figure 5.30.** Silt with coarse sand and gravel, with crustal / micro-braided cryostructure, borehole AUTC-4, depth 9.63-9.70 m, gravimetric moisture content 67%.



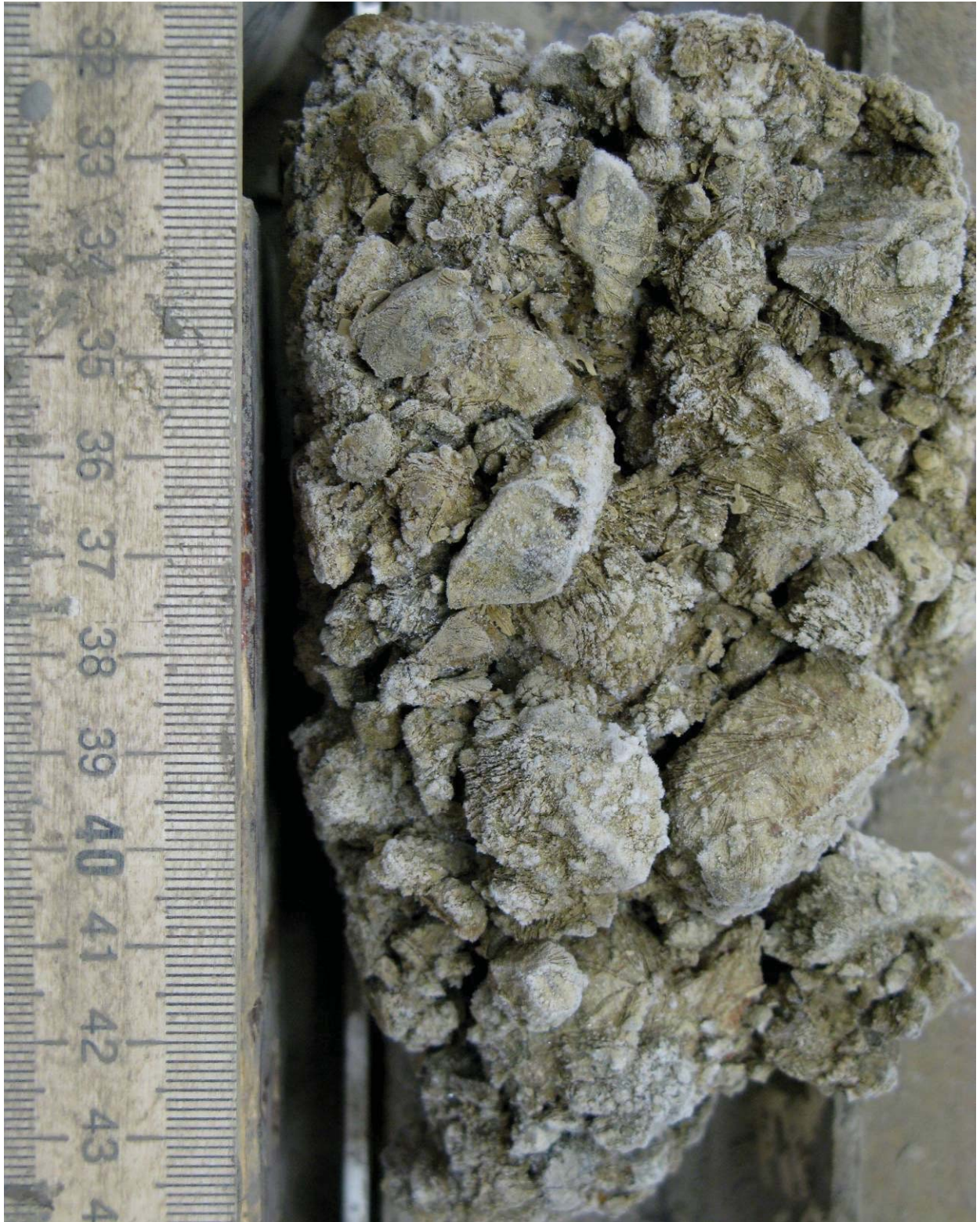


**Figure 5.31.** Gravel with crustal cryostructure, borehole AUTC-4, depth 12.08-12.20 m, gravimetric moisture content 14%.

**Borehole # AUTC08-5 (Figures 5.32-5.40).** May 14, 2008.

Coordinates: Latitude N 65°33'20"; Longitude W 148°54'6".

General description: burned black spruce stand (Erickson Creek 2003); burned hummocks; random thermokarst mounds up to 1-m-high, up to 10 m in diameter; forest floor is primarily *Ceratodon purpureus* and burned dead moss and burned fibric organic matter.

Vascular Plant Species: *Ledum palustre*, *Epilobium angustifolium*.

Moss Species: *Ceratodon purpureus*.

- 0.00-0.59 m Dark-brown peat and organic silt with layers of yellow-grey oxidized silt up to 10-cm-thick. Cryostructures: organic-matrix porphyritic, micro-lenticular, reticulate incomplete, ice lenses up to 0.2-cm-thick. Frozen active layer. Permafrost table – 0.59 m.
- 0.59-1.10 m Yellow-grey silt, with organic material (up to 3%), ice-rich. Cryostructures: micro-braided to micro-ataxitic, micro-lenticular, ice lenses up to 0.1-cm-thick. Gravimetric moisture content: 64-143%. Modern intermediate layer.
- 1.10-5.19 m The same soil, with layers of brown-grey silt (organic material up to 15%). Cryostructures: latent micro-lenticular, micro-porphyritic. Gravimetric moisture content: 55-88%. At 4.32-4.43, 4.55-4.73 – ice-rich layers; cryostructures: micro-braided to micro-ataxitic, ice lenses up to 0.2-cm-thick. Gravimetric moisture content: 90-99%. Syngenetic permafrost.
- 5.19-6.00 m The same soil, with organic material (up to 5%), ice-rich. Cryostructures: micro-ataxitic to micro-braided, ice lenses up to 0.2-cm-thick. At 5.65-5.74 –ice  
Gravimetric moisture content: 107-178%.
- 6.00-6.42 m The same soil, mostly ice-poor. Cryostructure: micro-porphyritic, reticulate, micro-braided. Gravimetric moisture content: 53%. Syngenetic permafrost.
- 6.42-7.48 m The same soil, ice-rich. Cryostructures: micro-ataxitic, micro-braided, mostly inclined or sub-vertical. Gravimetric moisture content: 103-176%. Presumably syngenetically frozen soil adjacent to the ice wedge or buried intermediate layer.

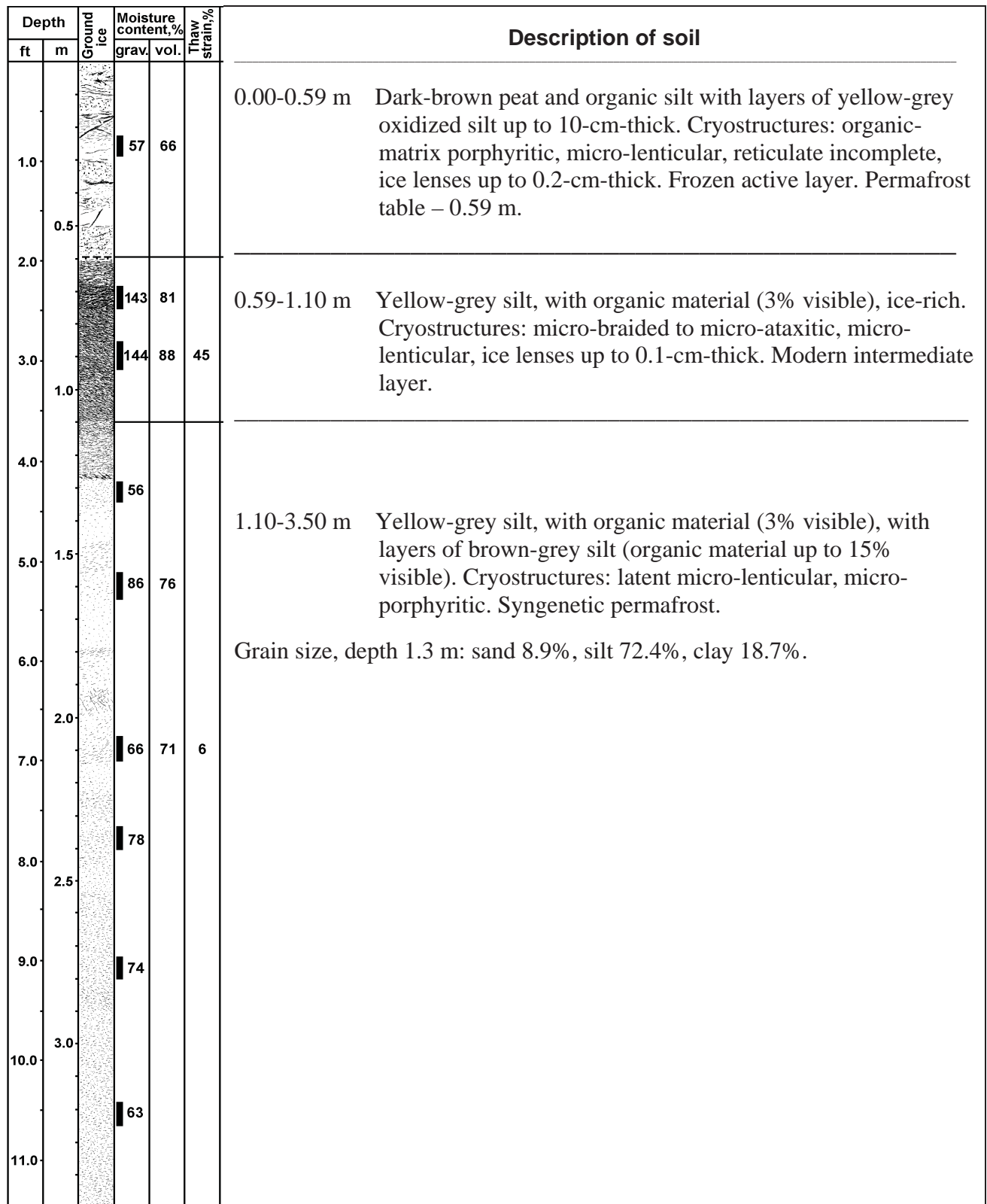


**Figure 5.32.** Cryogenic structure (ice is black) and properties of frozen soil, borehole AUTC-5, depth 0-11.5 ft (0-3.5 m).



Depth		Ground ice	Moisture content, %		Thaw strain, %	Description of soil
ft	m		grav.	vol.		
12.0			88	76	30	3.50-4.32 m Yellow-grey silt, with organic material (3% visible), with layers of brown-grey silt (organic material up to 15% visible). Cryostructures: latent micro-lenticular, micro-porphyrritic. Syngenetic permafrost.  Grain size, depth 3.85 m: sand 12.2%, silt 68.2%, clay 19.6%.
13.0	4.0		78	75		
14.0			99			4.32-4.73 m Yellow-grey silt, with organic material (3% visible), with layers of brown-grey silt (organic material up to 15% visible). Cryostructures: mostly micro-braided to micro-ataxitic, ice lenses up to 0.2-cm-thick. Syngenetic permafrost.
15.0	4.5		90			
16.0			55 66			4.73-5.19 m Yellow-grey silt, with organic material (3% visible), with layers of brown-grey silt (organic material up to 15% visible). Cryostructures: latent micro-lenticular, micro-porphyrritic. Syngenetic permafrost.
17.0	5.0					
18.0			178	92	37	5.19-6.00 m Yellow-grey silt, with organic material (5% visible), ice-rich. Cryostructures: micro-ataxitic to micro-braided, ice lenses up to 0.2-cm-thick. At 5.65-5.74 – ice layer. Presumably buried active layer.
19.0	5.5		107	80	12	
20.0			53			6.00-6.42 m Yellow-grey silt, with organic material (5% visible), mostly ice-poor. Cryostructure: micro-porphyrritic, reticulate, micro-braided. Syngenetic permafrost.  Grain size, depth 6.15 m: sand 9.1%, silt 75.8%, clay 15.1%.
21.0	6.0					
22.0			176			6.42-7.00 m Yellow-grey silt, with organic material (5% visible), ice-rich. Cryostructures: micro-ataxitic, micro-braided, mostly inclined or sub-vertical. Presumably syngenetically frozen soil adjacent to the ice wedge or buried intermediate layer.

**Figure 5.33.** Cryogenic structure (ice is black) and properties of frozen soil, borehole AUTC-5, depth 11.5-23 ft (3.5-7 m).

Depth		Ground ice	Moisture content, %		Thaw strain, %	Description of soil
ft	m		grav.	vol.		
	7.0		103			6.42-7.48 m Yellow-grey silt, with organic material (5% visible), ice-rich. Cryostructures: micro-ataxitic, micro-braided, mostly inclined or sub-vertical. Presumably syngenetically frozen soil adjacent to the ice wedge or buried intermediate layer.
24.0			126	88	44	
			105	80	41	

**Figure 5.34.** Cryogenic structure (ice is black) and properties of frozen soil, borehole AUTC-5, depth 23-24.5 ft (7-7.48 m).

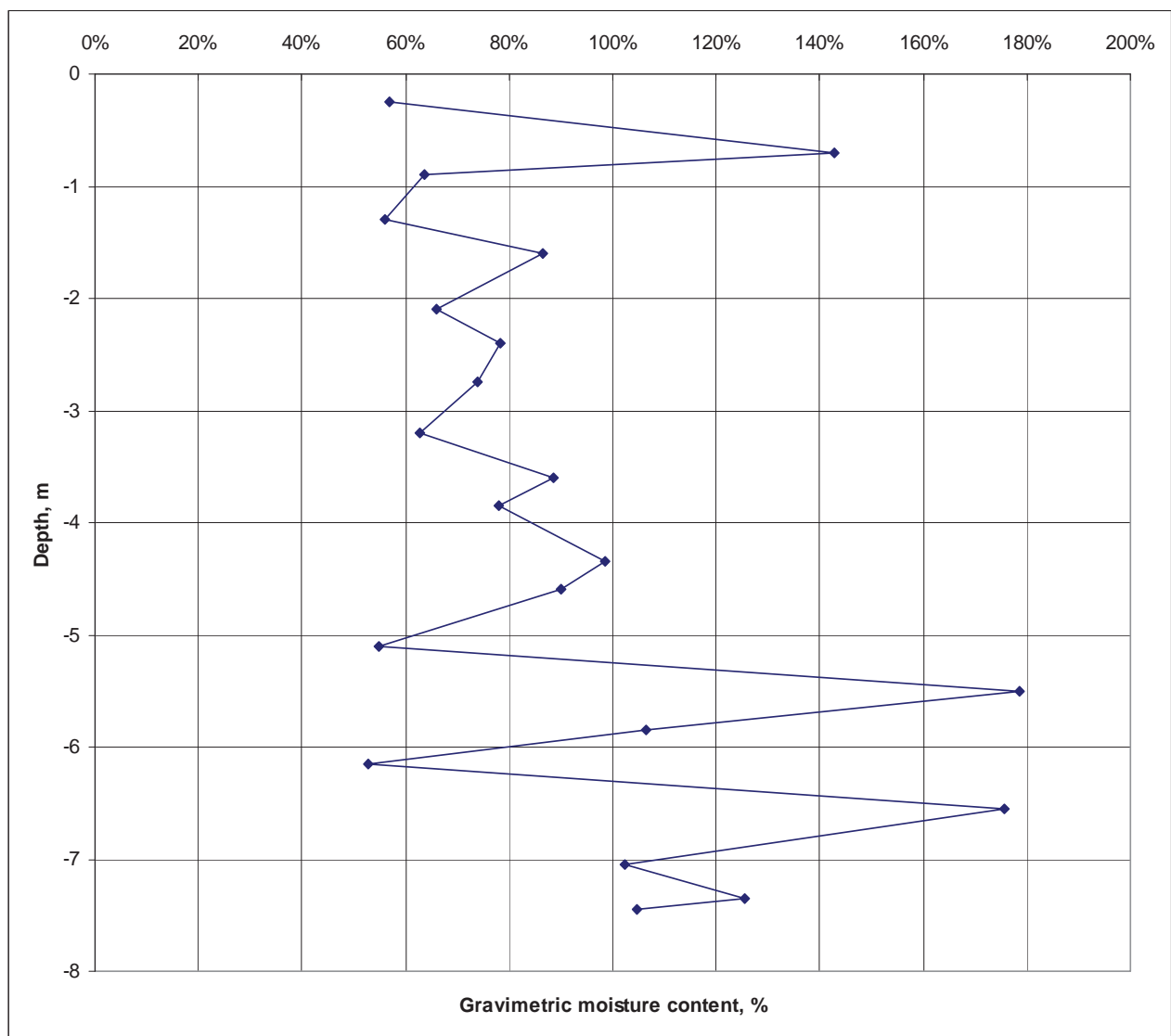


**Figure 5.35.** Gravimetric moisture content of frozen soil, borehole AUTC-5, syngenetic permafrost.

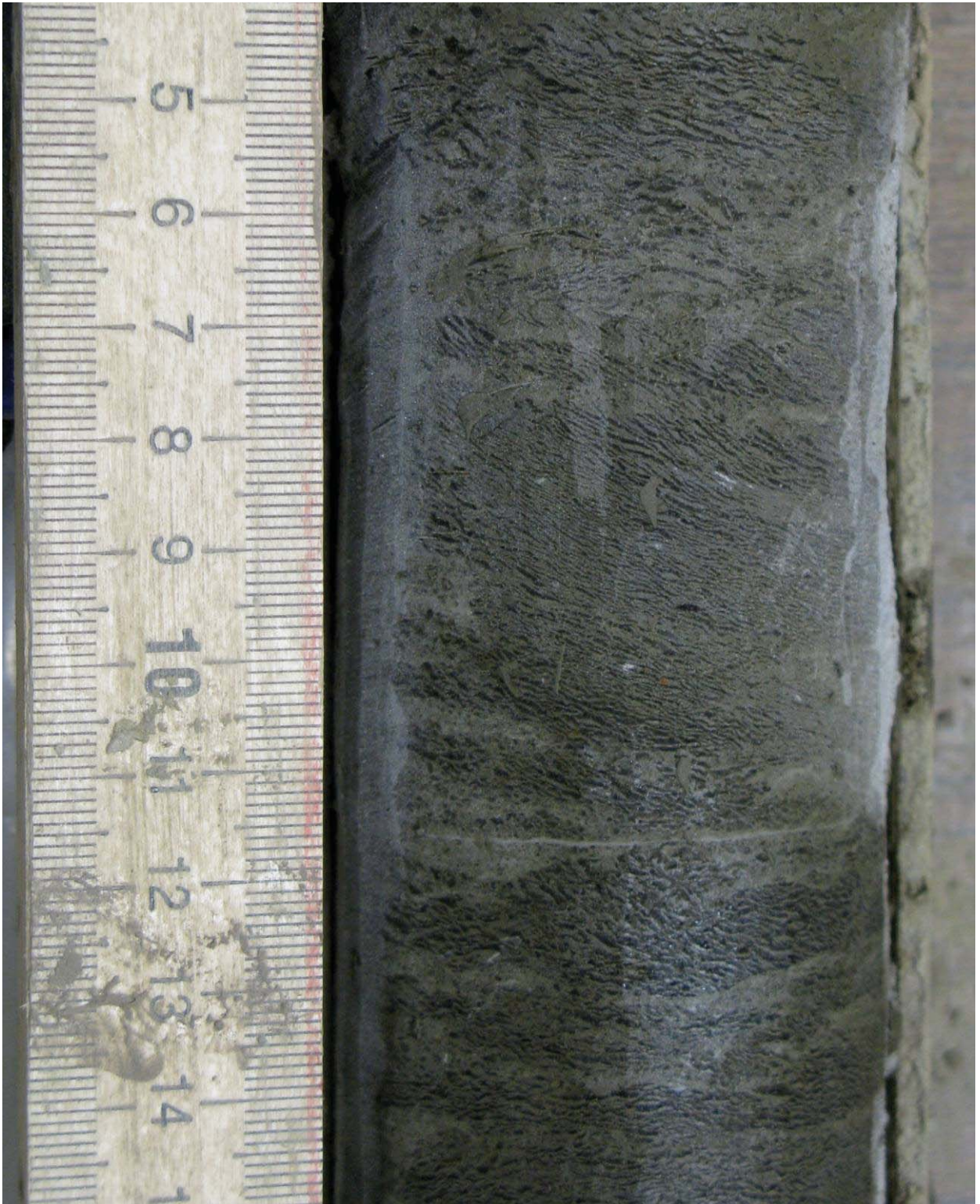


**Figure 5.36.** Silt with micro-braided cryostructure, borehole AUTC-5, depth 0.8-0.9 m, gravimetric moisture content 92%.





**Figure 5.37.** Silt with latent micro-lenticular cryostructure (inclined), borehole AUTC-5, depth 2.03-2.14 m, gravimetric moisture content 66%.





**Figure 5.38.** Silt with latent micro-lenticular cryostructure, borehole AUTC-5, depth 2.74-2.85 m, gravimetric moisture content 74%.





**Figure 5.39.** Silt with micro-lenticular – micro-braided cryostructure, borehole AUTC-5, depth 4.55-4.64 m, gravimetric moisture content 90%.





**Figure 5.40.** Silt with micro-ataxitic – micro-braided cryostructure, borehole AUTC-5, depth 7.30-7.38 m, gravimetric moisture content 126%.

**Borehole # AUTC08-6 (Figures 5.41-5.52).** May 15, 2008.

Coordinates: Latitude N 65°33'22"; Longitude W 148°54'18".

General description: burned black spruce forest (Erickson Creek 2003); random thermokarst depressions up to 0.5-m-deep, up to 3 m in diameter; several shallow erosional trenches.

Vascular Plant Species: *Ledum palustre*, *Epilobium angustifolium*, *Vaccinium vitis-idaea*.

Moss Species: *Pleurozium schreberi*, *Ceratodon purpureus*, *Aulacomnium palustre*, *Dicranum spp.*

- 0.00-0.08 m Dark-brown peat, ice-poor. Cryostructure: organic-matrix porphyritic.
- 0.08-0.80 m Yellow-grey oxidized silt, ice-poor. Cryostructures: micro-porphyrritic, from 0.28 m – porous invisible. From 0.60 m to 0.72 m – very dry, friable. Gravimetric moisture content: 30-43%. Frozen active layer. Permafrost table – 0.80 m.
- 0.80-1.08 m Yellow-grey silt. Cryostructures: micro-lenticular, from 0.91 – latent micro-lenticular. Gravimetric moisture content: 56%. Presumably modern intermediate layer (ice-poor, probably restored after the forest fire).
- 1.08-3.20 m Yellow-grey silt, with small rare inclusions of organic material (at 2.35-2.70 m – up to 3%), ice-poor, dense. Cryostructure: porous invisible. Gravimetric moisture content: 39-46%. From 2.90 m – brown-grey organic silt, ice-poor. Cryostructure: porous invisible. Gravimetric moisture content: 63%. Thawed and refrozen sediments.
- 3.20-13.15 m Wedge-ice. Vertical foliation, air bubbles.
- 13.15-15.66 m Brown-grey silt, with organic material (up to 5-7%). Cryostructures: latent micro-lenticular, micro-porphyrritic, from 15 m – mostly micro-braided with ice inclusions up to 0.8-cm-thick. Gravimetric moisture content: 69-131%.
- 15.66-16.62 m Grey and yellow-grey silt. Cryostructures: micro-braided, micro-lenticular; at 16.08 m – inclined ice lens 1.2 cm; from 16.30 m – latent micro-lenticular, micro-porphyrritic, several ice veins up to 0.7 cm. Gravimetric moisture content: 48-95%.
- 16.62-18.14 m Wedge-ice. Vertical foliation, numerous soil inclusions, air bubbles. At 17.79-18.14 m – boundary between the ice wedge and adjacent soil (yellow-grey oxidized silt). Cryostructure: mostly micro-braided.
- 18.14-18.91 m Yellow-grey silt, strongly oxidized, ice-poor. Cryostructures: latent micro-lenticular, micro-porphyrritic. Gravimetric moisture content: 39-42%. From 18.6 m – soil is very dense, epigenetic permafrost.
- 18.91-19.61 m The same soil, with gravel and coarse sand (up to 50%), ice-poor. Cryostructures: porous invisible, crustal (ice crusts up to 0.2 cm). Gravimetric moisture content: 21-24%. Epigenetic permafrost.
- 19.61-21.05 m Weathered bedrock (black schist), ice-poor. Cryostructures: porous invisible, crustal. Gravimetric moisture content: 21-24%. Epigenetic permafrost.

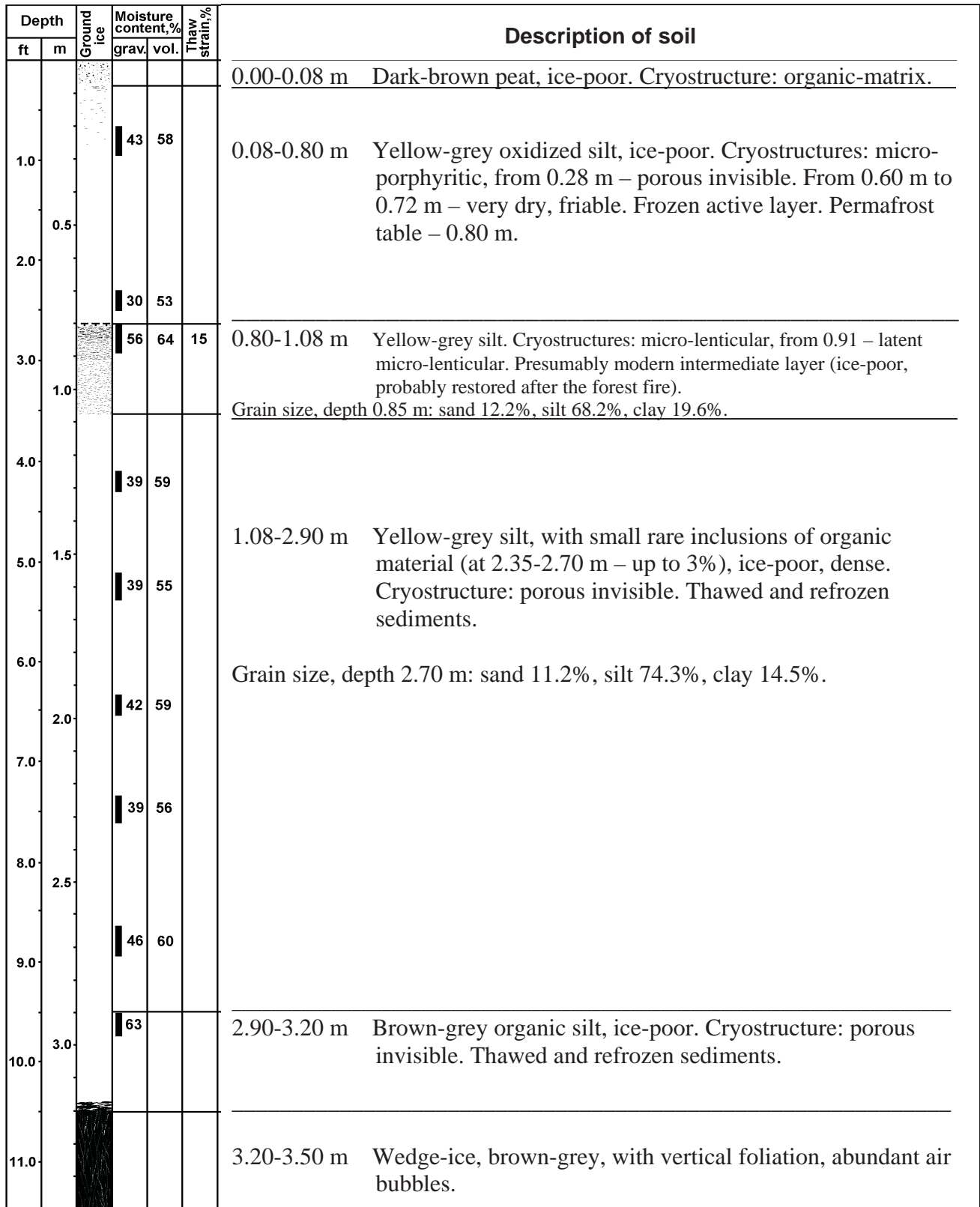


**Figure 5.41.** Cryogenic structure (ice is black) and properties of frozen soil, borehole AUTC-6, depth 0-11.5 ft (0-3.5 m).



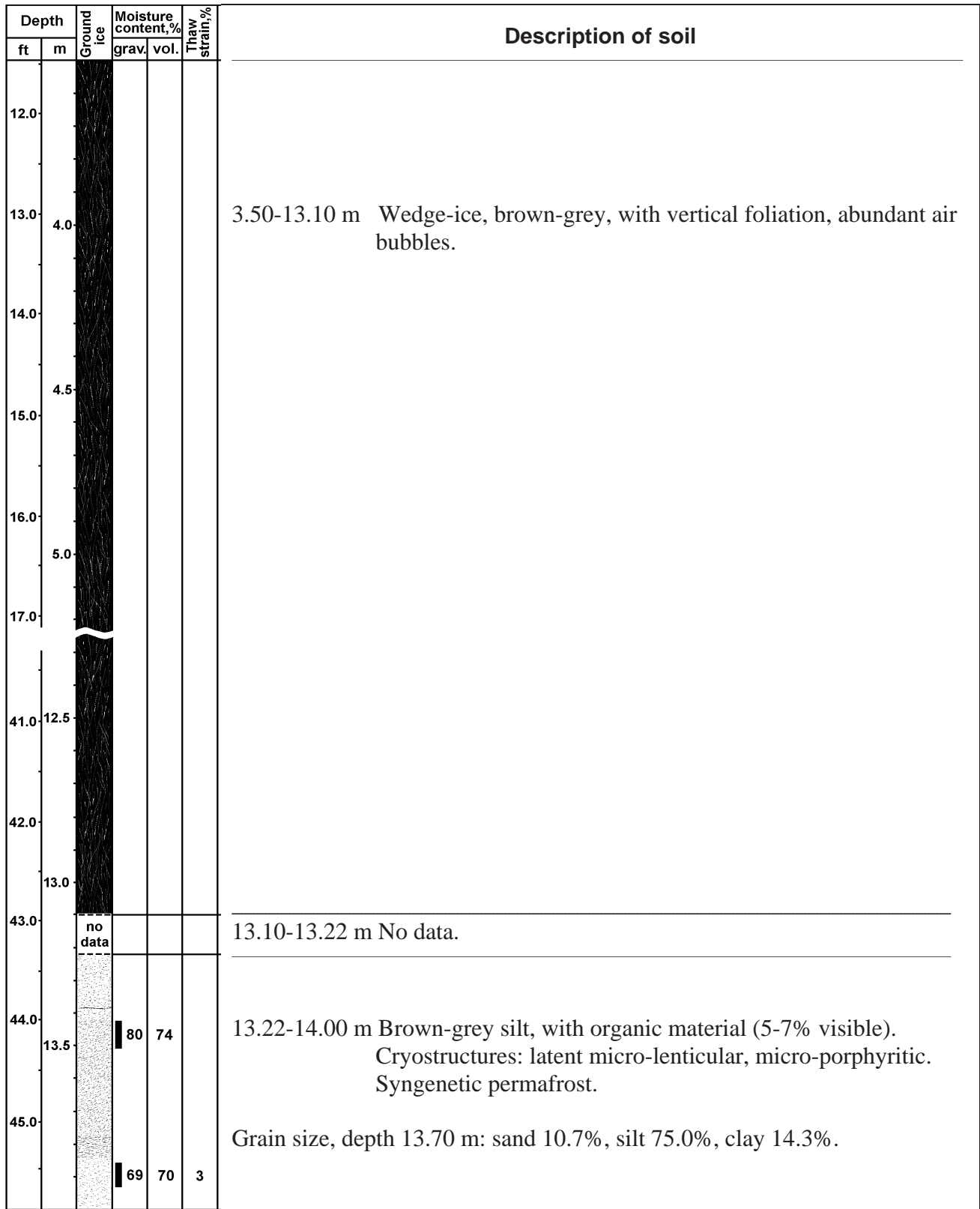


**Figure 5.42.** Cryogenic structure (ice is black) and properties of frozen soil, borehole AUTC-6, depth 11.5-46 ft (3.5-14 m).

Depth		Ground ice	Moisture content, %		Thaw strain, %	Description of soil
ft	m		grav.	vol.		
46.0			99			14.00-14.79 m Brown-grey silt, with organic material (5-7% visible). Cryostructures: latent micro-lenticular, micro-porphyrritic. Syngenetic permafrost.
47.0						
	14.5		97			
48.0						
49.0		no data				14.79-15.05 m No data.
	15.0					
50.0			131	87	29	15.05-15.66 m Brown-grey silt, with organic material (5-7% visible). Cryostructures: mostly micro-braided with ice inclusions up to 0.8-cm-thick. Syngenetic permafrost.
51.0						
	15.5					
52.0			95			15.66-16.02 m Grey and yellow-grey silt. Cryostructures: micro-braided, micro-lenticular. Syngenetic permafrost.
53.0						
	16.0					
53.0			68			16.02-16.62 m Grey and yellow-grey silt. Cryostructures: micro-lenticular, latent micro-lenticular, micro-porphyrritic, several ice veins up to 0.7 cm; at 16.08 m – inclined ice lens 1.2 cm. Syngenetic permafrost.
54.0						
	16.5		48	64	6	Grain size, depth 16.55 m: sand 8.4%, silt 78.4%, clay 13.2%.
55.0						
56.0						
	17.0					
57.0						

**Figure 5.43.** Cryogenic structure (ice is black) and properties of frozen soil, borehole AUTC-6, depth 46-57.5 ft (14-17.5 m).

Depth		Ground ice	Moisture content, %		Thaw strain, %	Description of soil
ft	m		grav.	vol.		
58.0						17.50-17.79 m Wedge-ice, brown-grey, with vertical foliation, abundant air bubbles, numerous soil inclusions.
59.0	18.0					17.79-18.14 m Boundary between the ice wedge and adjacent soil (yellow-grey oxidized silt). Cryostructure: mostly micro-braided. Syngenetic permafrost.
60.0			42	60		18.14-18.60 m Yellow-grey silt, strongly oxidized, ice-poor. Cryostructures: latent micro-lenticular, micro-porphyratic.
61.0	18.5		39	60		18.60-18.91 m Yellow-grey silt, strongly oxidized, ice-poor, soil is very dense. Cryostructure: lenticular. Epigenetic permafrost.
62.0			24	43		18.91-19.61 m Yellow-grey gravelly sandy silt, ice-poor. Cryostructures: porous invisible, crustal (ice crusts up to 0.2 cm). Epigenetic permafrost.
63.0						Grain size, depth 19.10 m: gravel 13%, sand 29%, silt 37.1%, clay 20.8%.
64.0	19.5		21			
65.0			24	42		19.61-21.05 m Weathered bedrock (black schist), ice-poor. Cryostructures: porous invisible, crustal. Epigenetic permafrost.
66.0						
67.0	20.5					
68.0			21	44		

**Figure 5.44.** Cryogenic structure (ice is black) and properties of frozen soil, borehole AUTC-6, depth 57.5-69 ft (17.5-21.05 m).



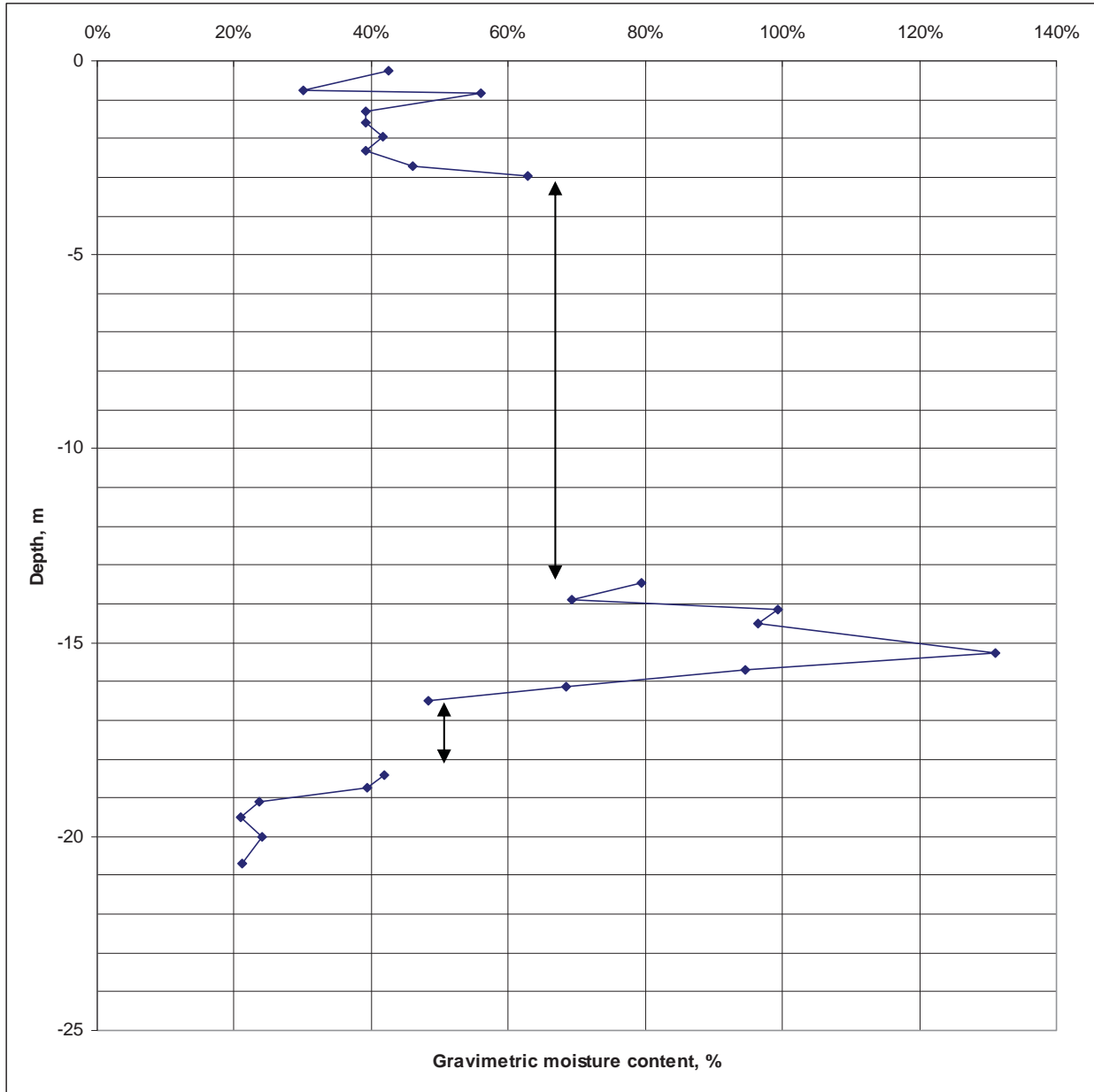


**Figure 5.45.** Gravimetric moisture content of frozen soil, borehole AUTC-6. Thawed and refrozen sediments on top, from 3.2 m – syngenetic permafrost. From 18.6 m – epigenetic permafrost.



**Figure 5.46.** Silt with micro-lenticular cryostructure (0-4cm – porous invisible), borehole AUTC-6, depth 0.76-0.88 m, gravimetric moisture content 56% (0.8-0.86 m).





**Figure 5.47.** Silt with porous cryostructure (no visible ice), borehole AUTC-6, depth 2.25-2.36 m, gravimetric moisture content 39%.





**Figure 5.48.** Organic silt with porous cryostructure (no visible ice), borehole AUTC-6, depth 2.90-3.03 m, gravimetric moisture content 63%.



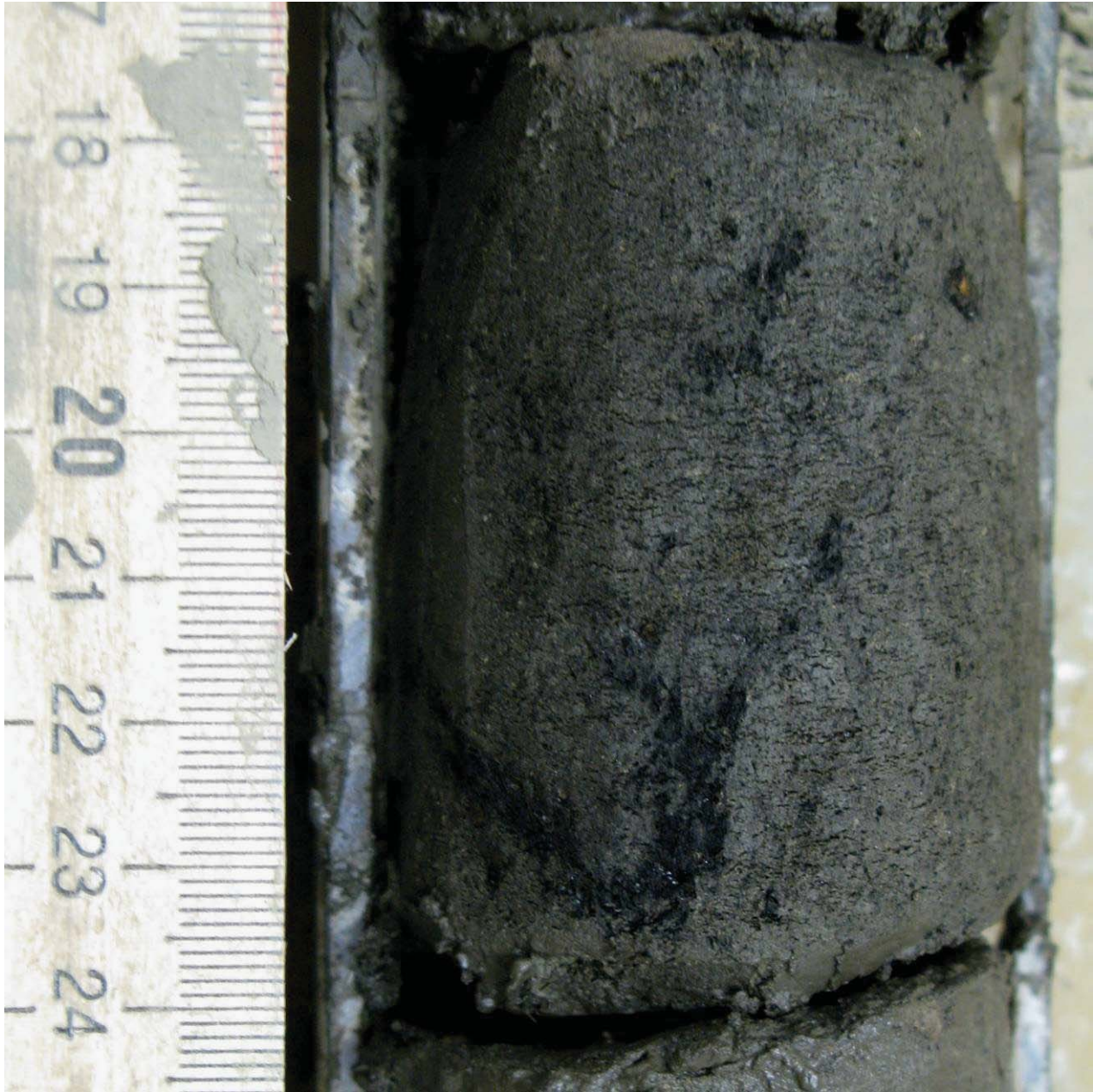


**Figure 5.49.** Silt with micro-lenticular – micro-braided cryostructure, borehole AUTC-6, depth 14.11-14.18 m, gravimetric moisture content 99%.





**Figure 5.50.** Ice-rich silt, boundary with ice wedge, borehole AUTC-6, depth 7.30-7.38 m.



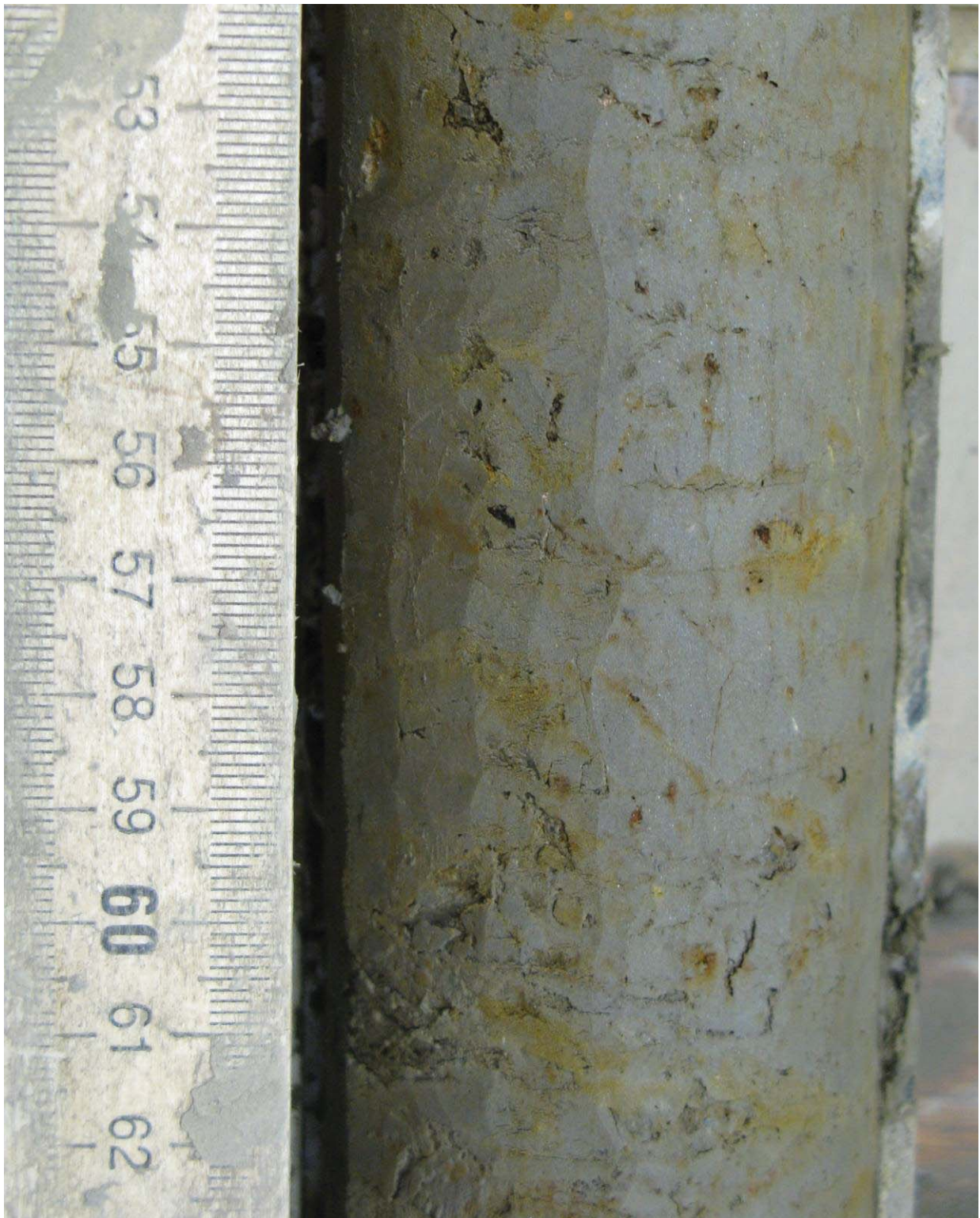


**Figure 5.51.** Ice-poor silt (epigenetic permafrost) with porous – lenticular cryostructure, borehole AUTC-6, depth 18.67-18.77 m, gravimetric moisture content 39%.





**Figure 5.52.** Gravelly sandy silt (epigenetic permafrost) with crustal cryostructure, borehole AUTC-6, depth 18.67-18.77 m, gravimetric moisture content 24%.

**Borehole # AUTC08-7 (Figures 5.53-5.63).** May 16, 2008.

Coordinates: Latitude N 65°33'26"; Longitude W 148°54'29".

General description: burned black spruce forest (Erickson Creek 2003); sporadic thermokarst depressions.

Vascular Plant Species: *Ledum palustre*, dead *Epilobium angustifolium*, *Vaccinium vitus-idaea*, *Salix spp.*, *Elymus innovatus*, *Picea mariana* saplings.

Moss Species: *Dicranum spp.*, *Ceratodon purpureus*, *Polytrichum spp.*

- 0.00-0.10 m Dark-brown peat, ice-poor, at 0.05-0.12 m – irregular ice lens. Cryostructure: organic-matrix porphyritic.
- 0.10-0.46 m Yellow-brown silt, with organic material (up to 5%). Cryostructures: micro-braided, micro-braided lenticular. Gravimetric moisture content: 59%. Frozen active layer.
- 0.46-0.98 m Yellow-grey silt, ice-poor. From 0.55 m – very dry, friable. Cryostructures: latent micro-braided lenticular, from 0.55 m – porous invisible. Gravimetric moisture content: 27%. Frozen active layer. Permafrost table – 0.98 m.
- 0.98-1.30 m The same soil, with organic material (up to 2%), dense. Cryostructures: latent micro-lenticular, from 1.16 m – porous invisible. Gravimetric moisture content: 45%. Thawed and refrozen sediments.
- 1.30-1.83 m Brown organic silt. Cryostructure: mostly porous invisible, from 1.56 m. – several ice lenses up to 0.2-cm-thick. Gravimetric moisture content: 49-76%. Previously thawed and refrozen.
- 1.83-3.90 m The same soil, ice-rich. Cryostructures: combined organic-matrix porphyritic, micro-braided and micro-lenticular, with ice lenses up to 0.3-cm-thick; several ice layers up to 1.5-cm-thick. Gravimetric moisture content: 109-246%. Syngenetic permafrost. From 2.61 to 2.76 m – grey silt; cryostructure reticulate-braided with ice lenses up to 0.3-cm-thick, at 2.77 m – ice layer up to 1.5-cm-thick. Gravimetric moisture content: 157%. Presumably buried intermediate layer.
- 3.90-6.88 m Grey silt, with organic material (up to 3%). Cryostructures: micro-braided, micro-lenticular, sometimes inclined; from 5.6 m – several layers with micro-porphyritic cryostructure; at 6.73-6.88 m – presumably contact with wedge-ice. Gravimetric moisture content: 60-102%.
- 6.88-7.53 m The same soil, mostly ice-rich. Cryostructure: mostly micro-braided, occasionally sub-vertical; at 7.36-7.43 m – presumably contact with wedge-ice. Gravimetric moisture content: 122-146%.
- 7.53-11.38 m Wedge-ice. Vertical foliation, air bubbles. At 10.0-10.95 and 11.19-11.38 – ice-rich breccia (Presumably contact with ice wedge).
- 11.38-11.82 m Yellow-grey silt. Cryostructure: mostly micro-braided, inclined. Gravimetric moisture content: 73%. From 11.75 – contact with ice wedge.
- 11.82-11.90 m Wedge-ice. Vertically foliated with air bubbles.






Depth		Ground ice	Moisture content, %		Thaw strain, %	Description of soil
ft	m		grav.	vol.		
						0.00-0.10 m Dark-brown peat, at 0.05-0.12 m irregular ice lens. Cryostructure: organic-matrix porphyritic.
1.0			59	67		0.10-0.46 m Yellow-brown silt, with organic material (5% visible). Cryostructures: micro-braided, micro-braided lenticular. Frozen active layer.
2.0	0.5		27	46		0.46-0.98 m Yellow-grey silt, ice-poor. From 0.55 m – very dry, friable. Cryostructures: latent micro-braided lenticular, from 0.55 m – porous invisible. Frozen active layer. Permafrost table – 0.98 m.
4.0	1.0		45	62	0.5	0.98-1.30 m The same soil, with organic material (2% visible), dense. Cryostructures: latent micro-lenticular, from 1.16 m – porous invisible. Thawed and refrozen sediments. Grain size, depth 1.05 m: sand 11.7%, silt 75.1%, clay 13.2%.
5.0	1.5		49			1.30-1.83 m Brown organic silt. Cryostructure: mostly porous invisible, from 1.56 m. – several ice lenses up to 0.2-cm-thick. Thawed and refrozen sediments.
6.0			76			
7.0	2.0		246			1.83-3.90 m Brown organic silt, ice-rich. Cryostructures: combined organic-matrix porphyritic, micro-braided and micro-lenticular, with ice lenses up to 0.3-cm-thick; several ice layers up to 1.5-cm-thick. Syngenetic permafrost.
8.0	2.5					
9.0			157			2.61-2.78 m Grey silt; cryostructure reticulate-braided with ice lenses up to 0.3-cm-thick, at 2.77 m – ice layer 1.5 cm. Presumably buried intermediate layer.
		no data				2.78-2.96 m No data
10.0	3.0		183			2.96-3.50 m Brown organic silt, ice-rich. Cryostructures: micro-braided and micro-lenticular. Syngenetic permafrost.
11.0						

**Figure 5.53.** Cryogenic structure (ice is black) and properties of frozen soil, borehole AUTC-7, depth 0-11.5 ft (0-3.5 m).





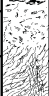

Depth		Ground ice	Moisture content, %		Thaw strain, %	Description of soil
ft	m		grav.	vol.		
12.0			109			3.50-3.90 m Brown organic silt. Cryostructures: micro-braided and micro-lenticular. Syngenetic permafrost.  Grain size, depth 3.55 m: sand 14.6%, silt 69.2%, clay 16.2%.
13.0	4.0		93			3.90-4.35 m Grey silt, with organic material (3% visible). Cryostructures: micro-braided, micro-lenticular, from 4.15 – inclined. Syngenetic permafrost.
14.0			81	77		
15.0	4.5	no data				4.35-4.58 m No data
16.0	5.0		61			
17.0			70			4.58-6.88 m Grey silt, with organic material (3% visible). Cryostructures: micro-braided, micro-lenticular, sometimes inclined; from 5.6 m – several layers with micro-porphyritic cryostructure; at 6.73-6.88 m – presumably contact with wedge-ice. Syngenetic permafrost.  Grain size, depth 6.2 m: sand 18.0%, silt 65.7%, clay 16.3%.
18.0	5.5		76			
19.0	6.0		60	68	0.3	
20.0			102			
21.0	6.5		69	74	16	
22.0			146			6.88-7.00 m Grey silt, with organic material (3% visible), ice-rich. Cryostructure: micro-braided, sub-vertical. Syngenetic permafrost.

**Figure 5.54.** Cryogenic structure (ice is black) and properties of frozen soil, borehole AUTC-7, depth 11.5-23 ft (3.5-7 m).

Depth		Ground ice	Moisture content, %		Thaw strain, %	Description of soil
ft	m		grav.	vol.		
23.0						7.00-7.53 m Grey silt, with organic material (3% visible), mostly ice-rich. Cryostructure: mostly micro-braided, sub-vertical; at 7.36-7.43 m – presumably contact with wedge-ice. Syngenetic permafrost.
24.0						
7.5						
25.0						7.53-11.38 m Wedge-ice, brown-grey, with vertical foliation, abundant air bubbles.
26.0						
8.0						
27.0						
28.0						
8.5						
29.0						10.0-10.95 m Ice-rich breccia. Presumably contact with ice wedge.
30.0						
31.0						
9.5						
32.0						
10.0						
33.0						
34.0						

**Figure 5.55.** Cryogenic structure (ice is black) and properties of frozen soil, borehole AUTC-7, depth 23-34.5 ft (7-10.5 m).



Depth		Ground ice	Moisture content, %		Thaw strain, %	Description of soil
ft	m		grav.	vol.		
35.0						10.50-10.95 m Ice-rich breccia. Presumably contact with ice wedge.
			228			
36.0	11.0					10.95-11.19 m Wedge-ice, brown-grey, with vertical foliation, air bubbles.
37.0						11.19-11.38 m Ice-rich breccia. Presumably contact with ice wedge.
38.0	11.5		73	74	26	11.38-11.82 m Yellow-grey silt. Cryostructure: mostly micro-braided, inclined. Gravimetric moisture content: 73%. From 11.75 – contact with ice wedge. Grain size, depth 11.55 m: sand 15.3%, silt 71.5%, clay 13.2%.
39.0						11.82-11.90 m Wedge-ice, brown-grey, sediment-rich.

**Figure 5.56.** Cryogenic structure (ice is black) and properties of frozen soil, borehole AUTC-7, depth 34.5-39 ft (10.5-11.9 m).

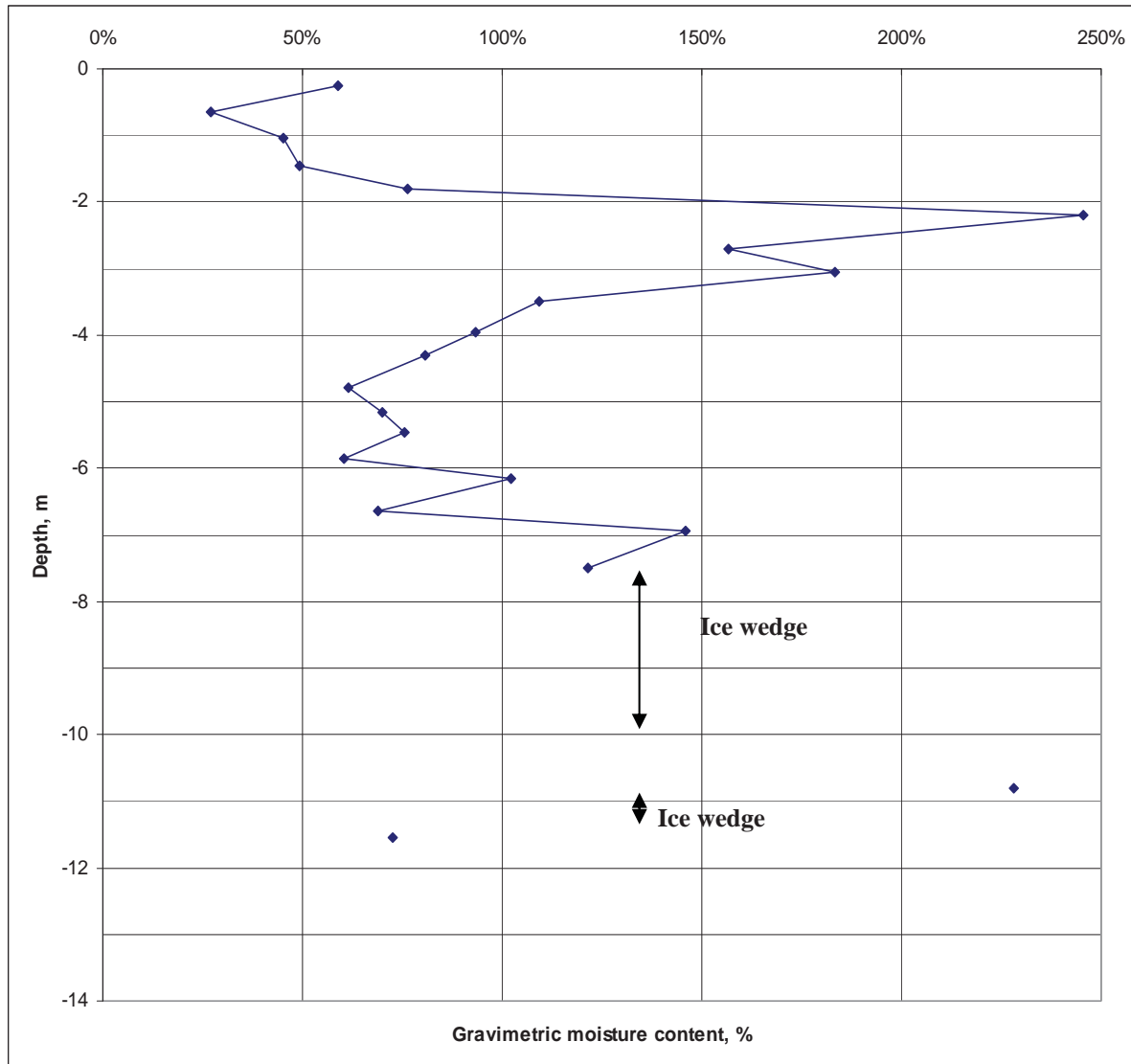


**Figure 5.57.** Gravimetric moisture content of frozen soil, borehole AUTC-7, syngenetic permafrost. From 1 to 1.8 m – thawed and refrozen sediments.



**Figure 5.58.** Silt with reticulate – braided cryostructure, borehole AUTC-7, depth 2.66-2.76 m, gravimetric moisture content 157%.





**Figure 5.59.** Organic silt with micro-braided cryostructure, borehole AUTC-7, depth 3.00-3.08 m, gravimetric moisture content 183%.





**Figure 5.60.** Silt with micro-lenticular – micro-braided cryostructure, borehole AUTC-7, depth 4.25-4.35 m, gravimetric moisture content 81%.





**Figure 5.61.** Silt with braided – micro-braided cryostructure, borehole AUTC-7, depth 11.5-11.6 m, gravimetric moisture content 73%.





**Figure 5.62.** Ice-rich silt, boundary with ice wedge, borehole AUTC-7, depth 11.77-11.9 m.



**Figure 5.63.** Sediment-rich wedge-ice with vertical foliation, borehole AUTC-7, depth 11.9 m.



**Borehole # AUTC08-8 (Figures 5.63-5.72).** May 17, 2008.

Coordinates: Latitude N 65°33'31"; Longitude W 148°54'36".

General description: burned black spruce stand with considerable downed woody debris; higher severity burn than most of the other sites; organic matter thickness ~3-4 cm; organic matter composition is primarily burned dead moss and burned fibric organic matter; ground cover is ~ 20% bare, 70% *Ceratodon*, 10% terrestrial leaf litter.

Vascular Plant Species: *Ledum palustre*, dead *Epilobium angustifolium*, *Vaccinium vitis-idaea*, sparse *Betula papyrifera*, rose.

Moss Species: *Ceratodon purpureus*.

- 0.00-0.14 m Dark-brown peat, ice-rich. Cryostructure: organic-matrix porphyritic to suspended.
- 0.14-0.49 m Brown-grey – yellow-grey silt, with organic material (up to 5%). Cryostructures: micro-braided, micro-braided lenticular. From 0.25 m – porous invisible, with inclined ice veins. At 0.35-0.42 m – dry, friable. At 0.48-0.50 m – inclined ice lenses. Gravimetric moisture content: 32%. Frozen active layer. Permafrost table – 0.49 m.
- 0.49-1.21 m Brown-grey silt, mostly ice-rich. Cryostructures: micro-braided to micro-ataxitic, from 0.75 m – mostly micro-lenticular. Gravimetric moisture content: 89-182%. Contemporary intermediate layer, from 0.75 m – syngenetic permafrost.
- 1.21-2.80 m Wedge-ice. Vertical foliation, air bubbles. At 1.21-1.33 m and 2.31-2.80 m – ice-rich breccia (presumably contact with ice wedge).
- 2.80-6.42 m Brown organic silt with layers of silt and silty peat. Cryostructures: mostly micro-braided (at 4.6-6.1 m – mostly sub-vertical), organic-matrix porphyritic; at 3.5-4.5 m – several inclined ice lenses (veins?) up to 2-cm-thick. Gravimetric moisture content: 93-195%. At 4.82-4.92 m, 5.22-5.43 m, and 6.32-6.42 m – ice-rich breccia (presumably contact with ice wedge).
- 6.42-7.03 m Brown-grey silt, with organic material. Cryostructures: micro-braided, micro-lenticular, inclined. Gravimetric moisture content: 115-150%.
- 7.03-14.24 m Wedge-ice. Vertical foliation, air bubbles. At 13.02-14.24 m – ice-rich breccia (presumably contact with ice wedge).
- 14.24-14.64 m Yellow-grey sandy silt, at 14.55 m – inclusion of weathered gravel 0.4 cm. Cryostructure: lenticular, ice lenses up to 0.05-cm-thick, spacings 2-7 cm. Gravimetric moisture content: 36%. Epigenetic permafrost (presumably thawed and refrozen sediments).



Depth		Ground ice	Moisture content, %		Thaw strain, %	Description of soil
ft	m		grav.	vol.		
						0.00-0.14 m Dark-brown peat, ice-rich. Cryostructure: organic-matrix porphyritic to suspended.
1.0						0.14-0.49 m Brown-grey – yellow-grey silt, with organic material (5% visible). Cryostructures: micro-braided, micro-braided lenticular. From 0.25 m – porous invisible, with inclined ice veins. 0.35-0.42 cm – dry, friable. 0.48-0.50 m – inclined ice lenses. Permafrost table – 0.49 m.
	0.5				32	
2.0						0.49-0.75 m Brown-grey silt, mostly ice-rich. Cryostructures: micro-braided to micro-atactic, Contemporary intermediate layer.
	2.0				182	89
3.0						0.75-1.21 m – Brown-grey silt. Cryostructures: micro-lenticular, micro-braided. Syngenetic permafrost.
	3.0				131	
4.0						
	4.0				89	
5.0						1.21-1.33 m Ice-rich breccia. Presumably contact with ice wedge.
	5.0					
6.0						1.33-2.31 m Wedge-ice, brown-grey, with vertical foliation, air bubbles.
	6.0					
7.0						
	7.0					
8.0						2.31-2.80 m Ice-rich breccia. Presumably contact with ice wedge.
	8.0					
9.0						
	9.0					
10.0						2.80-3.50 m Brown organic silt. Cryostructures: mostly micro-braided, organic-matrix porphyritic. Syngenetic permafrost.
	10.0				123	
	10.0				195	
11.0						
	11.0				141	

**Figure 5.64.** Cryogenic structure (ice is black) and properties of frozen soil, borehole AUTC-8, depth 0-11.5 ft (0-3.5 m).

Depth		Ground ice	Moisture content, %		Thaw strain, %	Description of soil
ft	m		grav.	vol.		
12.0			93	81	2	3.50-4.82 m Brown organic silt. Cryostructures: mostly micro-braided (at 4.6-4.82 m – mostly sub-vertical), organic-matrix porphyritic; at 3.5-4.5 m – several inclined ice lenses (veins?) up to 2-cm-thick. Syngenetic permafrost.
13.0	4.0		130	91		
14.0			157	89		
15.0	4.5		121	82	8	
16.0						4.82-4.92 m Ice-rich breccia. Presumably contact with ice wedge.
17.0	5.0		147			4.92-5.22 m Brown organic silt. Cryostructures: mostly micro-braided sub-vertical. Syngenetic permafrost.
18.0			177			5.22-5.43 m Ice-rich breccia. Presumably contact with ice wedge.
19.0	5.5		125			5.43-5.65 m Brown silty peat. Cryostructures: organic-matrix porphyritic with irregular ice lenses up to 2-cm-thick.
20.0			113			5.65-5.96 m Brown-grey silt, with organic material. Cryostructures: micro-porphyritic, micro-lenticular sub-vertical. Syngenetic permafrost.
21.0	6.0		109			5.96-6.32 m Brown silty peat. Cryostructures: organic-matrix porphyritic with irregular ice lenses up to 1.5-cm-thick. Syngenetic permafrost.
22.0			150			6.32-6.42 m Ice-rich breccia. Presumably contact with ice wedge.
	6.5		150			6.42-7.00 m Brown-grey silt, with organic material. Cryostructures: micro-braided, micro-lenticular, inclined. Syngenetic permafrost.
			118			

**Figure 5.65.** Cryogenic structure (ice is black) and properties of frozen soil, borehole AUTC-8, depth 11.5-23 ft (3.5-7 m).

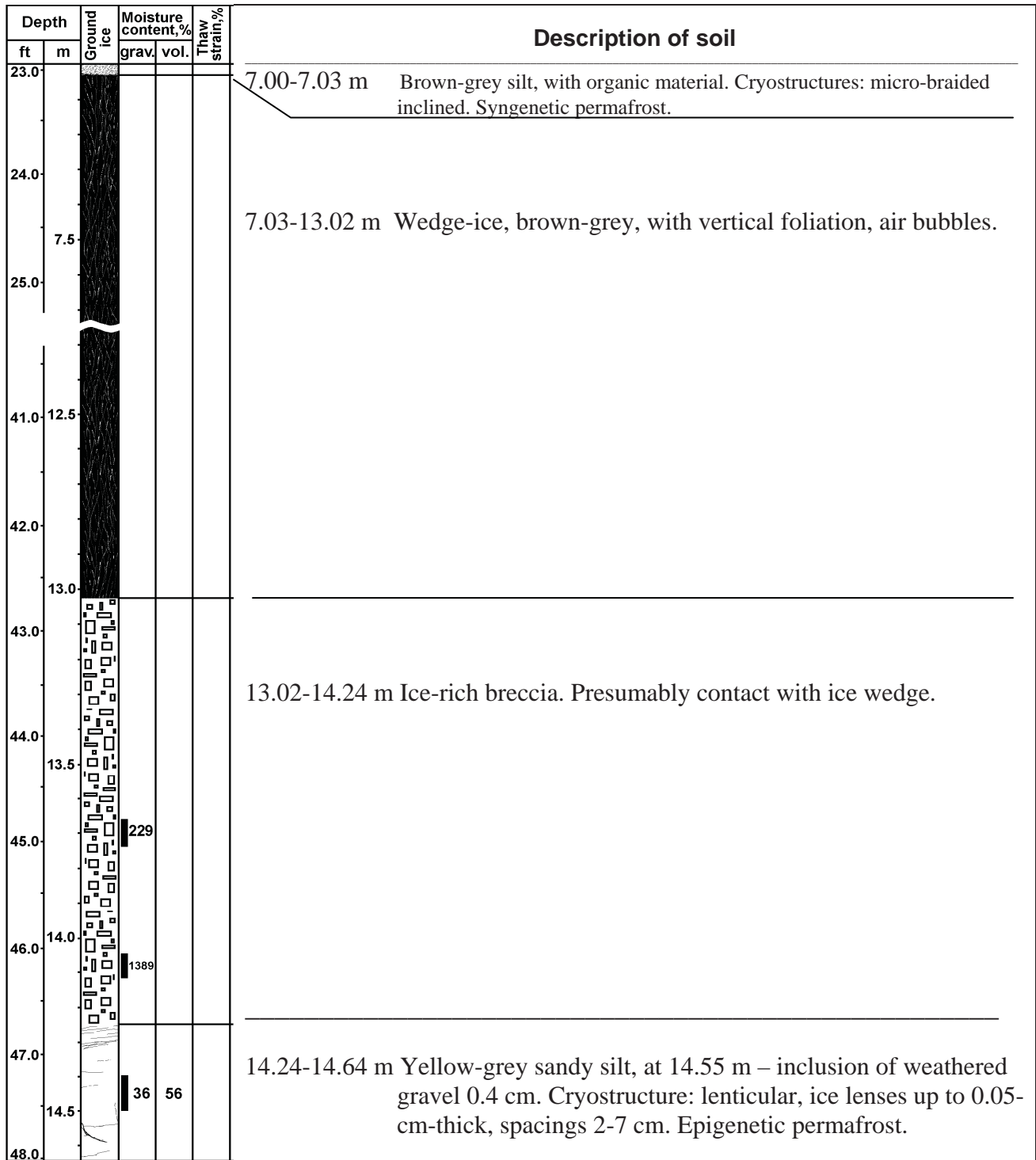


**Figure 5.66.** Cryogenic structure (ice is black) and properties of frozen soil, borehole AUTC-8, depth 23-48 ft (7-14.6 m).



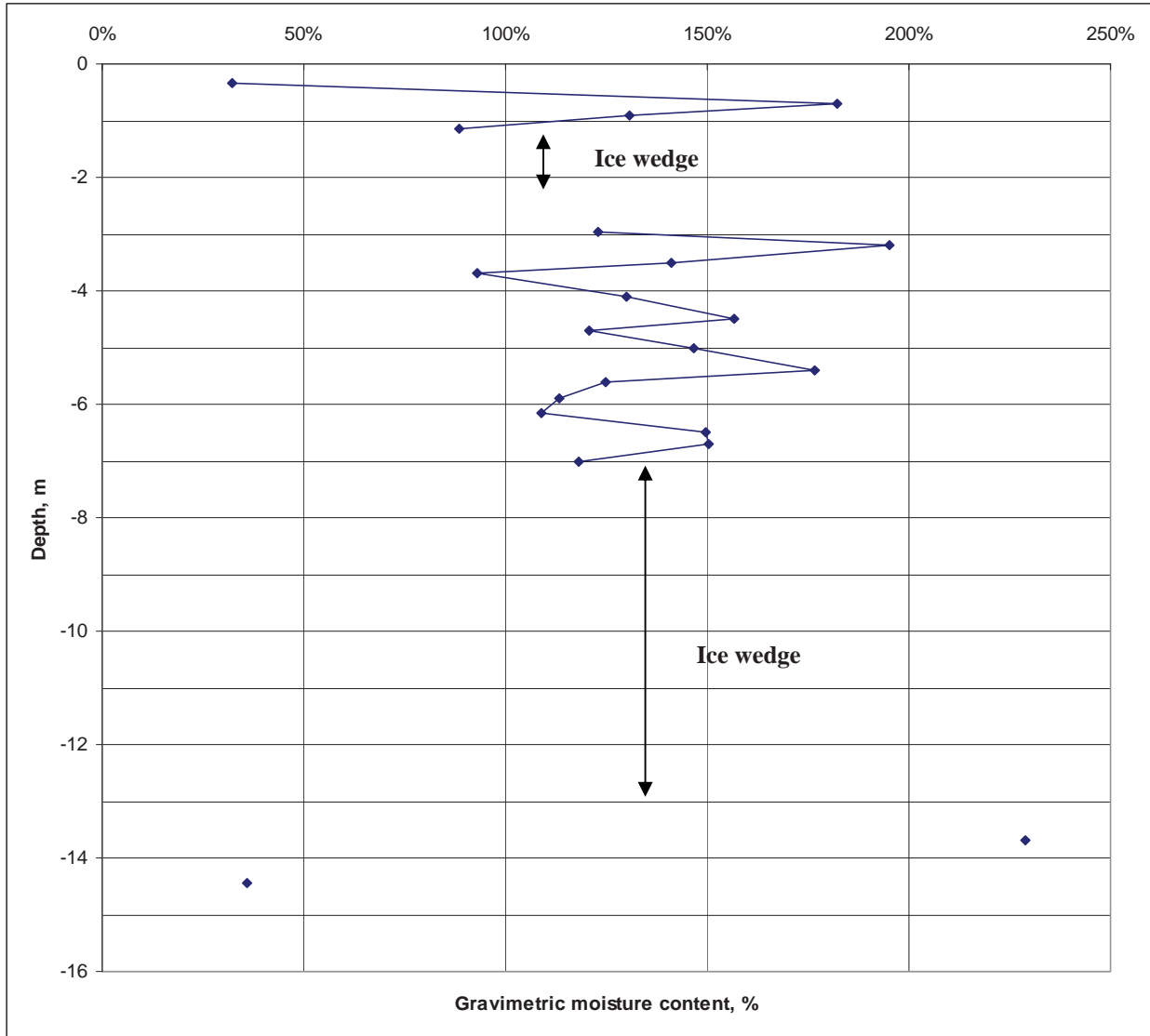


**Figure 5.67.** Gravimetric moisture of frozen soil, borehole AUTC-8 (syngenetic permafrost). From 14.2 m – epigenetic permafrost (presumably thawed and refrozen sediments).



**Figure 5.68.** Silt with micro-braided – micro-ataxitic cryostructure, borehole AUTC-8, depth 0.64-0.72 m, gravimetric moisture content 182%.





**Figure 5.69.** Organic silt with organic-matrix – micro-braided cryostructure, borehole AUTC-8, depth 3.60-3.72 m, gravimetric moisture content 93%.



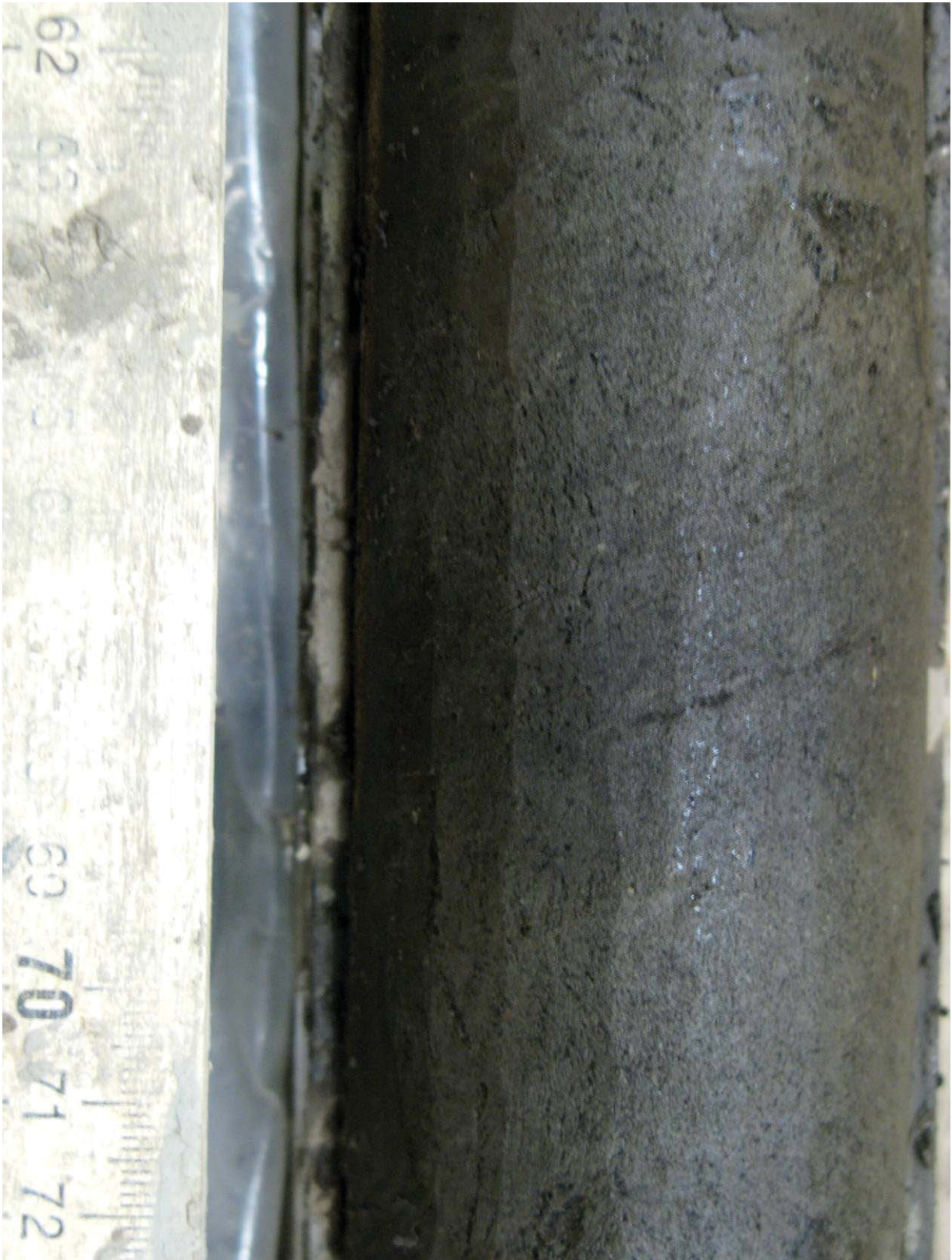


**Figure 5.70.** Organic silt with organic-matrix – micro-braided cryostructure, sub-vertical, borehole AUTC-8, depth 4.67-4.77 m, gravimetric moisture content 121%.



**Figure 5.71.** Silt with micro-braided – micro-lenticular cryostructure, inclined, borehole AUTC-8, depth 6.9-7.0 m, gravimetric moisture content 118%.





**Figure 5.72.** Ice-poor silt with layered – lenticular cryostructure, borehole AUTC-8, depth 14.28-14.43 m, gravimetric moisture content 36% (14.4-14.5 m, almost without visible ice).



**Borehole # AUTC08-9 (Figure 5.73-5.82).** May 18, 2008.

Coordinates: Latitude N 65°33'38"; Longitude W 148°54'43".

General description: burned black spruce stand with considerable downed woody debris; higher severity burn than most of the other sites small and shallow thermokarst pits; several active thermo-erosional gullies (presumably along ice wedges; organic matter thickness ~3-4 cm; organic matter composition if primarily burned dead moss and burned fibric organic matter; ground cover is ~ 20% bare, 70% *Ceratodon*, 10% terrestrial leaf litter.

Vascular Plant Species: *Ledum palustre*, dead *Epilobium angustifolium*, *Vaccinium vitus-idaea*, sparse *Betula papyrifera*, rose.

Moss Species: *Ceratodon purpureus*.

- 0.00-0.10 m Dark-brown peat. Cryostructure: organic-matrix porphyritic.
- 0.10-0.34 m Yellow-grey silt, oxidized, with organic material (up to 3%). Cryostructures: micro-braided, micro-braided lenticular. From 0.19 m – porous invisible. Gravimetric moisture content: 32%. Frozen active layer. Permafrost table – 0.34 m.
- 0.34-1.02 m Grey silt (at 0.54-0.90 m – brown-grey), mostly ice-rich. Cryostructures: mostly micro-braided, ice lenses up to 0.2-cm-thick, from 0.91 m – micro-braided to micro-ataxitic. Gravimetric moisture content: 114-160%. Contemporary intermediate layer.
- 1.02-1.50 m Brown organic silt with layers of grey and yellow-grey silt. Cryostructure: micro-braided.
- 1.50-10.00 m Wedge-ice. Vertically foliated with air bubbles.
- 10.68-14.39 m Brown-grey silt with layers of grey silt and brown-grey organic silt. Cryostructures: micro-braided, micro-porphyritic, micro-ataxitic. Gravimetric moisture content: 54-172%. At 10.68-10.90 m – sub-vertical cryostructure (micro-braided to micro-ataxitic) – presumably contact with ice wedge. At 11.13-11.41 – ice-rich silt (cryostructure: micro-braided to micro-ataxitic). Gravimetric moisture content: 160%. From 12.2 m – mostly ice-poor, with micro-porphyritic and latent micro-lenticular cryostructures; with several ice veins at different depths. Gravimetric moisture content: 47-93%.
- 14.39-16.61 m Wedge-ice. Vertically foliated with air bubbles.
- 16.96-21.35 m Grey silt, with organic material (up to 5%). Cryostructures: micro-braided, micro-lenticular, latent micro-lenticular, ice lenses up to 0.05 cm. At 17.95-18.13 m, 19.0-20.7 m silt is mostly ice-rich, with micro-braided cryostructure (sometimes – combined with micro-ataxitic cryostructure), ice lenses up to 0.1 cm. At 17.97 m, 19.92 m, 21.2-21.3 m – ice lenses up to 1 cm. Gravimetric moisture content: 51-166%.

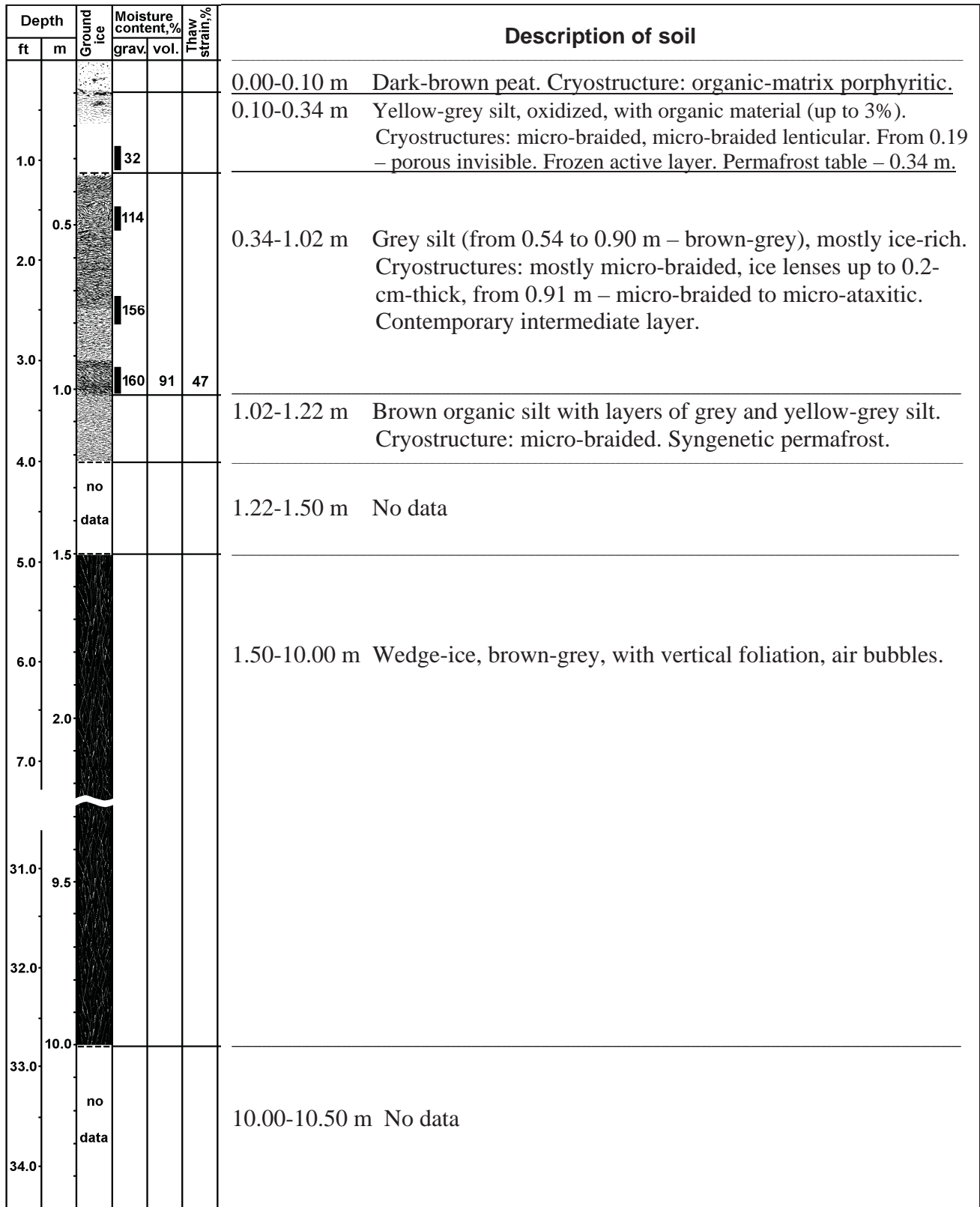





**Figure 5.73.** Cryogenic structure (ice is black) and properties of frozen soil, borehole AUTC-9, depth 0-34.5 ft (0-10.5 m).

Depth		Ground ice	Moisture content, %		Thaw strain, %	Description of soil
ft	m		grav.	vol.		
		no data				10.50-10.68 m No data
35.0			127	85	40	10.68-12.05 m Brown-grey silt with layers of grey silt and brown-grey organic silt. Cryostructures: micro-braided, micro-porphyrritic, micro-ataxitic, micro-lenticular. From 10.68 to 10.90 m – sub-vertical cryostructure, micro-braided to micro-ataxitic (presumably near the contact with ice wedge). From 10.90 to 11.13 m – mostly micro-lenticular cryostructure. From 11.13 to 11.41 m – ice-rich silt with micro-braided to micro-ataxitic cryostructure. From 11.41 to 11.94 m – mostly ice-poor soil with micro-porphyrritic cryostructure. From 11.94 to 12.05 m – ice-rich soil with micro-braided cryostructure. Syngenetic permafrost.
36.0	11.0		172			
37.0			54			
38.0	11.5		160	94	31	
39.0	12.0	no data				12.05-12.20 m No data
40.0			62			12.20-13.57 m Brown-grey silt with layers of grey silt and brown-grey organic silt, mostly ice-poor, with micro-porphyrritic and latent micro-lenticular cryostructures; with several ice veins at different depths. Syngenetic permafrost.
41.0	12.5		70	70	0.3	
42.0			93	81	2.5	
43.0	13.0		91	68		
44.0	13.5	no data				13.57-13.73 m No data
45.0			62	71	8	13.73-14.00 m Grey silt, ice-poor, with micro-porphyrritic cryostructure, with ice veins. Syngenetic permafrost.

**Figure 5.74.** Cryogenic structure (ice is black) and properties of frozen soil, borehole AUTC-9, depth 34.5-46 ft (10.5-14 m).



Depth		Ground ice	Moisture content, %		Thaw strain, %	Description of soil
ft	m		grav.	vol.		
46.0						14.00-14.39 m Grey silt, ice-poor, with micro-porphyritic cryostructure, with ice veins. Syngenetic permafrost.
47.0			47			
48.0	14.5					
49.0	15.0					14.39-16.61 m Wedge-ice, brown-grey, with vertical foliation, air bubbles.
52.0	16.0					
53.0						
54.0	16.5					
55.0			no data			16.61-16.96 m No data
56.0	17.0		59	70		16.96-18.00 m Grey silt, with organic material (5% visible). Cryostructures: micro-braided, micro-lenticular, latent micro-lenticular, ice lenses up to 0.05 cm. At 17.97 m – ice lenses up to 1 cm. Syngenetic permafrost.
57.0			51	64	19	
58.0	17.5		58			

**Figure 5.75.** Cryogenic structure (ice is black) and properties of frozen soil, borehole AUTC-9, depth 46-59 ft (14-18 m).

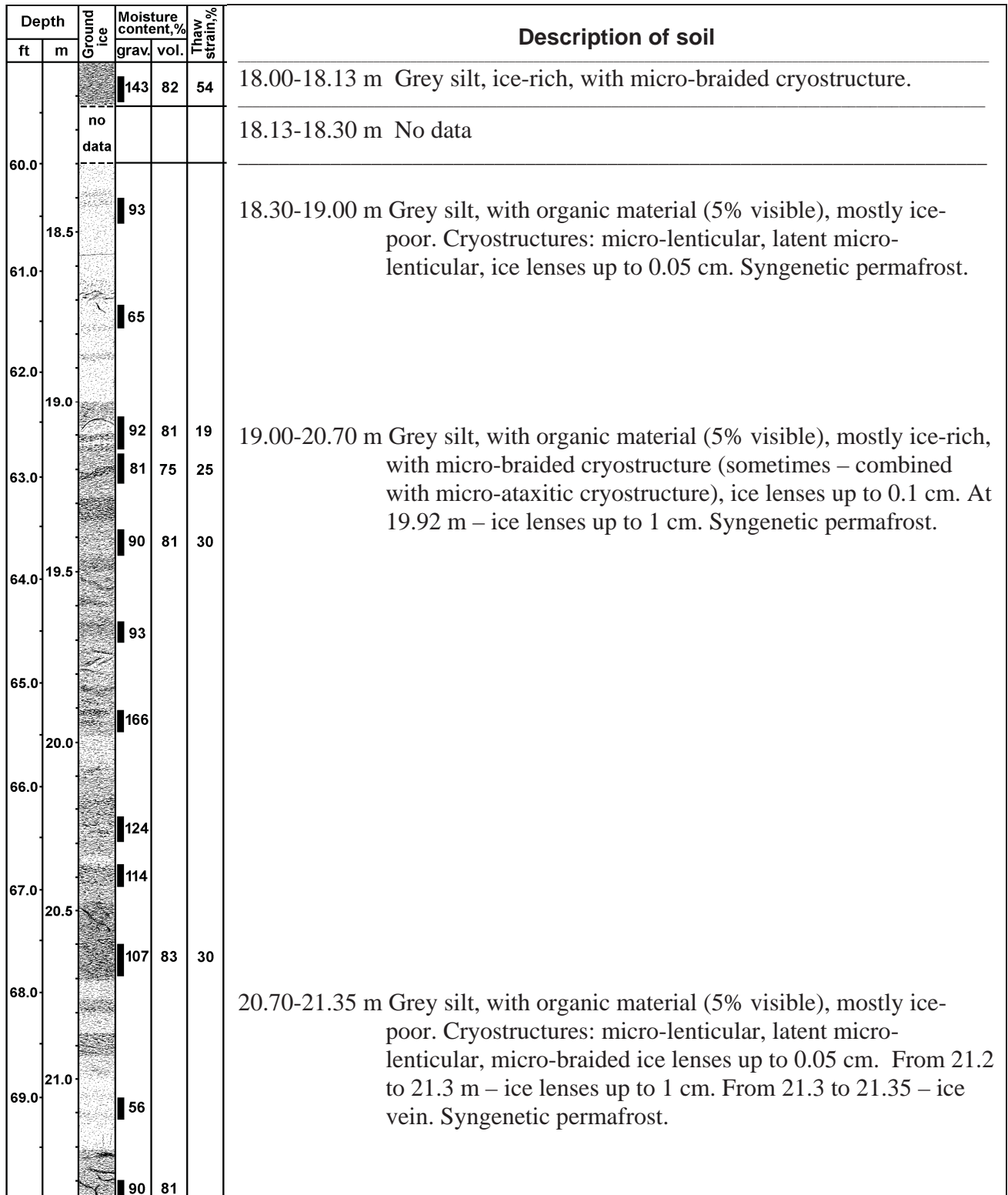


**Figure 5.76.** Cryogenic structure (ice is black) and properties of frozen soil, borehole AUTC-9, depth 59-70 ft (18-21.35 m).

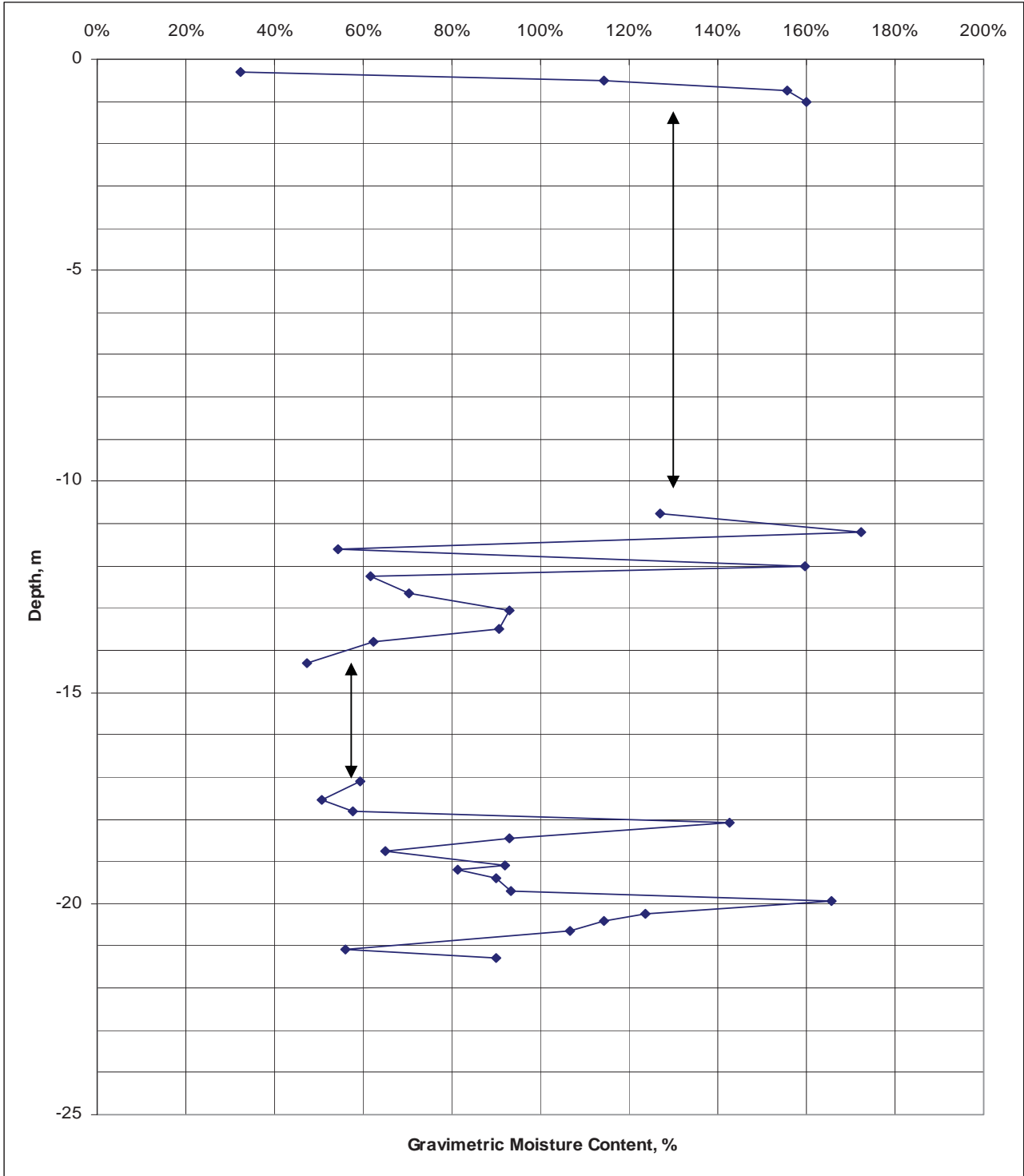


**Figure 5.77.** Gravimetric moisture content of frozen soil, borehole AUTC-9 (syngenetic permafrost).





**Figure 5.78.** Silt with micro-braided – micro-ataxitic cryostructure, borehole AUTC-9, depth 0.91-1.02 m, gravimetric moisture content 160%.





**Figure 5.79.** Silt with latent micro-lenticular – micro-porphyrific cryostructure, with small ice veins, borehole AUTC-9, depth 13.75-13.85 m, gravimetric moisture content 62%.





**Figure 5.80.** Silt with latent micro-lenticular – micro-lenticular cryostructure, borehole AUTC-9, depth 17.44-17.55 m, gravimetric moisture content 51%.





**Figure 5.81.** Silt with micro-braided – micro-lenticular cryostructure, borehole AUTC-9, depth 19.16-19.28 m, gravimetric moisture content 81%.





**Figure 5.82.** Silt with micro-braided – micro-lenticular cryostructure, with ice veins, borehole AUTC-9, depth 21.30-21.35 m, gravimetric moisture content 90%.

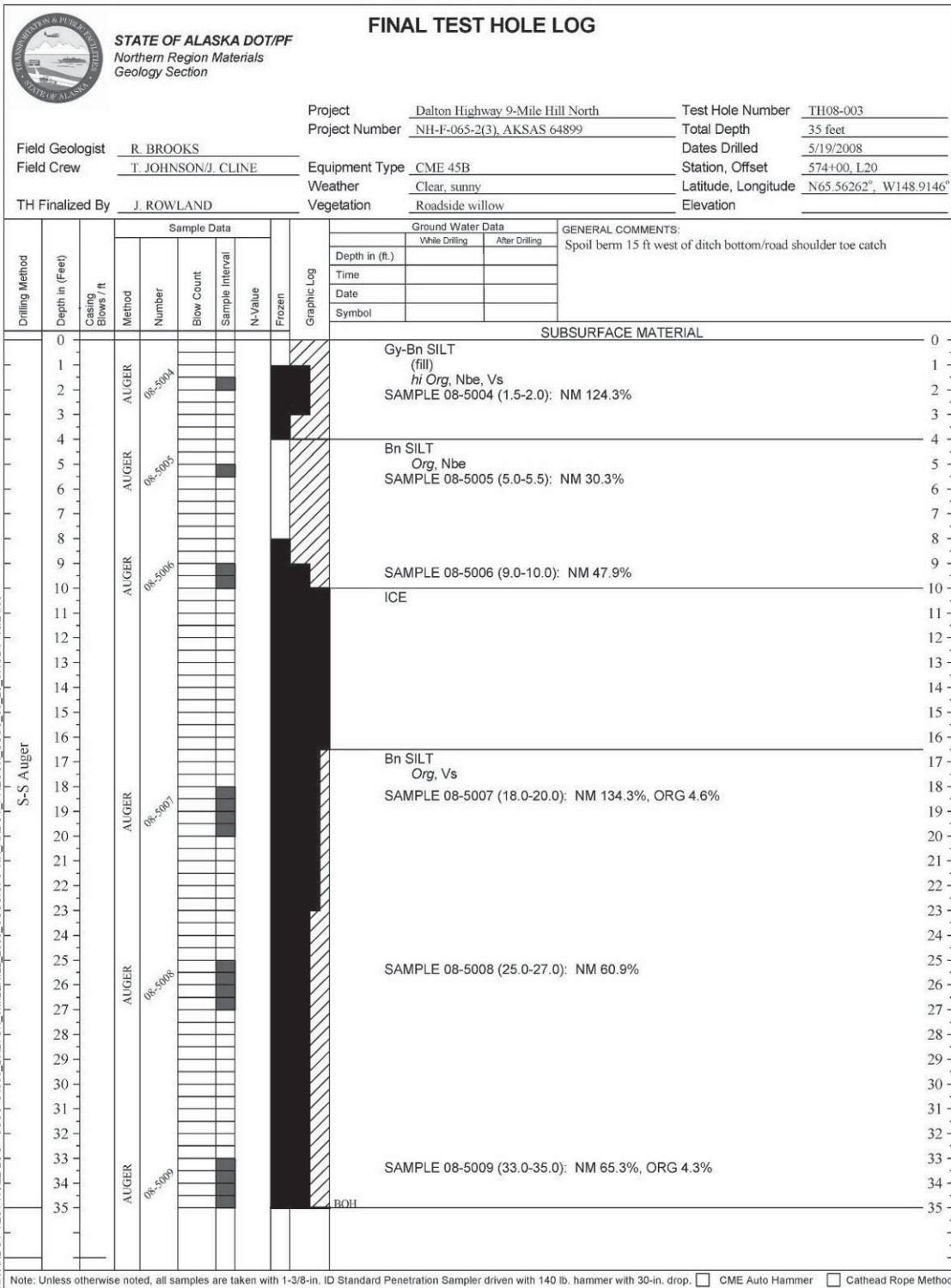


**Figure 5.83.** Example of DOT drilling log, Dalton Highway Innovation Project, test hole TH08-003 (for location, see **Figure 5.96**, DOT borehole #3).



### **5.3. Soil characteristics**

#### **Grain-size**

The grain-size of the sediments was found for 25 samples from six boreholes (AUTC08-2 – AUTC08-7). Soils in the study area are mostly silts with content of silt particles 70-80% (**Fig. 5.84**). Sand does not exceed 15%, and content of clay reaches 15-20% in several samples. The similarity of curves shows that the sediments in the study area are mostly uniform. According to AKDOT&PF data, contents of organic matter vary from 2% to 20% with the average value of 6.7% (**Fig. 5.85**). In the most of AUTC boreholes (except AUTC08-2 and AUTC08-5), horizons of organic silt or silty peat were encountered at different depths. For example, in the borehole AUTC08-4 soils rich in organic matter prevail in the depth interval 4.5-7.5 m, in the borehole AUTC08-7 – 1.5-4 m, and in the borehole AUTC08-8 – 3-6.5 m.

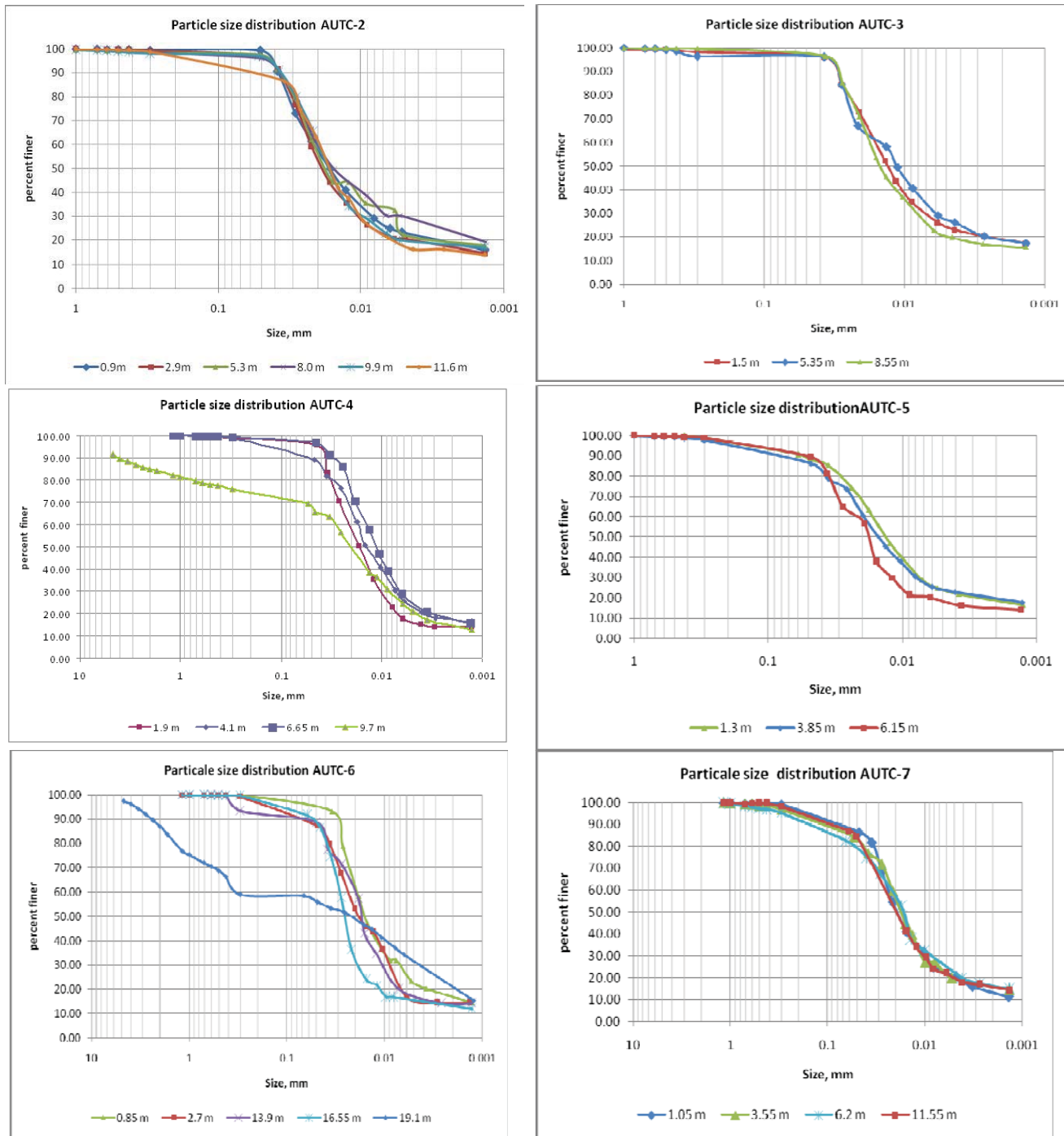
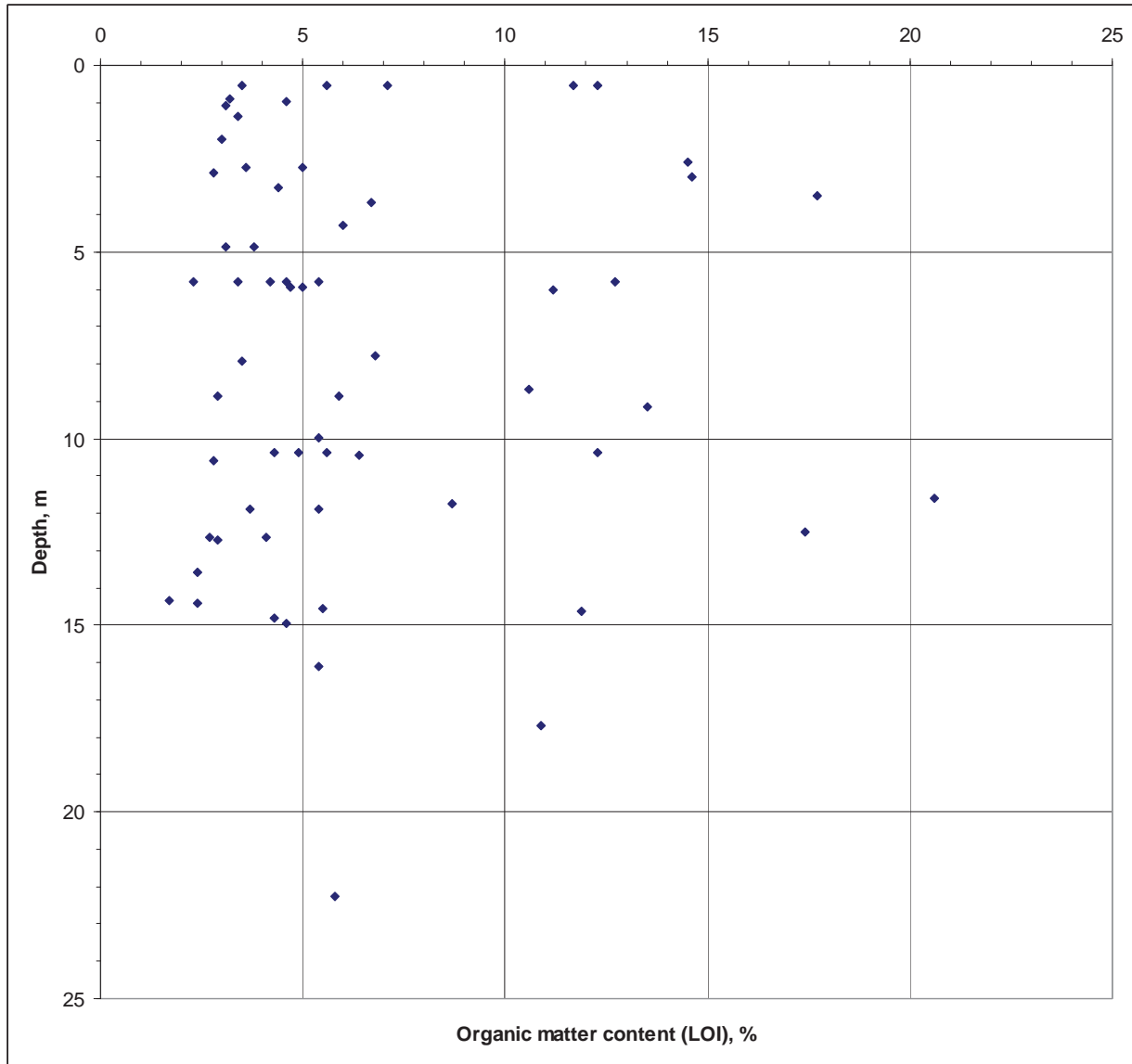


Figure 5.84. Grain size distribution, boreholes AUTC-2 – AUTC-7.





## Moisture content of soil between ice wedges

Gravimetric moisture content of soil between ice wedges was found for 189 samples from all boreholes. Volumetric moisture content was evaluated for 99 samples with measured volume. Moisture content of soil is presented in boreholes logs and summarized in **Figures 5.86** and **5.87**.

**Figure 5.86** shows distribution of gravimetric moisture content with depth. This diagram is based on the data from eight AUTC boreholes (189 samples). The wide range of gravimetric moisture content values (from ~40% up to 200% and more), which does not change significantly with depth, is typical for syngenetic permafrost. Average gravimetric moisture content is 85.5%. The lowest values (20-40%) are evidence that soil was thawed and later refrozen.

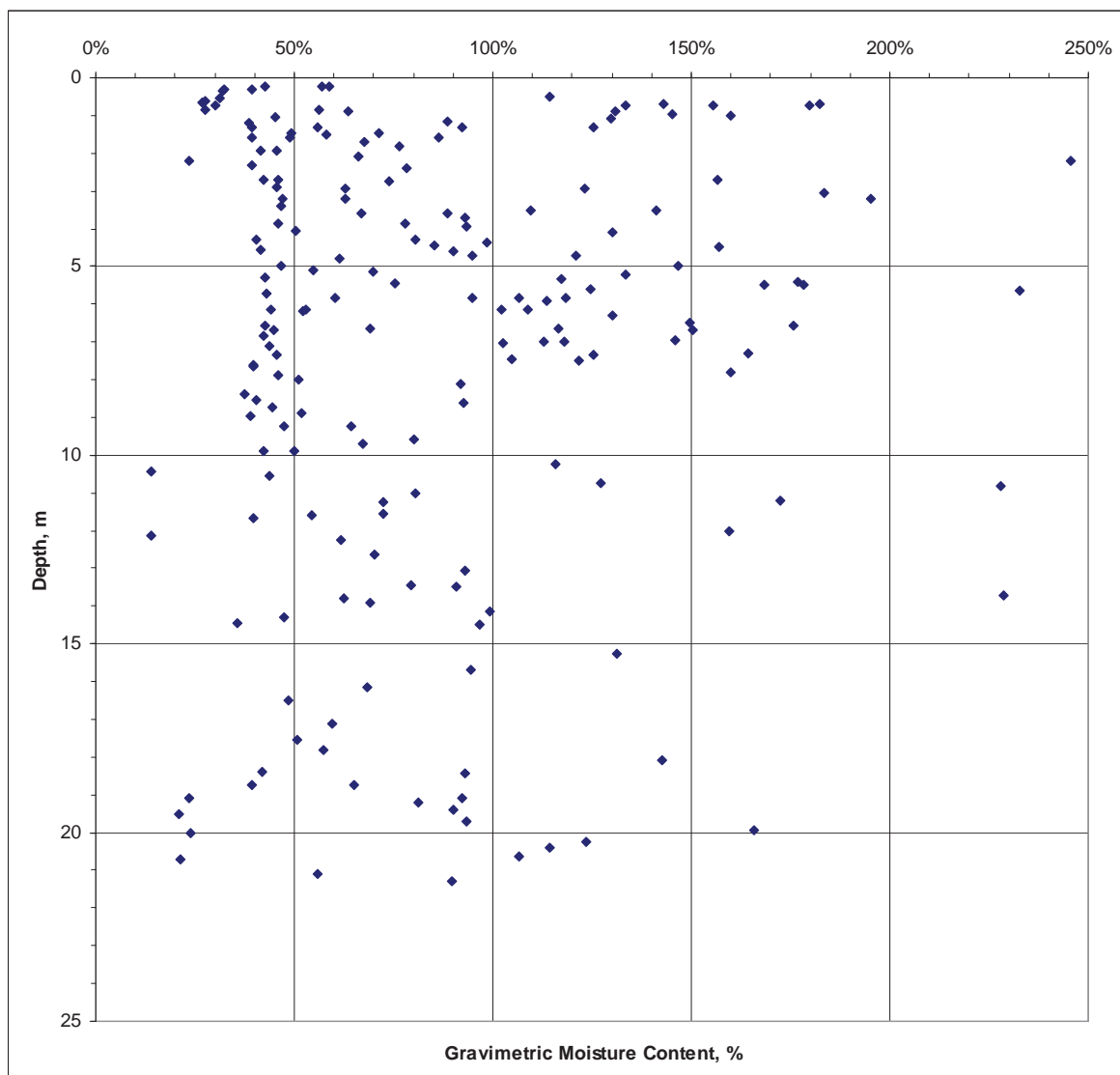


**Figure 5.86.** Gravimetric moisture content (without wedge ice) with depth (based on the data from eight AUTC boreholes, 189 samples). Average value: 85.5%.

**Figure 5.87** shows correlation between volumetric and gravimetric moisture content and can be used in future projects in areas with similar soils. Volumetric moisture content includes visible (segregated) and invisible (pore) ice, but does not include massive ice. Wedge-ice is the main type of massive ice in syngenetic permafrost and the only one recognized in boreholes in the studied area. It was found in most of AUTC and ADOT boreholes but its occurrence varies along the alignment.

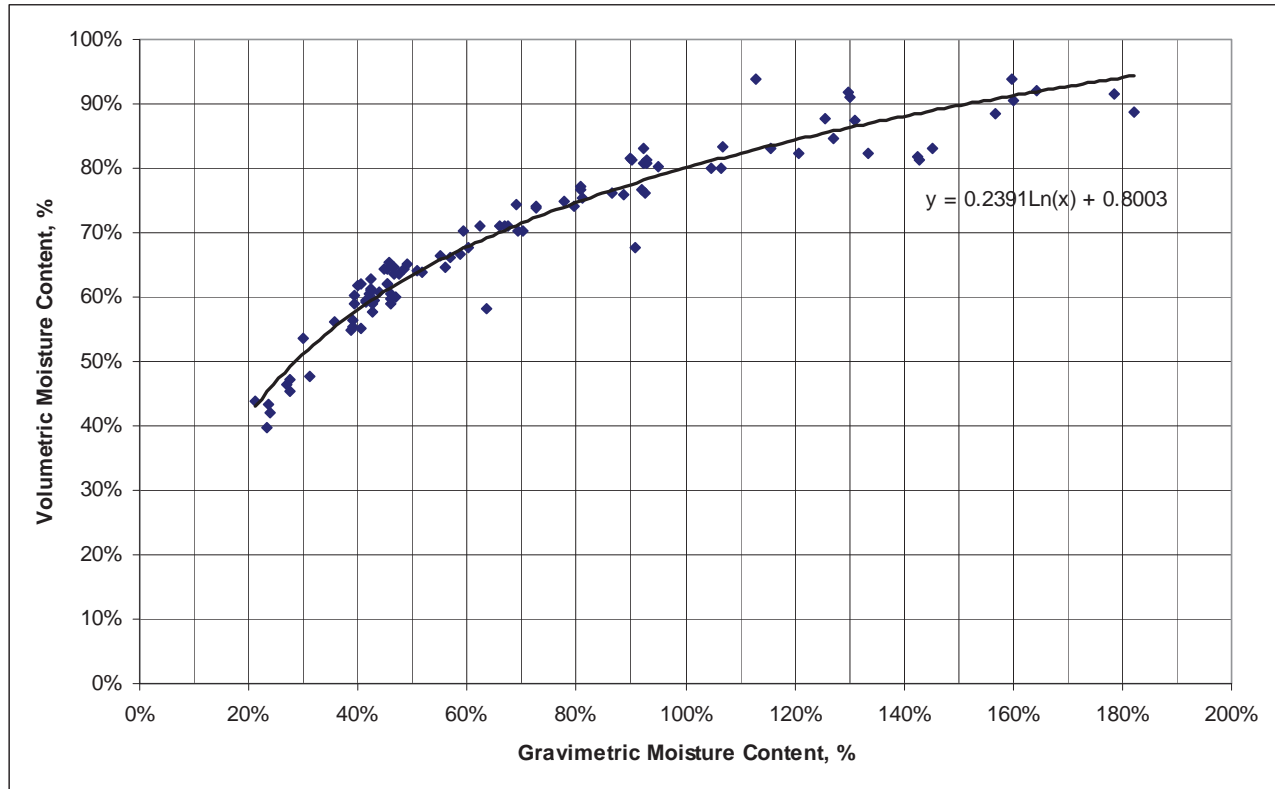


**Figure 5.87.** Volumetric vs gravimetric moisture contents (based on 99 samples with measured volume from eight AUTC boreholes).

#### ***5.4. Identification of alignment sections with different permafrost properties***

On the base of the wedge-ice distribution we identified four sections, two of which (sections 1 and 3) can be defined as rich in massive ice and two (sections 2 and 4) as poor in massive ice (**Figures 5.88, 5.89**). In further discussion they are defined as ice-rich and ice-poor sections. General characteristics of these sections are shown in **Table 5.1**. For the ice-rich section #1 wedge-ice was observed in 24 boreholes of 26 and for the section 3 it was found in eight boreholes of nine. In the section 2, wedge-ice was found in one borehole of 12 and in the section 4 in one borehole of 15. Wedge-ice occurs especially often in the section 3, where it occupies 47% of combined length of all boreholes.

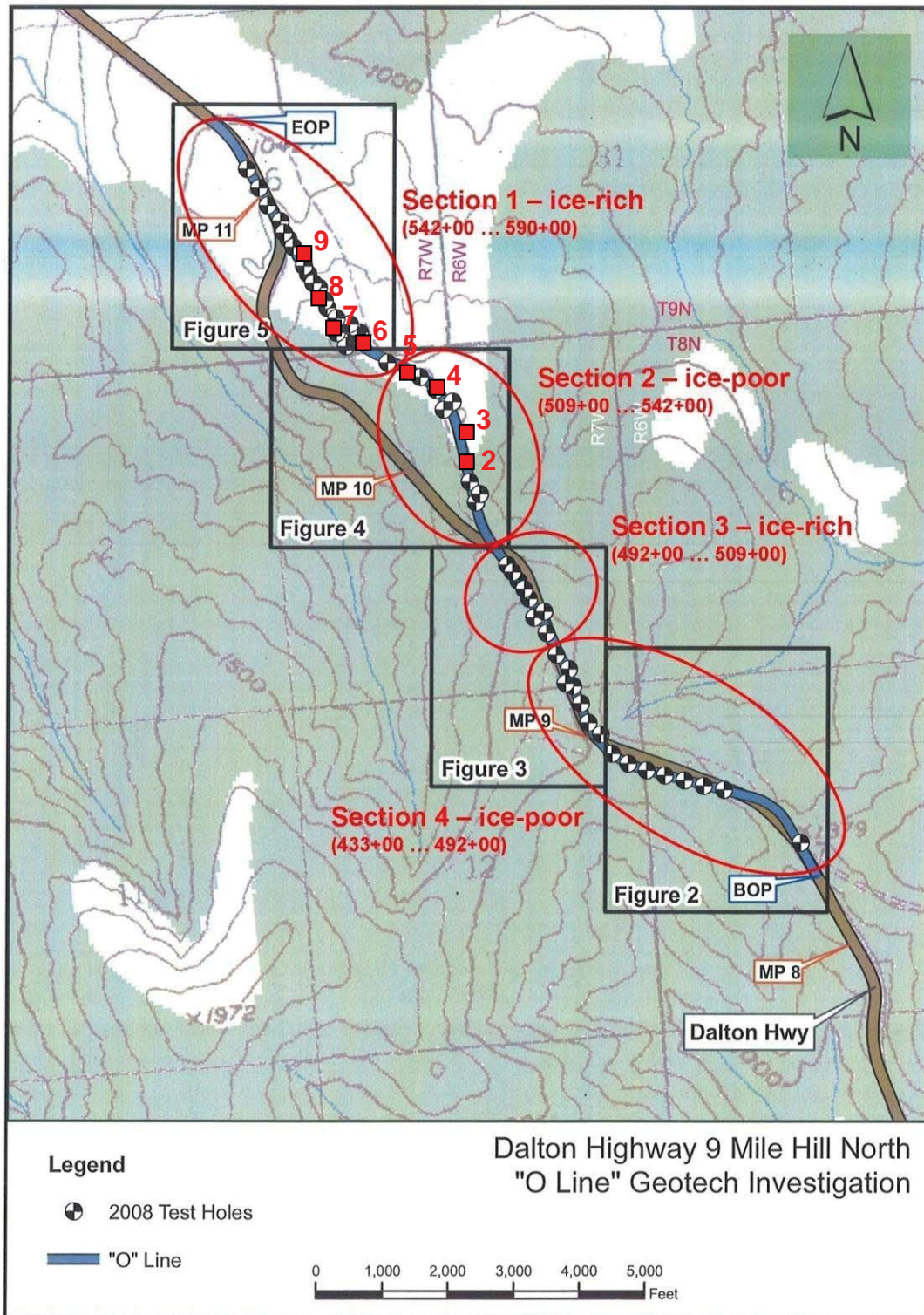
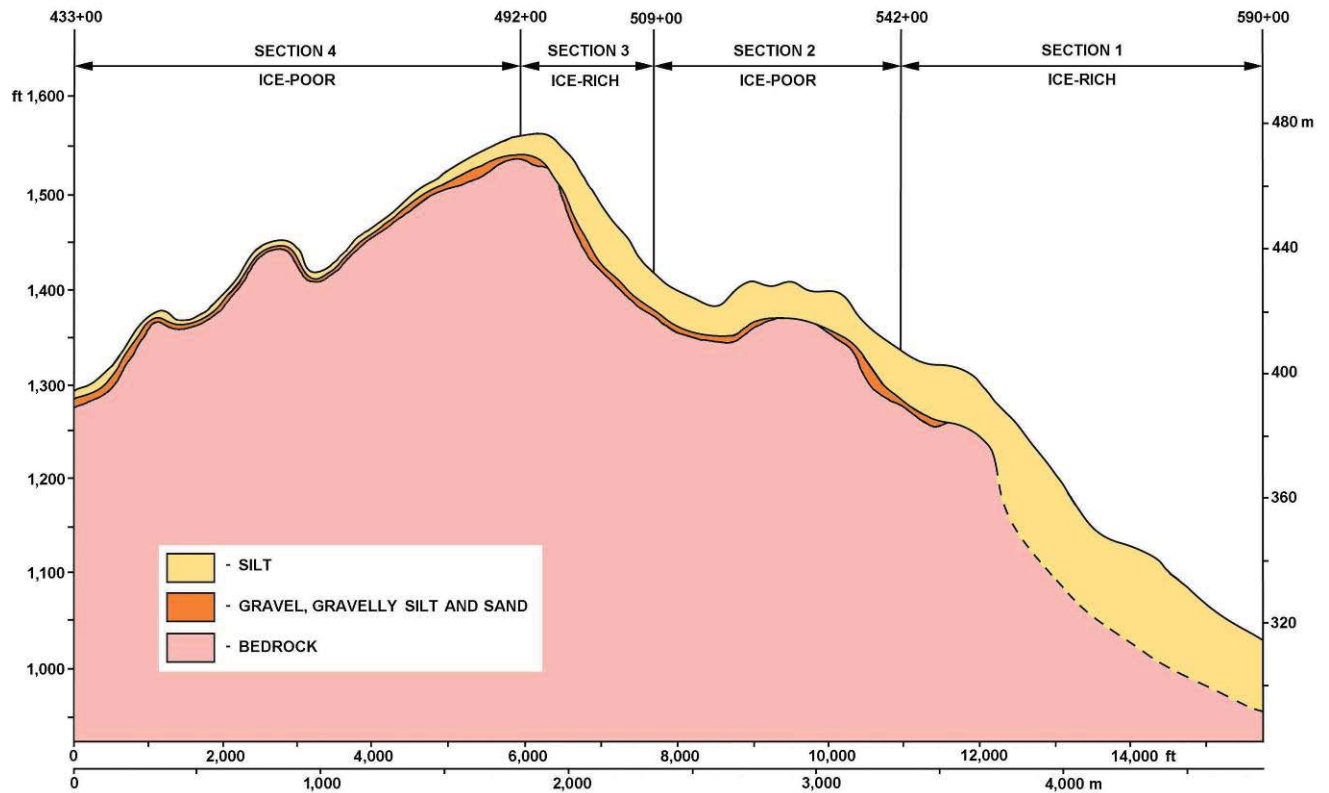


Figure 5.88. Ice-rich and relatively ice-poor sections (map).





**Figure 5.89.** Division of alignment in ice-rich and relatively ice-poor sections (profile).

**Table 5.1.** General characteristics of sections of ice-rich and relatively ice-poor sections. Based on drilling logs, AUTC and DOT boreholes.

	Sections			
	1 (ice-rich)	2	3 (ice-rich)	4
Number of AUTC boreholes	4	4	-	-
Number of DOT boreholes	22	8	9	15
Total number of boreholes	26	12	9	15
Number of boreholes with wedge ice	24	1	8	1
Wedge-ice occurrence, %	34.7	2.4	47.0	3.1
Thickness of silt, ft (m)	<b>52...&gt;85</b> (16...>26)	<b>31...39</b> (9.5...12)	<b>30...46</b> (9...14)	<b>2...13</b> (0.6...4)
Thickness of gravel over bedrock, ft (m)	<b>0...11</b> (0...3.4)	<b>0...16</b> (0...5)	<b>0...5</b> (0...1.6)	<b>1...7</b> (0.4...2.1)

Wedge-ice occurrence was estimated for different sections on the base of data from all boreholes (both AUTC and DOT). **Table 5.2** shows wedge-ice occurrence in the sections 1-4 calculated for different depth intervals as a percentage of the length of core with wedge-ice in the total length of core collected for these intervals. For example, if 26 boreholes are deeper than 5 m, the total length of core (gravel and bedrock core was not taken into account) for the depth interval from 4 to 5 m will be 26 meters. If 11.8 m of this core consist of wedge ice, it means that the wedge-ice occurrence for this depth interval will be  $11.8 \text{ m} / 26 \text{ m} * 100\% = 45.4\%$ .

**Table 5.2.** Wedge-ice occurrence at different depth intervals, sections 1-4.

Depth interval, m	Section 1			Section 2			Section 3			Section 4		
	Length of core with wedge-ice, m	Total length of core, m	Wedge-ice volume, %	Length of core with wedge-ice, m	Total length of core, m	Wedge-ice volume, %	Length of core with wedge-ice, m	Total length of core, m	Wedge-ice volume, %	Length of core with wedge-ice, m	Total length of core, m	Wedge-ice volume, %
0-1	0	26	<b>0</b>	0	12	<b>0</b>	0	9	<b>0</b>	0	15	<b>0</b>
1-2	3.8	26	<b>14.6</b>	0.1	12	<b>0.8</b>	0	9	<b>0</b>	0	7	<b>0</b>
2-3	9	26	<b>34.6</b>	1.0	12	<b>8.3</b>	1	9	<b>11.1</b>	0	4	<b>0</b>
3-4	12.4	26	<b>47.7</b>	1.0	12	<b>8.3</b>	1.5	9	<b>16.7</b>	0.9	3	<b>30.0</b>
4-5	11.8	26	<b>45.4</b>	1.0	12	<b>8.3</b>	3.8	9	<b>42.2</b>			
5-6	9.6	26	<b>36.9</b>	0	12	<b>0</b>	4.3	9	<b>47.8</b>			
6-7	13.6	26	<b>52.3</b>	0	12	<b>0</b>	4.9	9	<b>54.4</b>			
7-8	14.8	26	<b>56.9</b>	0	11	<b>0</b>	5.3	8	<b>66.3</b>			
8-9	14.1	26	<b>54.2</b>	0	11	<b>0</b>	6.9	8	<b>86.3</b>			
9-10	12.4	24	<b>51.7</b>	0	9	<b>0</b>	6.4	7	<b>91.4</b>			
10-11	9.1	24	<b>37.9</b>	0	7	<b>0</b>	5.7	7	<b>81.4</b>			
11-12	6.6	21	<b>31.4</b>	0	4	<b>0</b>	4.1	7	<b>58.6</b>			
12-13	5.2	19	<b>27.4</b>	0	1	<b>0</b>	4.0	4	<b>100</b>			
13-14	3.2	16	<b>20.0</b>	0	1	<b>0</b>	2.3	3	<b>76.7</b>			
14-15	1.8	15	<b>12.0</b>				0	1	<b>0</b>			
15-16	2.1	13	<b>16.2</b>									
16-17	2.9	10	<b>29.0</b>									
17-18	1.9	5	<b>38.0</b>									
18-19	1.1	4	<b>27.5</b>									
19-20	1.2	3	<b>40.0</b>									
20-21	0.4	2	<b>20.0</b>									
21-22	0	1	<b>0</b>									
22-23	0	1	<b>0</b>									
23-24	0	1	<b>0</b>									
24-25	0	1	<b>0</b>									
25-26	0	1	<b>0</b>									
Total	137.0	395	<b>34.7</b>	3.1	127.7	<b>2.4</b>	50.2	108	<b>47.0</b>	0.9	29	<b>3.1</b>

**Figure 5.90** shows the wedge-ice occurrence with depth, estimated for the ice-rich sections #1 and #3. Wedge-ice occurrence significantly increases from the depths of 3-4 meters. It means that significant part of ice wedges are covered by the layer of thawed and refrozen sediments (this layer was distinguished in several AUTC boreholes). Absence of ice wedges in the upper one meter of sequence can be explained by occurrence of intermediate layer beneath the active layer.

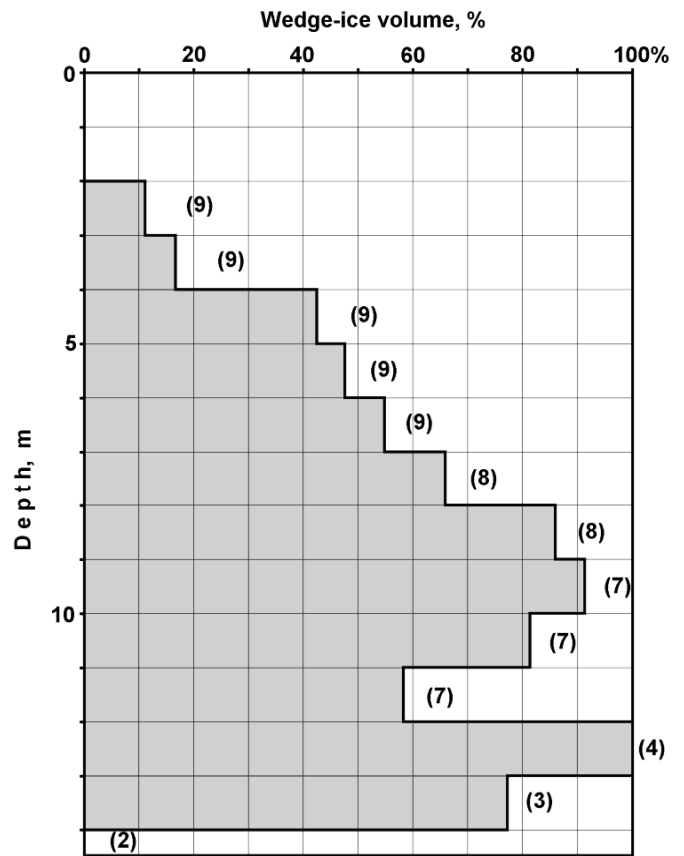
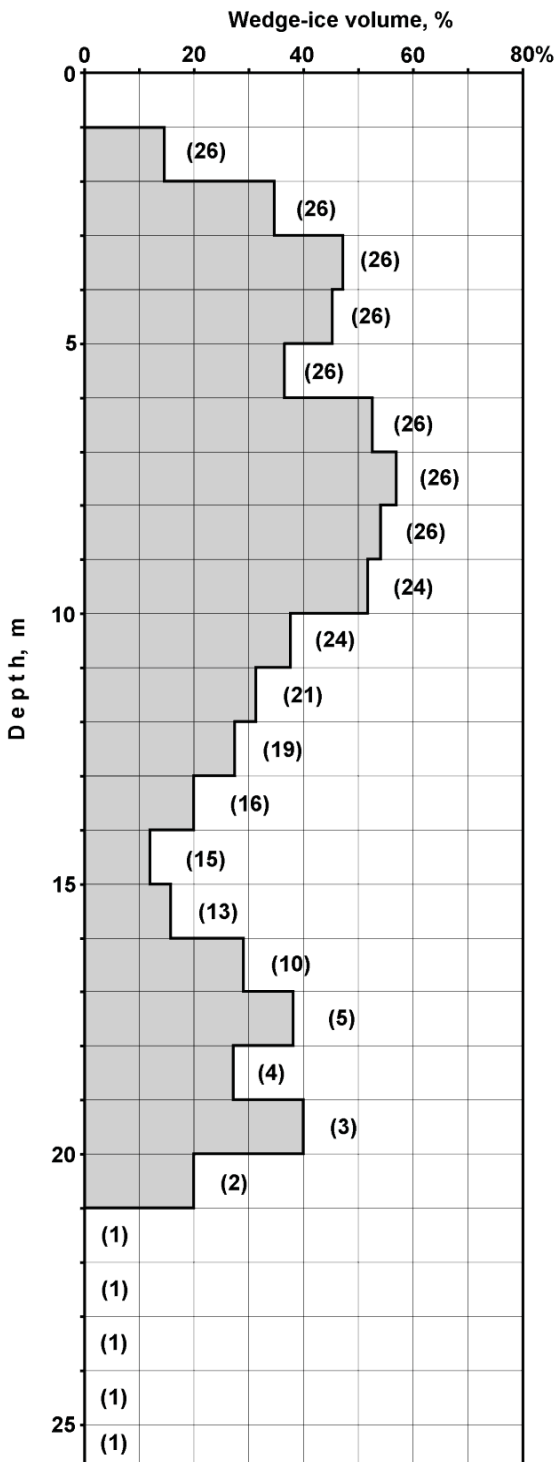


**Figure 5.90.** Wedge-ice occurrence with depth, sections #1 (left) and #3 (right). Numbers in parentheses show number of boreholes (both AUTC and DOT), which reached this depth interval. For locations of sections #1 and #3, see **Figures 5.88, 5.89.**



**Section #1 (542+00...590+00)** has a thick sequence of ice-rich syngenetically frozen silt (from 12 m to more than 26 m) with very high wedge-ice occurrence (35%). Wedge-ice distribution (**Fig. 5.90**) in this section can be described as following:

- from 0 to 1 m wedge-ice was not observed;
- from 1 to 8 m wedge-ice occurrence steadily increases (up to 57%);
- from 1 to 2 m – less than 15% in wedge-ice occurrence;
- from 3 to 10 m – more than 40% in wedge-ice occurrence,
- from 6 to 10 m wedge-ice occurrence exceeds 50% (measurements in 24-26 boreholes);
- from 8 to 15 m wedge-ice occurrence steadily decreases (up to 12%);
- from 15 to 20 m – new increase (up to 20-40%);
- from 21 m wedge-ice was not observed (only one borehole reached this depth).

Increase in the wedge-ice amounts from the depths of 2-3 meters we relate to occurrence of the layer of thawed and refrozen sediments on top of permafrost sequence (was observed in AUTC boreholes 6 and 7).

Average values of gravimetric moisture content of perennially frozen silt are 102% (based on the samples from four AUTC boreholes) and 103% (based on the samples from 22 DOT boreholes). Distribution of ice content with depth shows significant random variations typical of syngenetic permafrost (**Fig. 5.91**). The lowest values ( $MC_{grav} < 40-50\%$ ) were obtained mostly from the depth interval from 0 to 3 m (they correspond to the active layer and the layer of thawed and refrozen sediments encountered by several boreholes) and from 14 to 21 m (gravelly soil and bedrock in several boreholes). Distribution of ground ice volume (due to pore, segregated, and wedge ice) with depth in section #1 is shown in **Figure 5.92**.

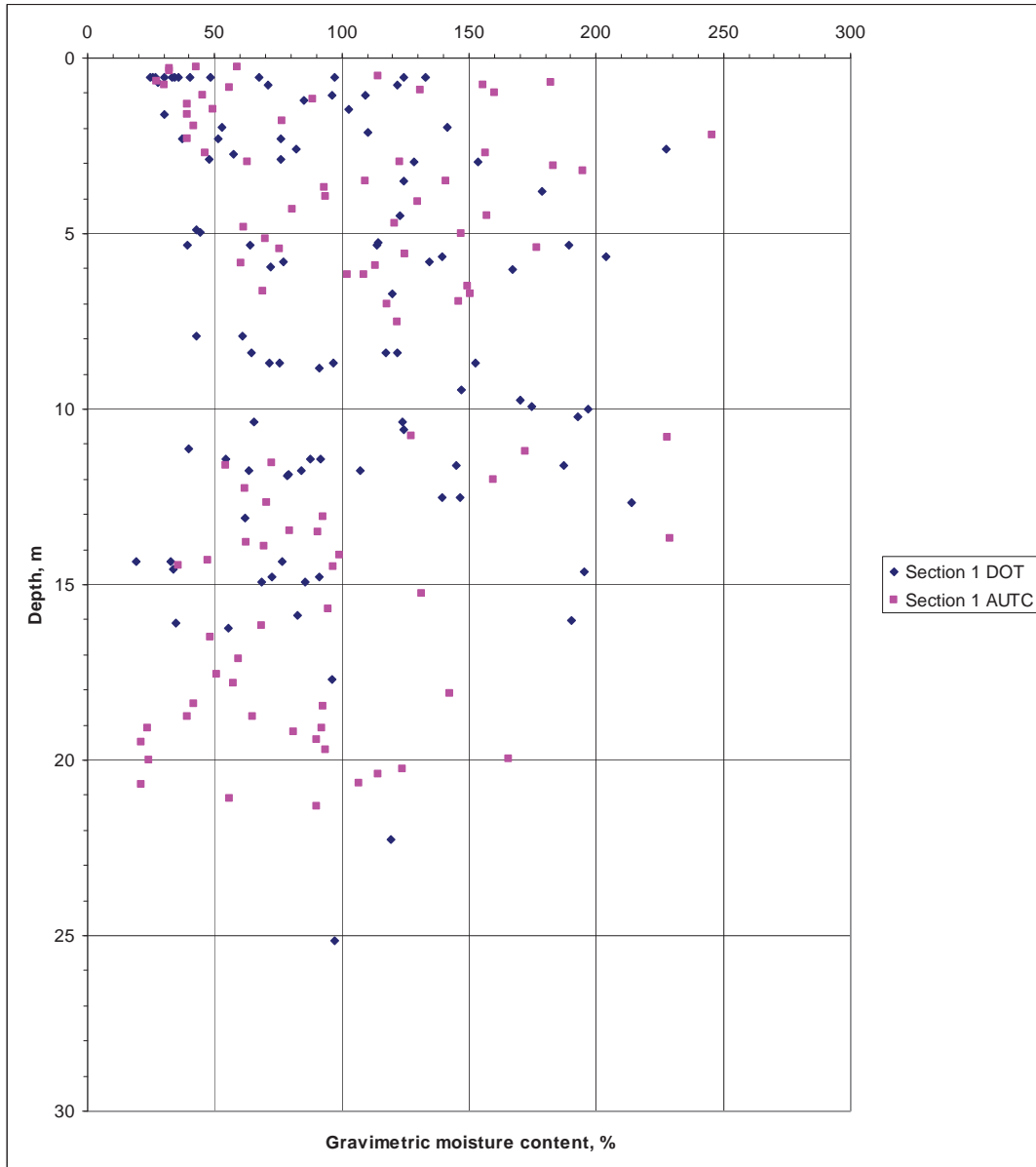


**Figure 5.91.** Gravimetric moisture content with depth, Section #1, based on DOT and AUTC data (four and 22 boreholes, correspondingly).

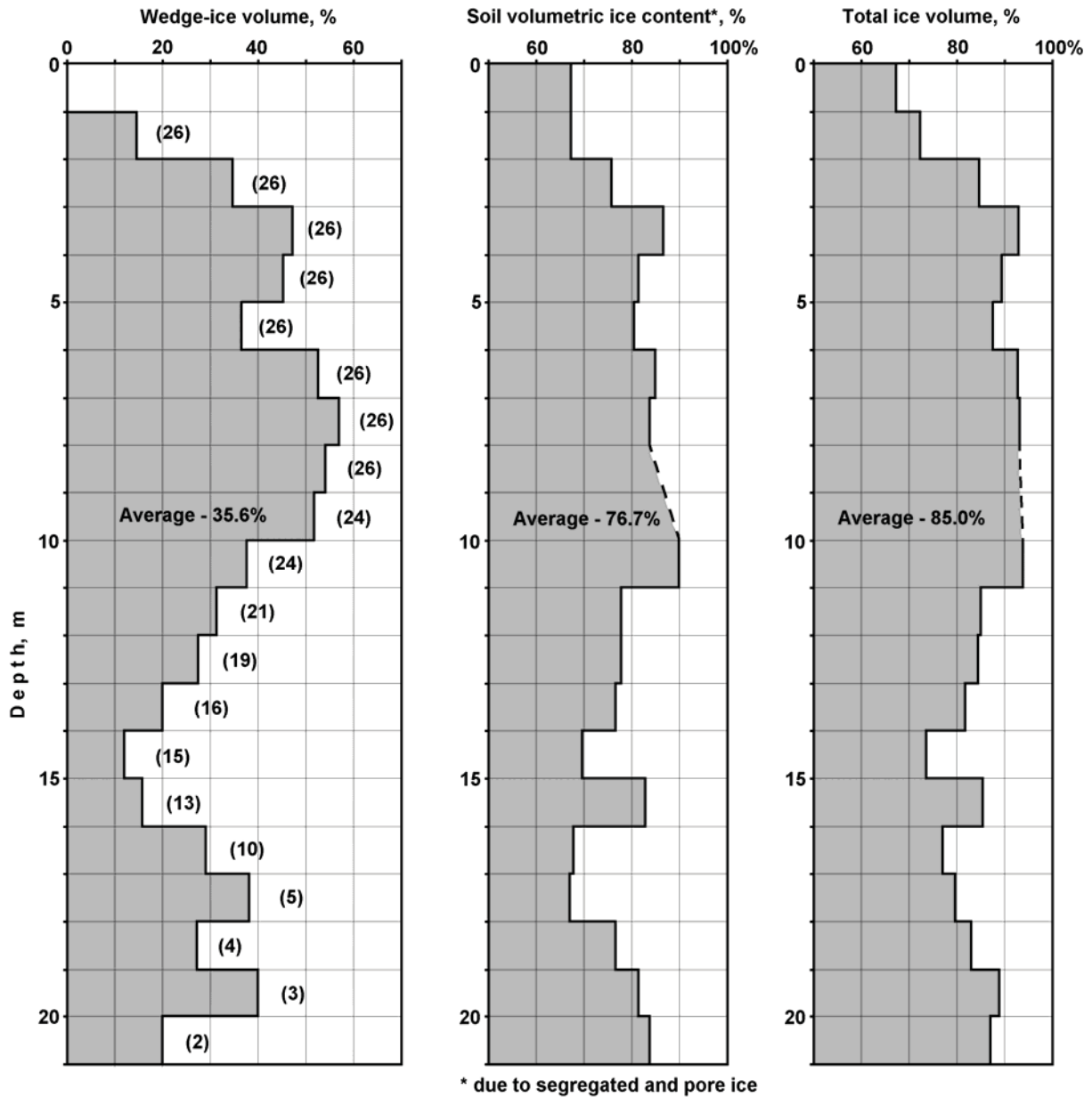


**Figure 5.92.** Distribution of ground ice volume with depth (Section #1). Numbers in parentheses show number of boreholes (both AUTC and DOT), which reached this depth interval. Volumetric ice content distribution is based on AUTC data.



**Section #2 (509+00...542+00)** is presented by 10-12-m-thick (31-39 ft) sequence of silt (partially ice-rich syngenetically frozen, partially ice-poor thawed and refrozen); very small wedge-ice occurrence (2%), but relatively high ice content of silt. Only one borehole (of 12) encountered ice wedge (borehole AUTC08-3, from 1.8 to 4.8 m) but inclined ice lenses in the other AUTC boreholes show the possibility of occurrence of other ice wedges. Syngenetic permafrost was identified in every AUTC borehole, although it can be overlaid by the layer of thawed and refrozen sediments up to 9-m-thick (in borehole AUTC-2). Ice contents of soil in section #2 are lower in comparison with section #1 but they are still relatively high. Average values of gravimetric moisture content of perennially frozen silt are 79% (based on the samples from four AUTC boreholes) and 64% (based on the samples from eight DOT boreholes). Distribution of ice content with depth is shown in **Figure 5.93**. The lowest values correspond either to the active layer and the layer of thawed and refrozen sediments (up to the depth about 10 m), or to gravelly soil and bedrock (below 10 m). Randomly distributed high values ( $MC_{grav} > 50\%$ ) belong mostly to syngenetic permafrost.

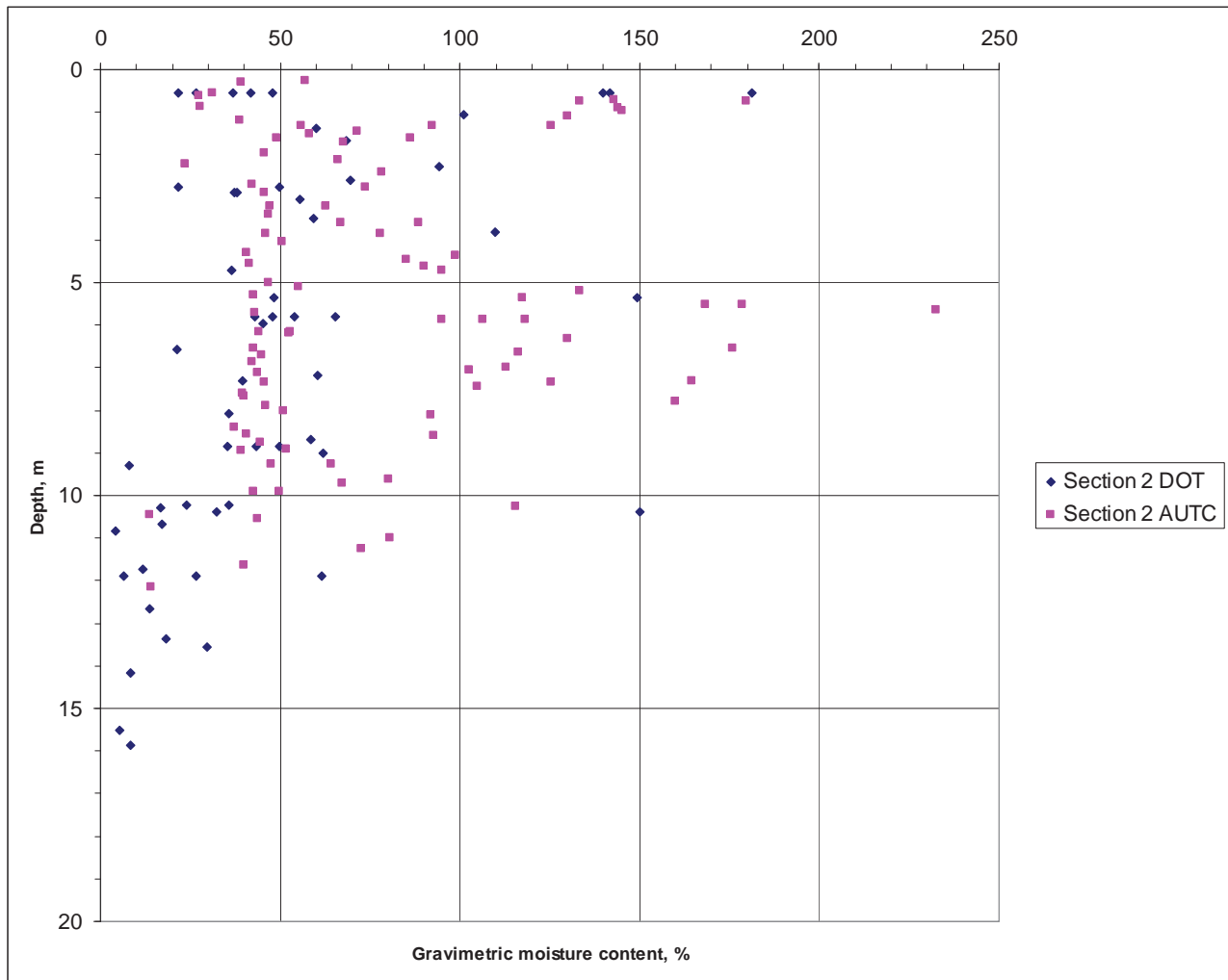


**Figure 5.93.** Gravimetric moisture content with depth, Section #2, based on DOT and AUTC data (eight and four boreholes, correspondingly).

**Section #3 (492+00...509+00)** is characterized by 9-14-m-thick sequence of ice-rich syngenetically frozen silt, extremely high wedge-ice occurrence (47%) and high gravimetric moisture content of perennially frozen silt (81% average, based on 38 samples from nine DOT boreholes).

Wedge-ice occurrence in the section 3 (**Fig. 5.90** right) can be described as following:

- from 0 to 2 m wedge-ice was not observed;
- from 2 to 4 m – less than 20% in wedge-ice occurrence;
- from 4 to 14 m –amount of wedge-ice exceeds 40%;
- from 4 to 10 m wedge-ice occurrence steadily increases (up to 92%);
- from 8 to 14 m wedge-ice occurrence usually exceeds 80%;
- from 9 to 10 m wedge-ice occurrence reaches 92% (measurements in 7 boreholes);
- from 12 to 13 m wedge-ice occurrence reaches 100% (measurements in 4 boreholes);
- from 14 m wedge-ice was not observed (in 2 boreholes).

Small amount of the wedge-ice up to the depth of 4 meters (**Fig. 5.90**, right) and low moisture content at the same depth interval (**Fig. 5.94**) we can explain by occurrence of the layer of thawed and refrozen sediments on top of permafrost sequence (similarly to section #1).

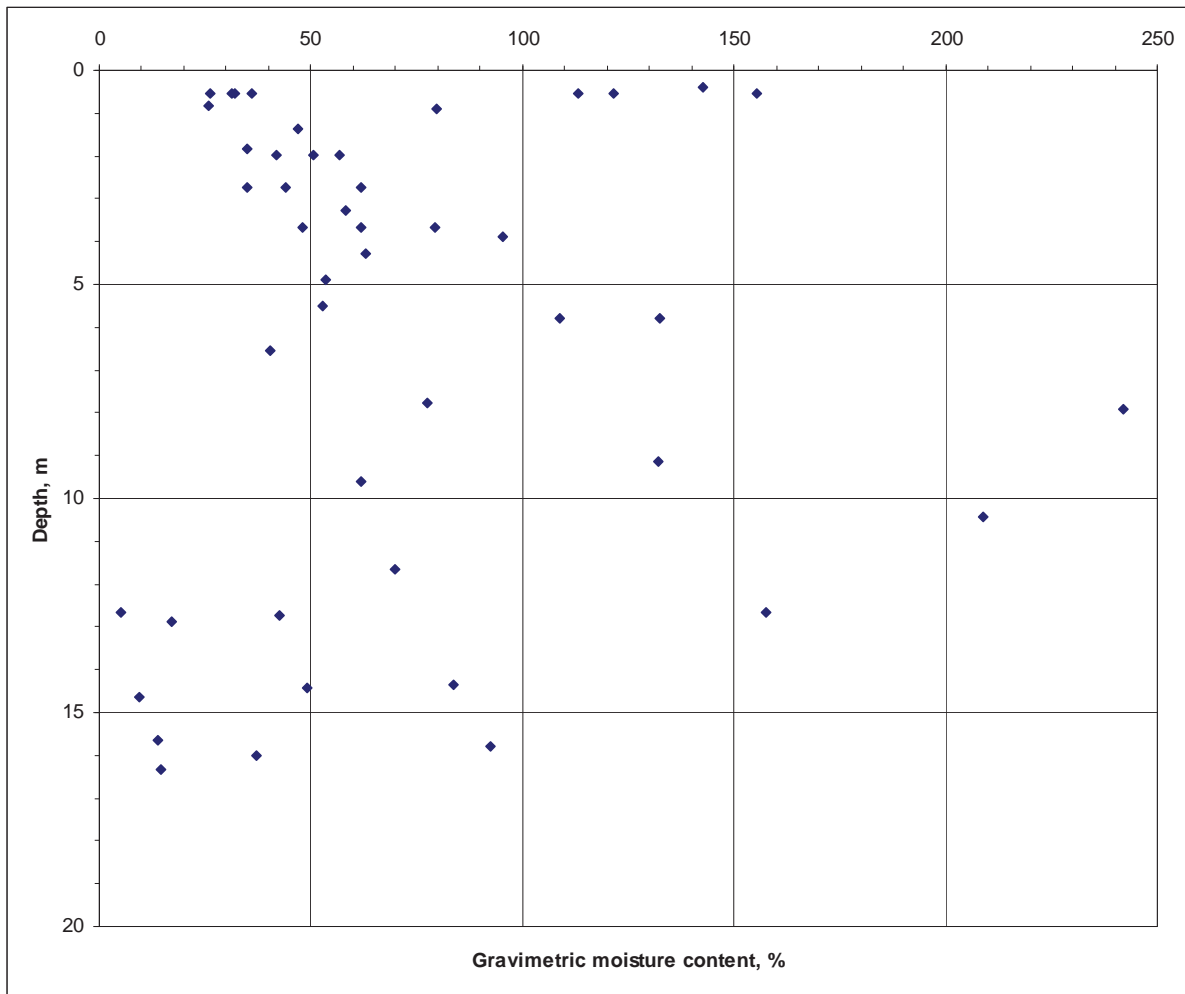


**Figure 5.94.** Gravimetric moisture content with depth, Section #3, based on DOT data (nine boreholes).

**Section #4 (433+00...492+00)** is characterized by very thin (0.5-4-m-thick) sequence of silt overlaying gravel and weathered bedrocks. Wedge-ice occurrence in this section is very small (3%), only one borehole (of 15) encountered ice wedge (borehole DOT-21). At the same time, but the gravimetric moisture content of perennially frozen silt is still relatively high (63% average, based on 21 samples from 15 DOT boreholes). Distribution of ice content with depth is shown in **Figure 5.95**.

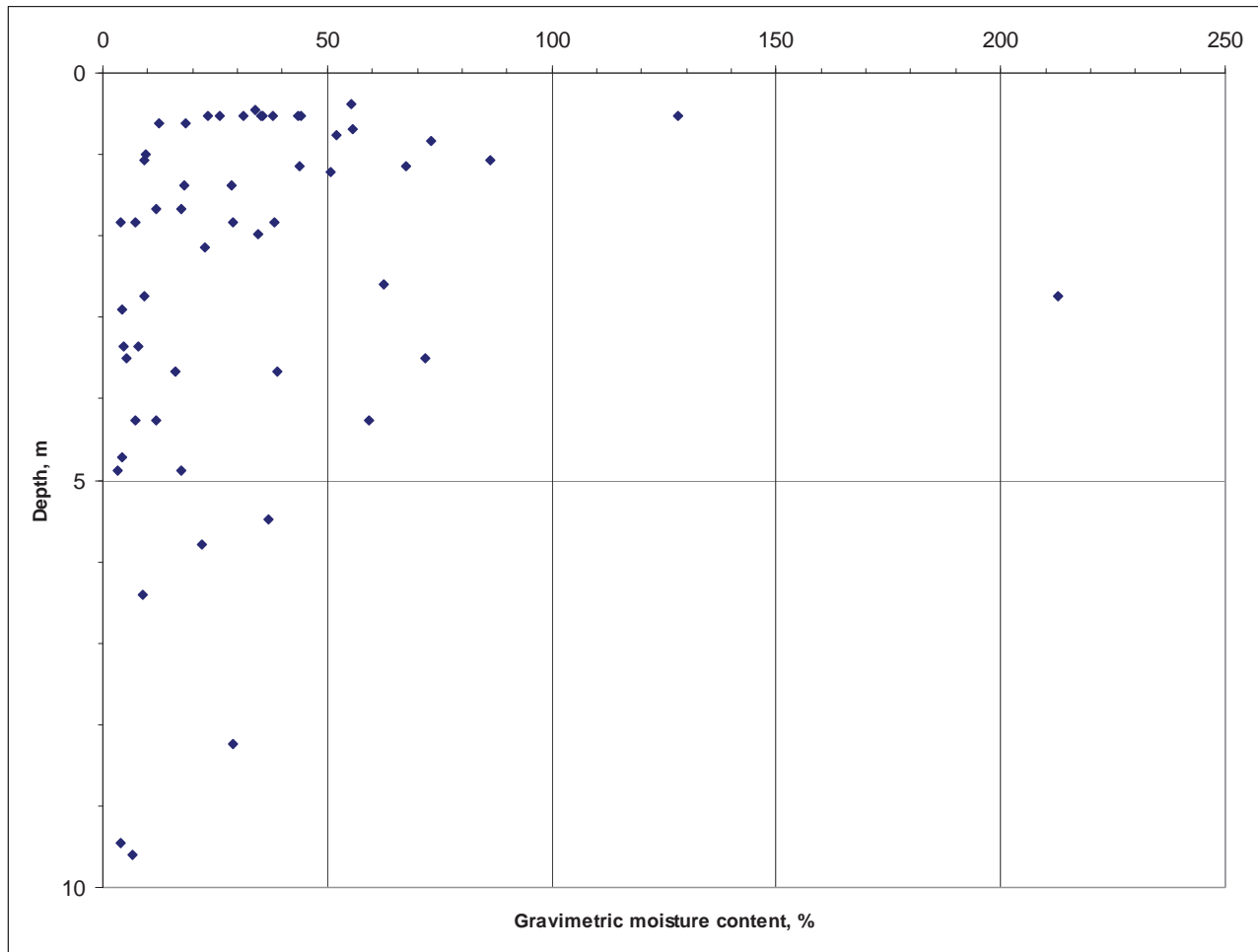


**Figure 5.95.** Gravimetric moisture content with depth, Section #4, based on DOT data (15 boreholes).

On the base of data from AUTC and DOT boreholes, we developed a cryostratigraphic profile for the sections 1 and 2 of the study site (**Figure 5.96**). Expected wedge-ice distribution in all four sections of the proposed alignment is shown in **Figure 5.97**. The maximum thickness of the syngenetic ice-rich permafrost in the area varies along the slope but could be more than 25 m (at the base of the slope). A width of ice-wedges in their upper part can reach 3-5 m, and the distance between ice wedges usually varies from 5 m to 15 m. It is common for such sediments that ice wedges can penetrate slightly deeper than layer of soil, in which they are developing.



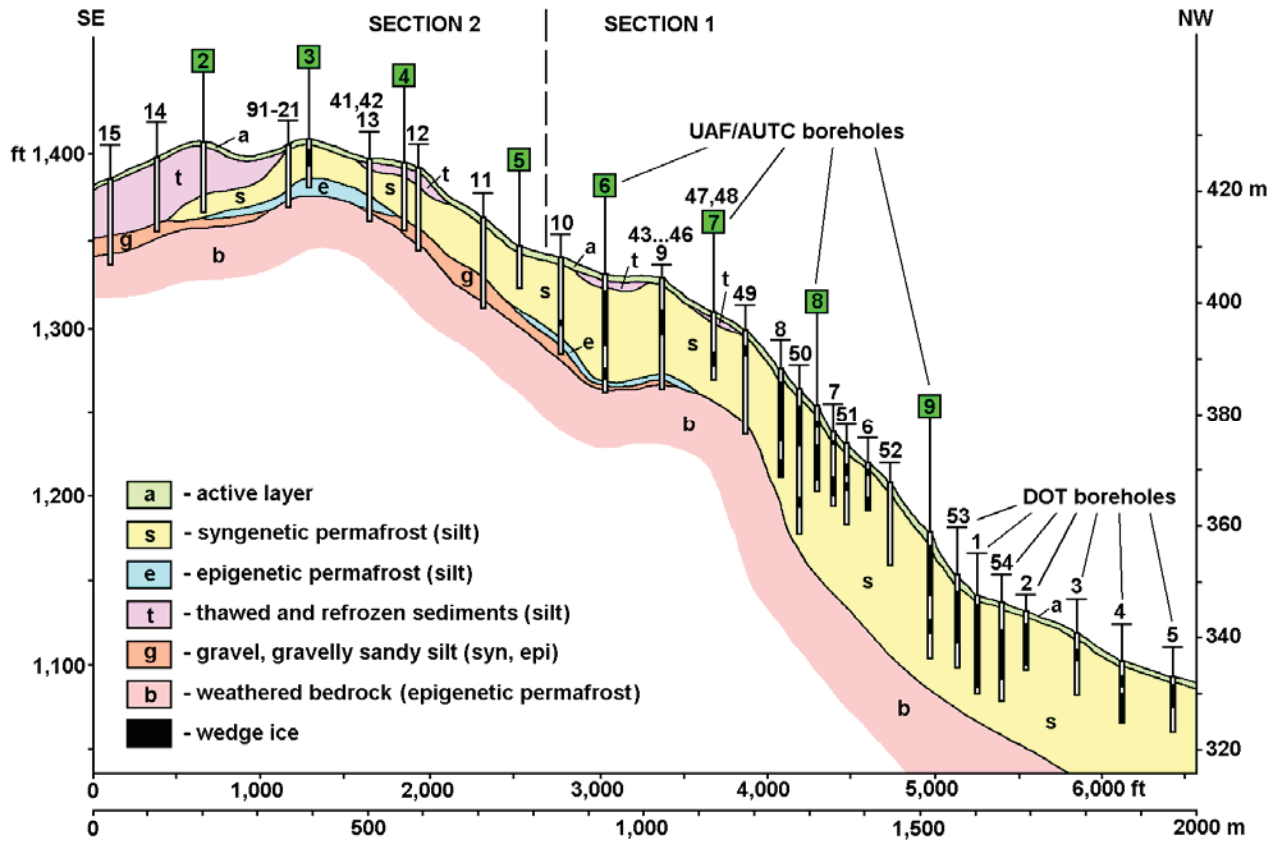


**Figure 5.96.** Cryostratigraphic profile. AUTC boreholes marked by green squares and the rest are DOT boreholes. Boundaries of sections #1 (ice-rich) and #2 (relatively ice-poor) are shown in **Figures 5.88, 5.89.**

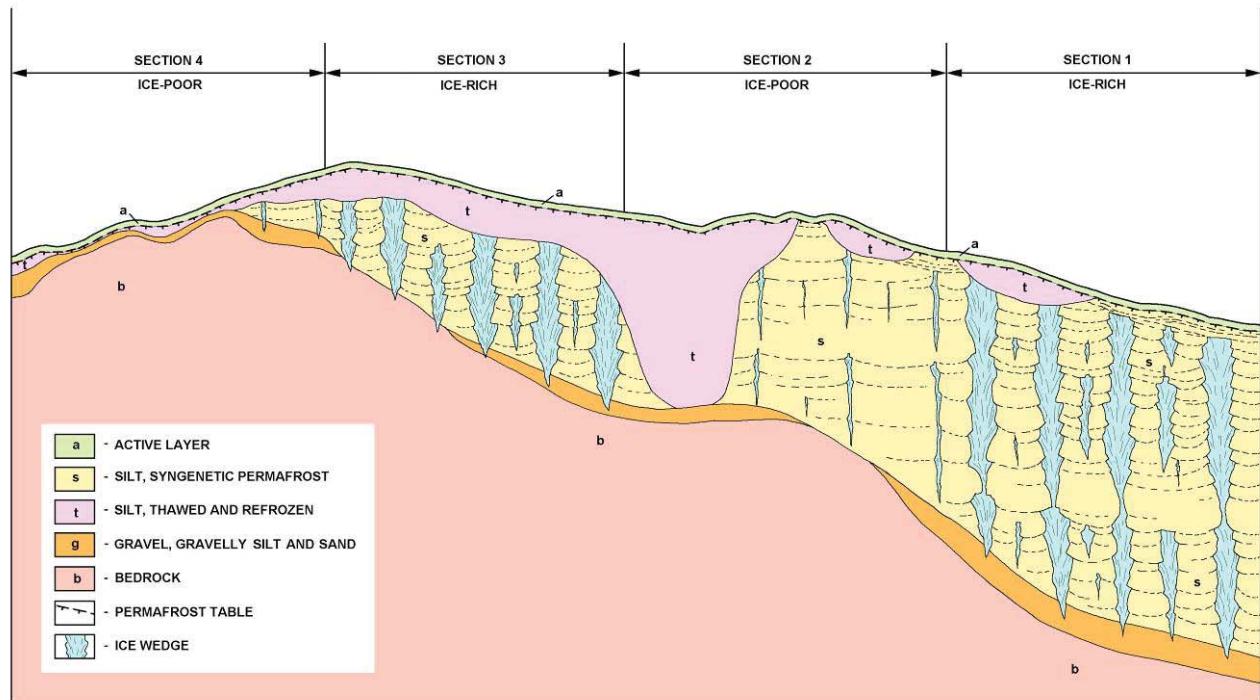


**Figure 5.97.** Expected wedge-ice distribution in different sections of the proposed alignment (not to scale).

### 5.5. Thaw strain of frozen soils

Evaluation of thaw strain of frozen soils is based on 44 tests of thawing without external load (free thawing) and five consolidation tests. **Figure 5.98** shows correlation between thaw strain in free thawing and gravimetric moisture content. Average thaw strain value is 23.2%. **Figure 5.99** shows the same correlation for 35 samples of mineral soils only. **Figure 5.100** shows correlation for 9 samples of organic soils. Average thaw strain values for mineral and organic soils are 0.26 and 0.13 correspondingly. Ice-rich mineral soils in free thawing completely lose their structure and a process of their disintegration can be compared with sedimentation in water (**Figure 5.101**).

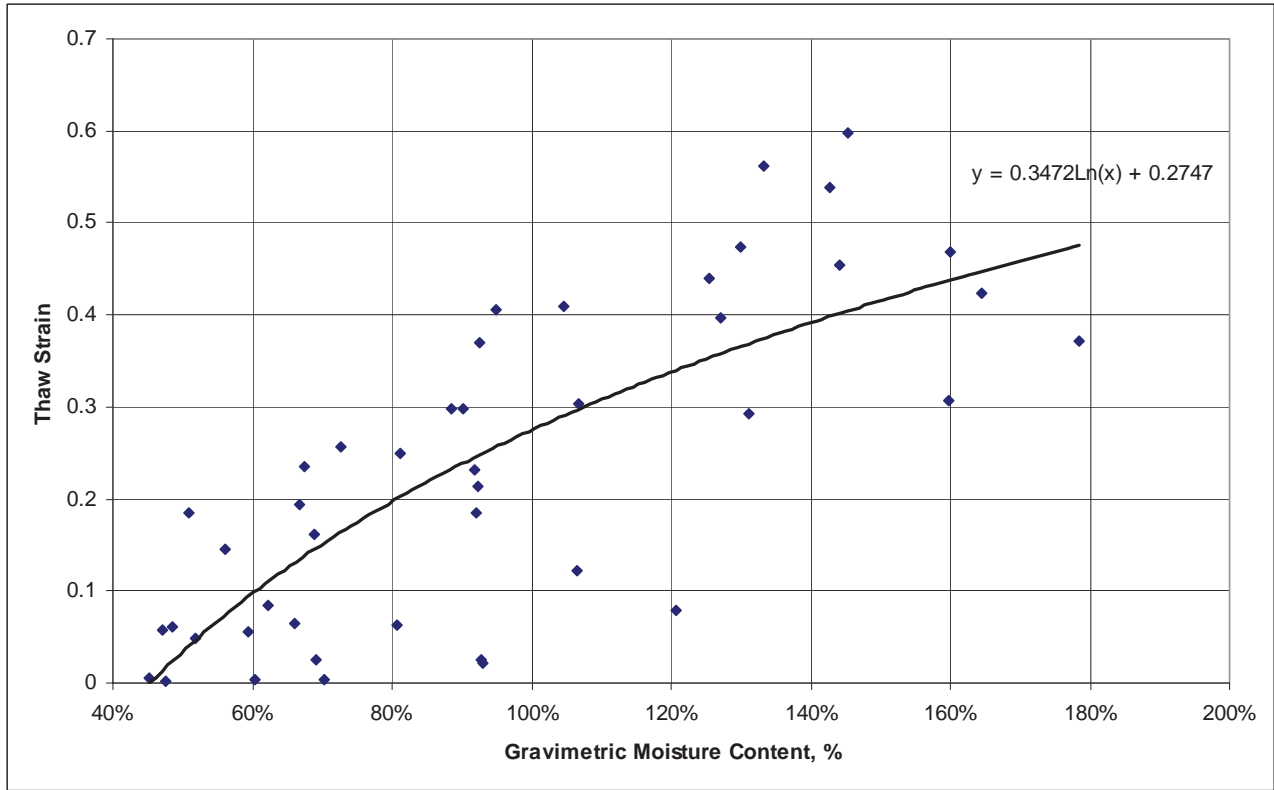


**Figure 5.98.** Correlation between thaw strain of mineral and organic-rich soil (without external load) and their moisture content (based on data from AUTC boreholes, 44 samples).



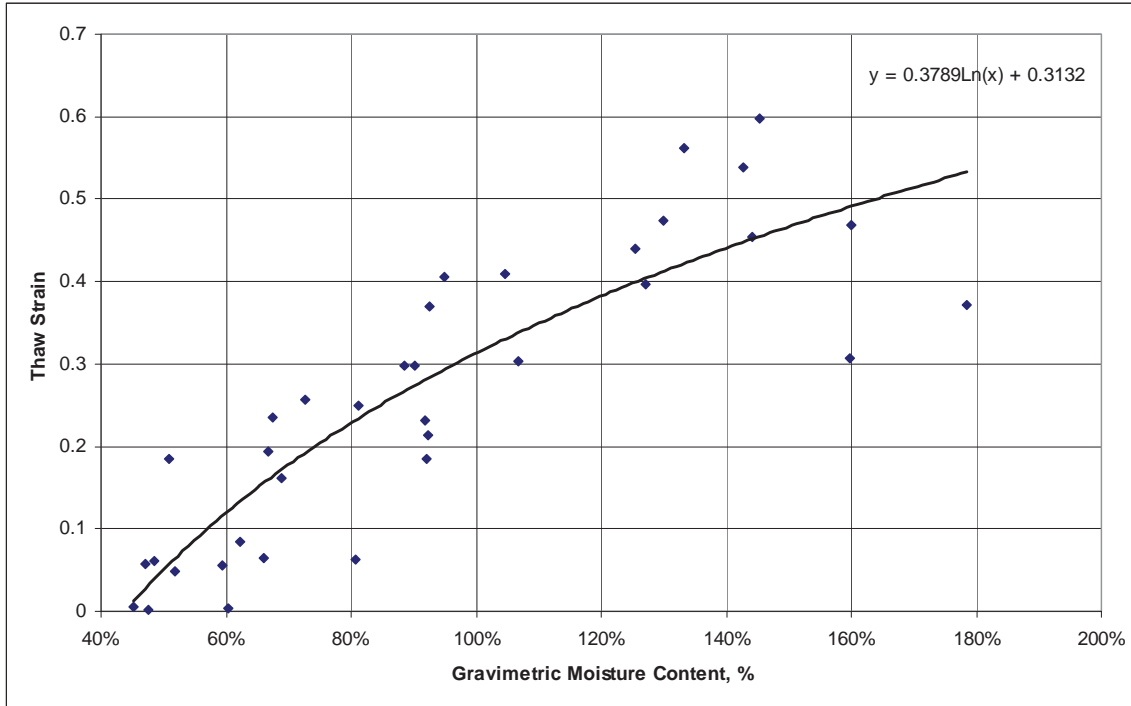


**Figure 5.99.** Correlation between thaw strain of mineral soil (without external load) and their moisture content (based on the data for 35 samples from AUTC boreholes).

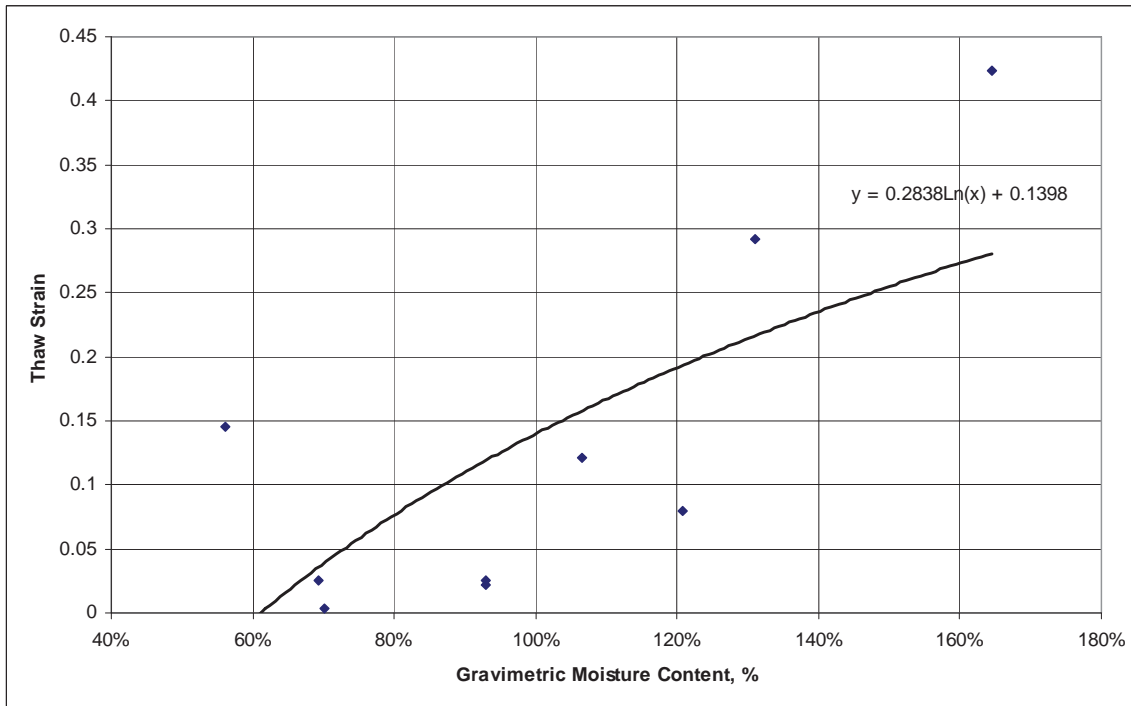


**Figure 5.100.** Correlation between thaw strain of organic-mineral soil (without external load) and their moisture content (based on the data for 9 samples from AUTC boreholes).

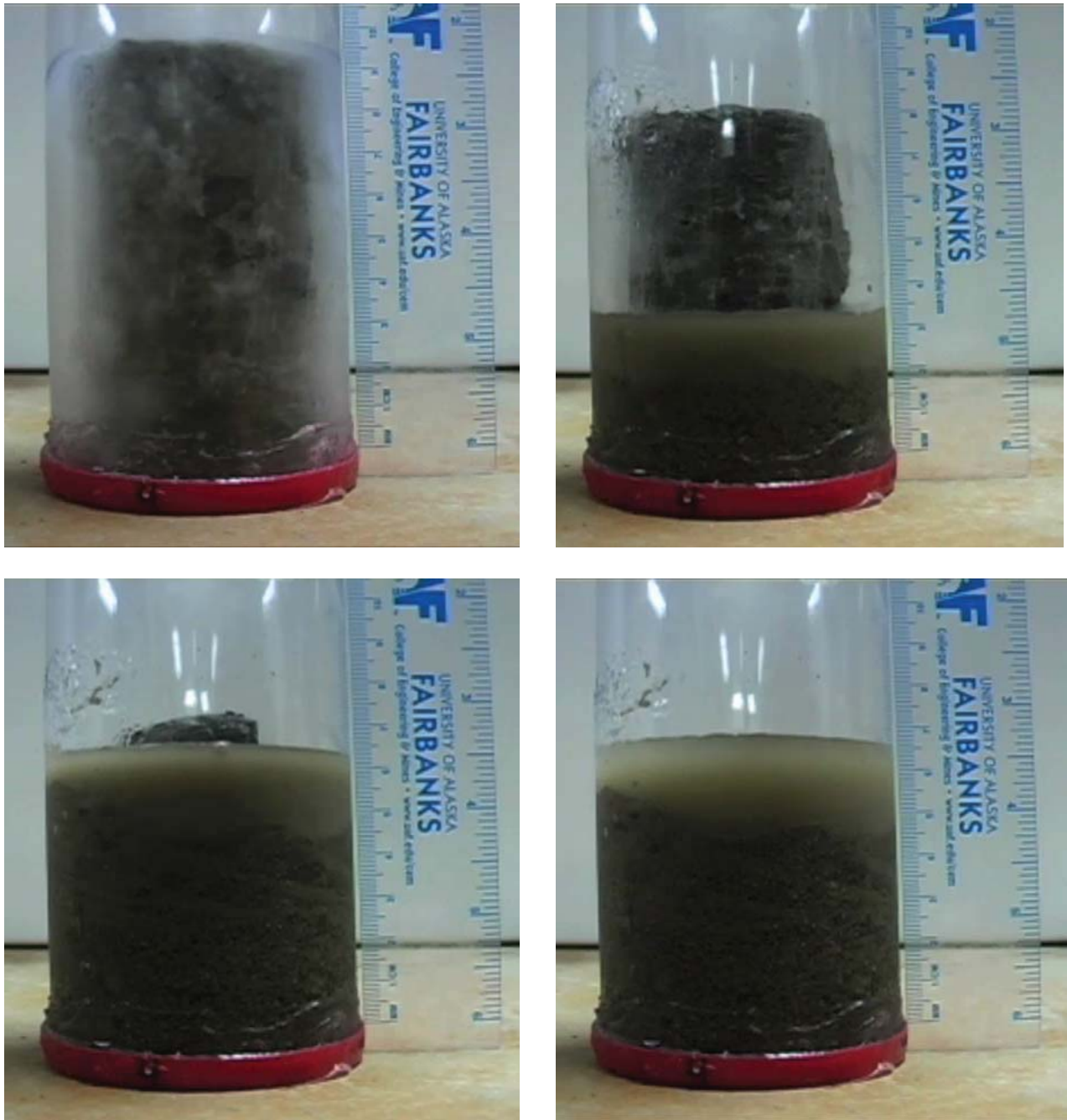


**Figure 5.101.** Thaw strain analysis of soils, borehole AUTC-4, depth 9.7 m, elapsed time 7 hrs.

We found that organic soils behave differently from mineral soils, and their thaw strain in free thawing is much lower. In consolidation test the part of the thaw strain of organic soils related to the impact of a load was greater than that of mineral soils and the total thaw strain of organic soils was comparable to the thaw strain of mineral soils (Figures 5.102, 5.103).

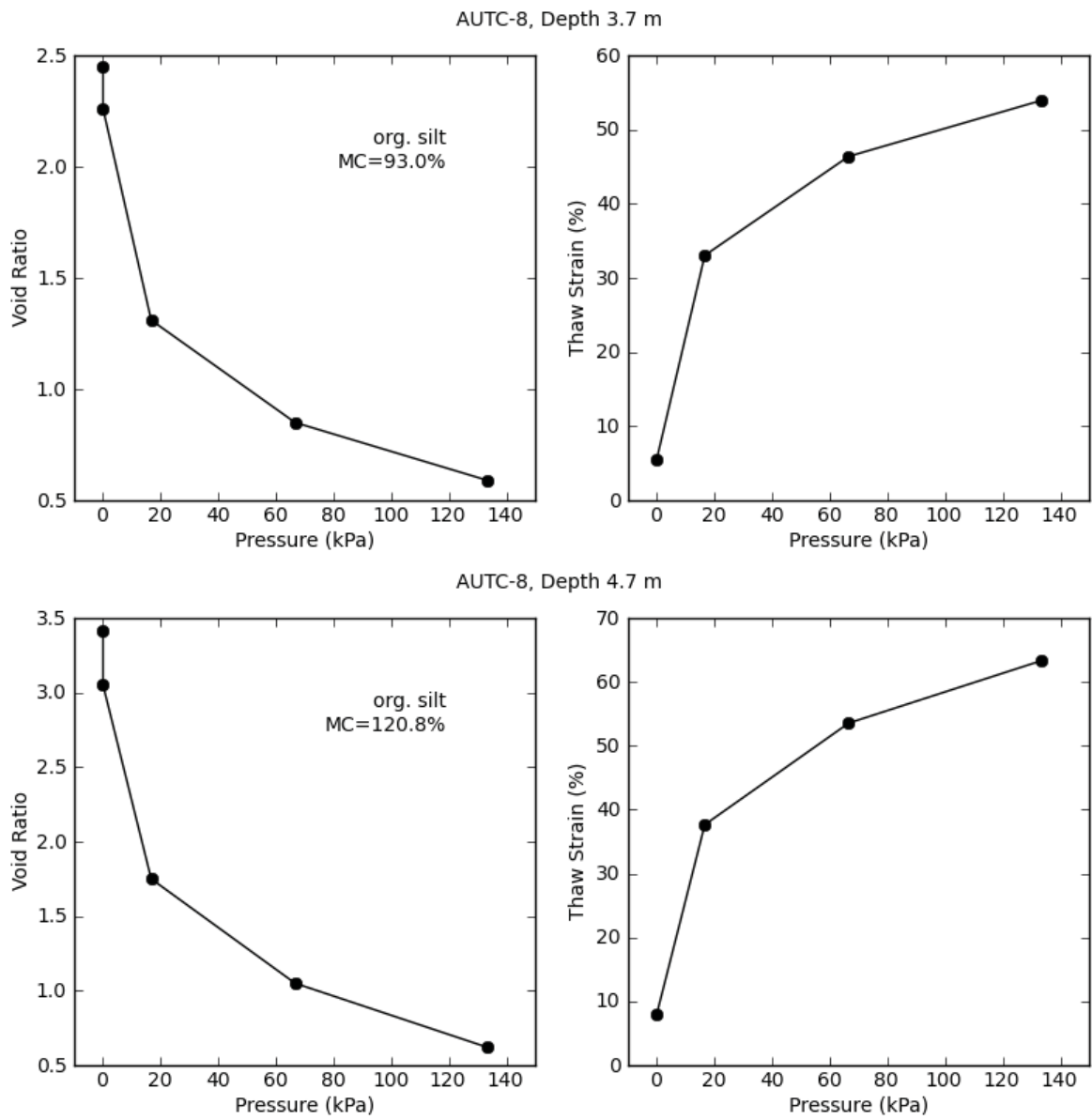


**Figure 5.102.** Consolidation of organic-mineral soils. Organic matter contents (LOI): 14.1% (AUTC-8, 3.7 m); 17.6% (AUTC-8, 4.7 m)



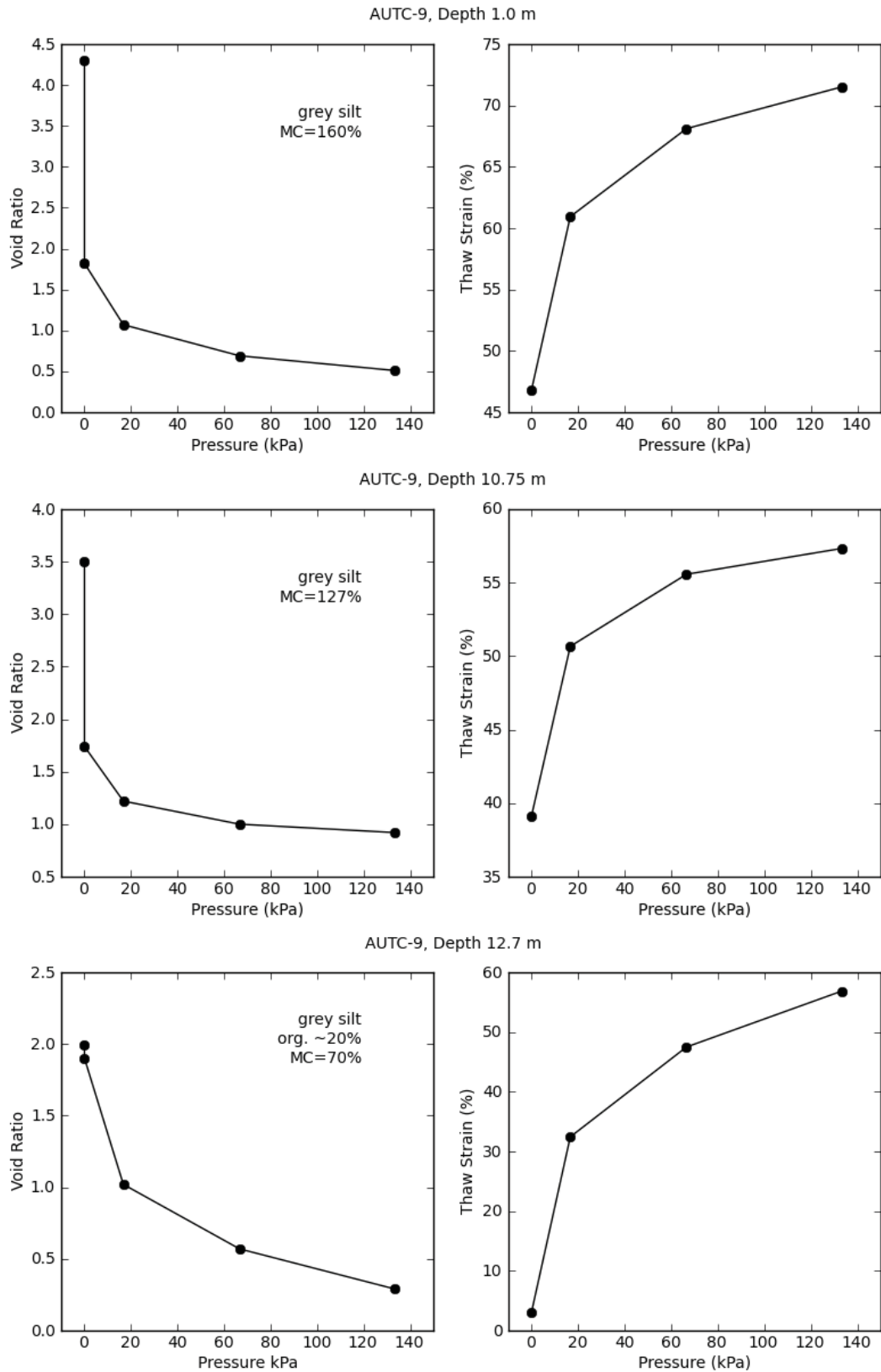


**Figure 5.103.** Consolidation of mineral soils. Organic matter contents (LOI): 6.5% (AUTC-9, 1.0 m); 9.2% (AUTC-9, 10,75 m); 9.0% (AUTC-9, 12.7 m).

We evaluated thaw strain of mineral soils (**Figure 5.104**) as a function of soil water content for two final void ratios 0.8 and 0.5, which correlates with loads about 50kPa (7.5 psi) and 140 kPa (20 psi). Thaw strain was evaluated using the the well-known equation:

$$\delta = \frac{e_{in} - e_{fn}}{1 + e_{in}},$$

where  $e_{in}$  = initial void ratio,  $e_{fn}$  = final void ratio.

The initial void ratio was found from the equation:

$$e_{in} = 1.09WG_s,$$

where  $W$  = moisture content (unit fraction),  $G_s$  = specific gravity of solids for mineral soils assumed 2.65.

The results of evaluation are shown in **Figure 5.104**. Thaw strain in **Figure 5.104** is not conservative because it does not take into account settlement due to wedge ice melting. Most of soils in the project area are extremely ice-rich and have excessive thaw settlement upon thawing.

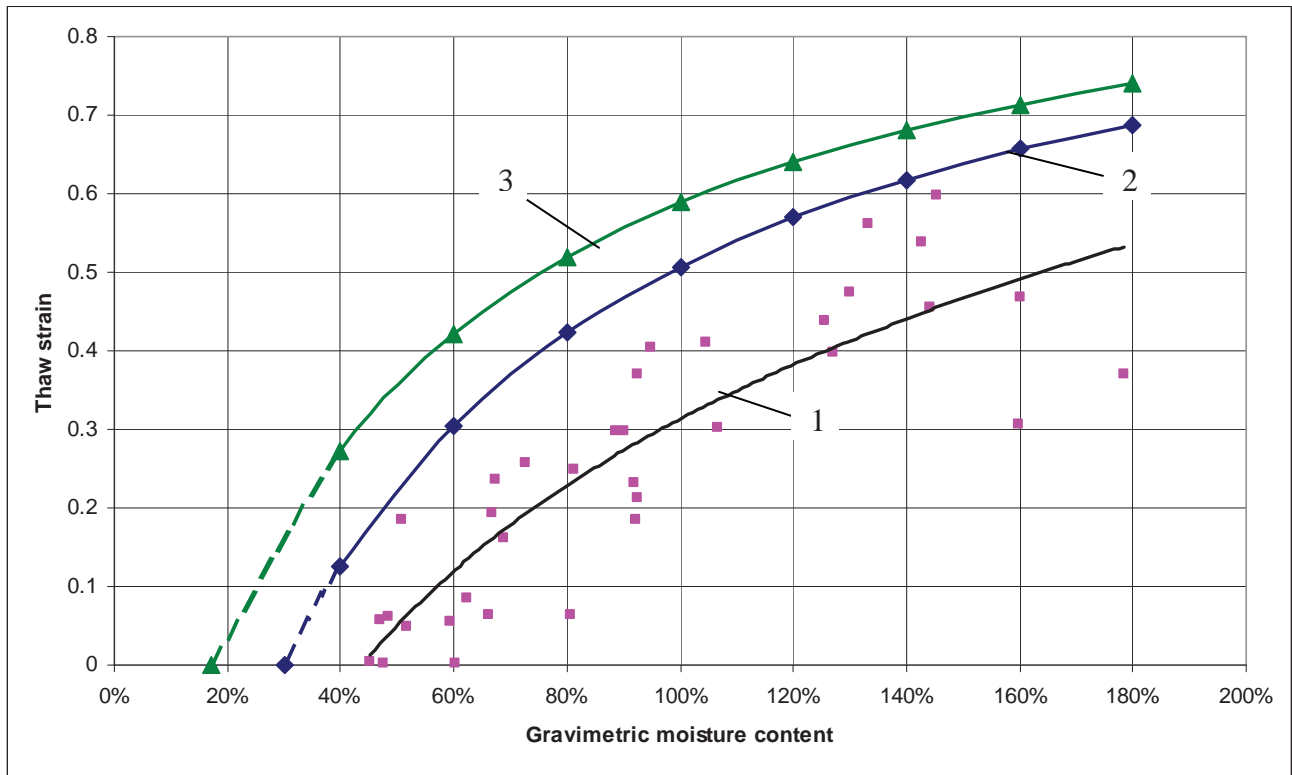


**Figure 5.104.** Thaw strain of mineral soil vs moisture content. 1 – without external load (based on experimental data, see **Figure 5.99**); 2 – under the stress 50 kPa (7.5 psi); 3 – under the stress 140 kPa (20 psi).

## Conclusions

Field data proved our preliminary evaluation of permafrost genesis and its properties in the project area. Most of soils in the project area are extremely ice-rich and have excessive thaw settlement upon thawing. Four sections with different permafrost properties are identified along the proposed alignment. They are:

**Section #1 (542+00...590+00)** is characterized by thick sequence of ice-rich syngenetically frozen silt (from 12 m to more than 26 m) with very high wedge-ice occurrence (35%) and gravimetric moisture content of perennially frozen silt (102%<sup>a</sup>/103%<sup>b</sup> average). The average thaw strain due to segregated ice is 32%, so the total thaw strain (due to wedge-ice and segregated ice) is 56%. This thaw strain is not conservative, because reflects only settlement upon thawing without load.

**Section #2 (509+00...542+00)** is characterized by 10-12-m-thick sequence of silt (partially ice-rich syngenetically frozen, partially ice-poor thawed and refrozen); very small wedge-ice occurrence (2%), but relatively high gravimetric moisture content of perennially frozen silt (79%<sup>a</sup>/64%<sup>b</sup> average). The average thaw strain due to segregated ice is 23%, and total thaw strain is 25%.

**Section #3 (492+00...509+00)** is characterized by 9-14-m-thick sequence of ice-rich syngenetically frozen silt, extremely high wedge-ice occurrence (47%) and gravimetric moisture content of perennially frozen silt (81%<sup>b</sup> average). The average thaw strain due to segregated ice is 23%, and total thaw strain is 59%.

**Section #4 (433+00...492+00)** is characterized by very thin (0.5-4-m-thick) sequence of silt overlaying gravel and weathered bedrocks; wedge-ice occurrence is very small (3%), but the gravimetric moisture content of perennially frozen silt is still relatively high (63%<sup>b</sup> average). The average thaw strain due to segregated ice is 13%, and total thaw strain is 16%.

Sections #1 and #3 are extremely ice-rich and permafrost thawing in these parts of alignment will bring unbearable settlement. Wedge-ice occurrence at sections #2 and #4 is not so significant, but the soils themselves contain great amount of segregated ice, and the thaw settlement cannot be neglected.

In the study area, ice wedges are usually separated from the base of the active layer by 1-4-m-thick protective layer of thawed and refrozen soils. Existence of the intermediate layer and the ice-poor stratum of thawed and refrozen soils on top of original syngenetic permafrost is extremely important for the road integrity in fill areas. In cut areas this layer will be destroyed, therefore permafrost will be more vulnerable to climatic and local impacts. This ice-poor layer can significantly reduce the period of stabilization of exposed surfaces of cut slopes (in cases when large massive ice bodies are located right below the permafrost table, the process of complete stabilization of exposed bluffs can take dozens of years) .

---

<sup>a</sup> Based on AUTC data

<sup>b</sup> Based on DOT data



Extremely high ice content of the ice-rich syngenetic permafrost with ice wedges determines its high thaw susceptibility and potential settlement harmful to any structures. The main potential hazards are the following: (1) significant thaw settlement of soils beneath the road; (2) rapid retreat of the road slopes in cut areas; (3) contamination of surface water due to thawing of ice-rich silts at the slopes; (4) formation of ponds in the road-side ditches, which will cause talik formation and thaw settlement of sediments beneath the water layer.

We understand that only design engineers accumulate whole information and have knowledge and experience required for comprehensive design of a road. We also understand that geotechnical information, despite its importance, is only one part of it. This is why we do not provide our recommendations for a road design but we are willing to cooperate with ADOT geotechnical and design engineers in evaluations of permafrost related hazards, which can associate with road construction and service, and impacts of possible construction modes on permafrost and permafrost potential reaction.

## REFERENCES

- American Society of Testing and Materials. ASTM D 422 (Reapproved 1998): Standard test method for particle-size analysis of soils. Annual book of ASTM standards, ASTM, West Conshohocken, PA (accessed online).
- Andersland, O. B. & Anderson, D. M. 1978. *Geotechnical engineering for cold regions*. McGraw-Hill Book Company, 566 pp.
- Black, R. F. 1978. Fabrics of ice wedges in central Alaska. *Proceedings of the Third International Conference on Permafrost, Edmonton, July 10-13, 1978*. Ottawa: National Research Council of Canada, 248-253.
- Blott, S. J., Pye, K. 2001. Gradistat: a grain size distribution statistics package for the analysis of unconsolidated sediments. *Earth Surface Processes and Landforms* 26: 1237-1278.
- Bray, M. T., French, H. M. & Shur, Y. 2006. Further cryostratigraphic observations in the CRREL permafrost tunnel, Fox, Alaska. *Permafrost and Periglacial Processes* 17 (3): 233-243.
- Brown, J. & Kreig, R. A. (Eds.) 1983. *Guidebook to permafrost and related features along the Elliott and Dalton Highways, Fox to Prudhoe Bay, Alaska*. 230 pp.
- Carter, L. D. 1988. Loess and deep thermokarst basins in Arctic Alaska. *Proceedings of the Fifth International Conference on Permafrost*. Tapir publishers, Trondheim, Norway: 706-711.
- Fortier, D., Kanevskiy, M., Shur, Y. 2008. Genesis of reticulate-chaotic cryostructure in permafrost. In: *Proceedings of the Ninth International Conference on Permafrost, June 29 – July 3, 2008, Fairbanks, Alaska*. Kane, D.L. & Hinkel, K.M. (eds). Institute of Northern Engineering, University of Alaska Fairbanks, vol. 1: 451-456.
- French, H. M. 2007. *The Periglacial Environment, Third Edition*. John Wiley and Sons Ltd, Chichester, UK, 458 pp.
- Gasanov, S. S. 1963. *Morphogenetic classification of cryostructures of frozen sediments*. Trudy SVKNII, Vol. 3, Magadan (in Russian).
- Gasanov, S. S. 1969. *Structure and history of formation of permafrost in Eastern Chukotka*. Moscow: Nauka, 168 pp. (in Russian).
- Geotechnical report, Dalton Highway 9 mile Hill North, Federal Project No. NH-F-065-2(3) / State Project No. 64899, Northern Region. 2006. Alaska Department of Transportation and Public Facilities, Northern Region.
- Hamilton, T. D. 1979. *Geologic road log, Alyeska haul road, Alaska, June-August 1975*. U.S. Geological Survey Open-File Report 79-227, 64 p.
- Hamilton, T. D., Ager, T. A., & Robinson, S. W. 1983. Late Holocene ice wedges near Fairbanks, Alaska, USA: environmental setting and history of growth. *Arctic and Alpine Research* 15 (2): 157-168.
- Hamilton, T. D., Craig, J. L. & Sellmann, P. V. 1988. The Fox permafrost tunnel: a late Quaternary geologic record in central Alaska. *Geological Society of America Bulletin* 100: 948-969.
- Jorgenson, T., Yoshikawa, K., Kanevskiy, M., Shur, Y., Romanovsky, V., Marchenko, S., Grosse, G., Brown, J., and Jones, B. 2008. Permafrost Characteristics of Alaska. In: *Proceedings of the Ninth International Conference on Permafrost, extended abstracts, June 29 – July 3, 2008, Fairbanks, Alaska*. Kane, D.L. & Hinkel, K.M. (eds). Institute of Northern Engineering, University of Alaska Fairbanks: 121-122.

- Kanevskiy, M. Z. 1991. The role of quasi-syngeneses in formation of Quaternary sediments cryogenic structure in Northern Yakutia. In: Melnikov, P. and Shur, Y. (eds.), *The upper horizon of permafrost*. Moscow: Nauka, 47-63 (in Russian).
- Kanevskiy, M. 2003. Cryogenic structure of mountain slope deposits, northeast Russia. In: Phillips, M., Springman, S., Arenson, L. (eds) *Proceedings of the Eighth International Conference on Permafrost*, 21-25 July 2003, Zurich, Switzerland, Swets & Zeitlinger B.V., Lisse, The Netherlands, vol. 1: 513-518.
- Kanevskiy, M., Fortier, D., Shur, Y., Bray, M., Jorgenson, T. 2008. Detailed cryostratigraphic studies of syngenetic permafrost in the winze of the CRREL permafrost tunnel, Fox, Alaska. In: *Proceedings of the Ninth International Conference on Permafrost, June 29 – July 3, 2008, Fairbanks, Alaska*. Kane, D.L. & Hinkel, K.M. (eds). Institute of Northern Engineering, University of Alaska Fairbanks, vol. 1: 889-894.
- Katasonov, E. M. 1962. Cryogenic textures, ice and earth wedges as genetic indicators of perennially frozen Quaternary deposits. *Issues of Cryology in Studies of Quaternary Deposits*. Moscow: Izd-vo AN SSSR, 86–98 (in Russian).
- Katasonov, E. M. 1969. *Composition and cryogenic structure of permafrost*. National Research Council of Canada, Ottawa, Technical Translation 1358, 25-36.
- Katasonov, E. M. 1978. Permafrost-facies analysis as the main method of cryolithology. *Proceedings of the Second International Conference on Permafrost, July 13-28, 1973. USSR Contribution*. Washington: National Academy of Sciences, 171-176.
- Kreig, R. A. & Reger, R. D. 1982. *Air-photo analysis and summary of landform soil properties along the route of the Trans-Alaska Pipeline System*. DGGs, College, Alaska, Geologic report 66: 149 pp.
- Kudryavtsev, V. A. (ed.). 1978. *General Permafrost Science (Geocryology)*. 2<sup>nd</sup> edn. Moscow: Moscow University Press, 463 pp. (in Russian).
- Lachenbruch, A. H. 1962. *Mechanics of thermal contraction cracks and ice-wedge polygons in permafrost*. Geol. Soc. of Am. Special Paper 70.
- Lawson, D. E. 1983. Ground ice in perennially frozen sediments, northern Alaska. In: *Proceedings of the Fourth International Conference on Permafrost*. National Academy Press, Washington, D.C.: 695-700.
- Leffingwell, E. de K. 1915. Ground-ice wedges, the dominant form of ground-ice on the north coast of Alaska. *Journal of Geology*, Vol. 23: 635-654.
- Linell, K. A. & Kaplar, C. W. 1966. Description and classification of frozen soils. *Permafrost: International Conference Proceedings*, National Academy of Sciences – National Research Council, Washington, DC, Publication 1287: 481-487.
- Lotspeich, F. B. 1971. *Environmental guidelines for road construction in Alaska*. Environmental Protection Agency, Alaska, Water Laboratory, College, Alaska, Report No. 1610 GOI 08/71, 127 pp.
- Matheus, P., Begét, J., Mason, O. & Gelvin-Reymiller, C. 2003. Late Pliocene to Late Pleistocene environments preserved at the Palisades Site, central Yukon River, Alaska. *Quaternary Research* 60: 33-43.
- Melnikov, V. P. & Spesivtsev, V. I. 2000. *Cryogenic Formations in the Earth's Lithosphere*. Novosibirsk: Siberian Publishing Center UIGGM, Siberian Branch, Russian Academy of Sciences, 343 pp.
- Meyer, H., Yoshikawa, K., Schirrmeister, L., Andreev, A. 2008. The Vault Creek Tunnel (Fairbanks Region, Alaska) – A Late Quaternary Palaeoenvironmental Permafrost Record. In:



- Proceedings of the Ninth International Conference on Permafrost, June 29 – July 3, 2008, Fairbanks, Alaska.* Kane, D.L. & Hinkel, K.M. (eds). Institute of Northern Engineering, University of Alaska Fairbanks, vol. 2: 1191-1196.
- Murton, J. B. & French, H. M. 1994. Cryostructures in permafrost, Tuktoyaktuk coastlands, western arctic Canada. *Canadian Journal of Earth Sciences* 31: 737–747.
- Péwé, T. L. 1966. Ice wedges in Alaska – classification, distribution and climatic significance. *Permafrost: International Conference Proceedings*, National Research Council of Canada - National Academy of Sciences, Washington, DC, Publication 1287, 76-81.
- Péwé, T. L. 1975. Quaternary geology of Alaska. *United States Geological Survey, Professional Paper* 835, 145 pp.
- Pihlainen, J.A. & Johnston, G.H. 1963. *Guide to a field description of permafrost for engineering purposes*. National Research Council of Canada, Associate Committee on soil and snow mechanics, Technical Memorandum 79, 23 pp.
- Popov, A. I. 1967. *Cryogenic phenomena in the Earth crust (Cryolithology)*. Moscow: Moscow University Press, 304 pp. (in Russian).
- Popov, A. I., Rozenbaum, G. E. & Tumel, N. V. 1985. *Cryolithology*. Moscow: Moscow University Press, 239 pp. (in Russian).
- Porter L. 1986. Jack Wade Creek: an in situ Alaskan late Pleistocene vertebrate assemblage. *Arctic* 39, pp. 297–299.
- Porter L. 1988. Late Pleistocene fauna of Lost Chicken Creek, Alaska, *Arctic* 41, pp. 303–313.
- Romanovskii, N. N. 1993. *Fundamentals of cryogenesis of lithosphere*. Moscow: Moscow University Press, 336 pp. (in Russian).
- Sellmann, P. V. 1967. *Geology of the USA CRREL permafrost tunnel, Fairbanks, Alaska*. Hanover, New Hampshire, US Army CRREL Technical Report 199, 22 pp.
- Shur Y. L. 1988a. *Upper horizon of the permafrost soils and thermokarst*. Novosibirsk: Nauka, Siberian Branch, 210 pp. (in Russian).
- Shur Y. L. 1988b. The upper horizon of permafrost soils. In *Proceedings of the Fifth International Conference on Permafrost*, Vol. 1. Tapir Publishers, Trondheim: Norway, 867–871.
- Shur, Y., Hinkel, K.M. & Nelson, F.E. 2005. The transient layer: implications for geocryology and climate-change science. *Permafrost and Periglacial Processes* 16 (1): 5-17.
- Shur, Y., and Jorgenson, M.T. 1998. Cryostructure development on the floodplain of the Collville River Delta, northern Alaska. In: *Proceedings of the Seventh International Conference on Permafrost*. Yellowknife, Canada: 993-999.
- Shur, Y., French, H. M., Bray, M. T. & Anderson, D. A. 2004. Syngenetic permafrost growth: cryostratigraphic observations from the CRREL Tunnel near Fairbanks, Alaska. *Permafrost and Periglacial Processes* 15 (4): 339-347.
- Smith, N. & Berg, R. 1973. Encountering massive ground ice during road construction in central Alaska. *Proceedings of the Second International Conference on Permafrost, July 13-28, 1973*. Washington: National Academy of Sciences, 730-736.
- Soloviev, P. A. 1959. *Permafrost of northern part of Lena-Amga plain*. Moscow: Academy of Sciences of the USSR Publishing House, 144 pp (in Russian).
- Tart, R. G. 2003. Heave and solifluction on slopes. In: Phillips, M., Springman, S., Arenson, L. (eds) *Proceedings of the Eighth International Conference on Permafrost, 21-25 July 2003, Zurich, Switzerland*, Swets & Zeitlinger B.V., Lisse, The Netherlands, vol. 2: 1135-1140.
- Tuck, R. 1940. *Origin of the muck-silt deposits at Fairbanks, Alaska*. *Bulletin of the Geological Society of America* 51: 1295-1310.

- van Everdingen, R. O. (edit) 1998. Multi-Language glossary of permafrost and related ground-ice terms. Univ. of Calgary Press: Calgary.
- Vtyurin, B. I. 1964. *Cryogenic structure of Quaternary deposits*. Moscow: Nauka, 151 pp. (in Russian).
- Wahrhaftig, C. 1965. Physiographic divisions of Alaska. USGS professional paper 482. Washington: United States Government Printing Office, 52 pp.
- Weber, F. R., Wheeler, K. L., Rinehart, C. D., and Light, T. D., 1997. Generalized geologic map of the Livengood Quadrangle, Alaska: U.S. Geological Survey Open-File Report 97-484-A, scale 1:250,000.
- Williams, J.R. 1962. *Geologic reconnaissance of the Yukon Flats district, Alaska*. U.S. Geological Survey Bulletin 111-H, Washington, DC, pp. 290–311.
- Wilkerson, A. S. 1932. Some frozen deposits in the goldfields of interior Alaska. *American Museum Novitates*, 525, 22 pp.
- Yanovsky V. K. 1933. Expedition to Pechora River to determine the position of the southern permafrost boundary. In *Reports of the Committee for Permafrost Investigations*, Vol. 5(2). Akademiia Nauk SSSR: Moscow-Leningrad, 65–149 (in Russian).
- Zhestkova T. N. 1982. *Formation of the cryogenic structure of ground*. Moscow: Nauka, 209 pp. (in Russian).